Politecnico di Torino

MASTER'S DEGREE IN ENERGY AND NUCLEAR ENGINEERING
Renewable Energy Systems
A.y. 2025/2026
Graduation session September 2026

Assessment of Geothermal Energy Exploitation Pathways for the Repurposing of Decommissioned Offshore Oil & Gas Platforms

Supervisor

Prof. Andrea Carpignano

Co-supervisor

Prof.ssa Raffaella Gerboni

Candidate

Anna Giuliano

“We do not inherit the Earth from our ancestors,

we borrow it from our children.”

Abstract

From an energy transition perspective, evaluating sustainable repurposing strategies for industrial facilities, including offshore Oil & Gas assets, has become increasingly important. Italy currently hosts 139 offshore platforms, many of which are approaching the end of their production life or have already entered the decommissioning phase. This thesis assesses the potential of exploiting the low-enthalpy geothermal resource available in depleted offshore hydrocarbon reservoirs and investigates the most suitable repurposing pathways.

The analysis first evaluates the geothermal resource available in Italian offshore reservoirs to identify technologies compatible with the expected temperature range. Two categories of applications are considered: Power-to-X, including biological methanation, LOHC hydrogenation and ammonia synthesis, and Seawater-based applications, including reverse osmosis, vacuum thermal distillation, membrane distillation and thermally-assisted fish farming. For each pathway, simplified process models are developed to estimate geothermal heat utilization, energy demand and product output.

Given the multidisciplinary nature of the proposed pathways, a Multi-Criteria Decision Analysis (MCDA) is implemented to compare the alternative scenarios according to technical, structural, logistical, environmental and socio-economic criteria within a common evaluation framework. The robustness of the methodology is assessed through sensitivity analyses involving both criterion weighting and an alternative continuous power supply scenario.

The results show that low-enthalpy geothermal resources are more effectively exploited by processes requiring continuous low-temperature heat, whereas chemical synthesis routes benefit from geothermal energy only during start-up operations, resulting in geothermal resource utilization for less than 5% of the annual operating time. Consequently, Seawater-based pathways achieve significantly higher overall adaptability than Power-to-X alternatives. The proposed methodology provides a systematic framework for supporting future decisions on the sustainable repurposing of decommissioned offshore platforms.

Table of Contents

1 Introduction 1
1.1 Project context 1
1.1.1 Overview of the Italian offshore infrastructure 4
1.1.2 The decommissioning process: challenges and economics 5
1.2 Purpose of the project 6
1.3 Thesis structure 8
2 Geothermal energy 11
2.1 Synergies with the Oil and Gas industry 15
2.2 The Italian geothermal landscape 16
2.2.1 Methodological framework for the realization of the Italian geothermal map 18
2.2.2 Data integration and spatial domain 18
2.2.3 Statistical refinement and practical application 18
2.3 Reservoir characterization 19
2.3.1 Reservoir temperature 21
2.3.2 Geothermal fluid chemistry & scaling mitigation 25
2.4 Technical configurations for geothermal energy recovery 26
2.4.1 Closed-loop geothermal systems 26
2.4.2 Open-loop geothermal systems 27
2.4.3 Comparison in the offshore context 27
2.4.4 Water disposal and reinjection 28
3 Prefeasibility study of reconversion scenarios 33
3.1 Biological methanation 34
3.1.1 Process fundamentals 34
3.1.2 Comparison of process configurations 35
3.1.3 Technical parameters and reactor design 35
3.1.4 Infrastructure and logistics 37
3.1.5 Conclusion 38
3.2 Liquid Organic Hydrogen Carriers (LOHC) system 38
3.2.1 Process fundamentals 38
3.2.2 Dibenzyltoluene (DBT) systems 39
3.2.3 Infrastructure and logistics 41
3.2.4 Thermal integration 41
3.2.5 Conclusion 44

3.3 Ammonia production 44
3.3.1 Process fundamentals 44
3.3.2 Comparison between different exothermic reactions 45
3.4 Reverse Osmosis (RO) desalination 45
3.4.1 Theoretical background 45
3.4.2 Process phases 46
3.4.3 Criticalities 47
3.4.4 Role of geothermal energy in Reverse Osmosis 47
3.5 Advanced thermal desalination scenarios 48
3.5.1 Energy requirements 48
3.5.2 Selection criteria for geothermal integration 49
3.5.3 The industrial benchmark: Vacuum Thermal Distillation (VTD) 50
3.5.4 The innovative frontier: Membrane Distillation (MD) 52
3.5.5 Comparative analysis 55
3.6 Geothermal-assisted aquaculture 57
3.6.1 Aquaculture for fish production 57
3.6.2 The role of geothermal energy and fish biology 58
3.6.3 Infrastructure, logistics and the Italian context 59
3.6.4 Environmental impact and mitigation 60
3.6.5 Seawood cultivation 61
3.7 Repurposing for artificial reefs 61
3.7.1 Different modes of artificial reef creation 62
3.7.2 The Gulf of Mexico and California cases 63
3.7.3 The Italian example: the Paguro wreck 63
3.8 Multi-Use Platforms Approach 64
3.8.1 Potential offshore energy resources 64
3.8.2 Mineral extraction from brine 65
3.8.3 Example of MUP starting from the proposed scenario 65
3.9 Summary of pre-feasibility scenarios for platform repurposing 66
4 Thermodynamic performance and energy assessment of reconversion scenarios 69
4.1 Definition of the project framework and constraints 69
4.2 Energy and mass balances for chemical synthesis scenarios 71
4.2.1 Thermodynamic and technical feasibility of Biological Methanation 72
4.2.2 Thermodynamic and technical feasibility of LOHC hydrogenation 76
4.2.3 Thermodynamic and technical feasibility of Ammonia production 79

4.2.4 Final thermodynamic comparison between different exothermic reactions 84
4.2.5 Energy analysis and operating scenarios 85
4.2.6 Exploitation and strategic role of the geothermal source 89
4.3 Energy and mass balances for seawater-based pathways 91
4.3.1 Thermodynamic and technical feasibility of Reverse Osmosis 92
4.3.2 Thermodynamics and technical feasibility of Vacuum Thermal Distillation 93
4.3.3 Thermodynamics and technical feasibility of Membrane Distillation 95
4.3.4 Final thermodynamic comparison between different desalination systems 98
4.3.5 Energy analysis for desalination systems 99
4.3.6 Energy analysis for thermally assisted fish farming 101
5 Guidelines: definition of the methodology 105
5.1 Multi-Criteria Decision Analysis (MCDA) 106
5.1.1 Advantages and disadvantages of multi-criteria analysis 106
5.2 Weighted Sum Method (WSM) 107
5.3 Guideline analysis procedure 108
5.3.1 Definition of criteria 109
5.3.2 Definition of the importance of each criterion 110
5.3.3 Attribution of an index to each criterion 111
5.3.4 Assigning weight to each criterion 114
5.3.5 Allocation of weights and indices 114
5.3.6 Elaboration of the results 115
6 Elaboration of the final results 119
6.1 Base Case results 119
6.2 Sensitivity analysis: Equal Weights Scenario 121
6.3 Sensitivity analysis: Intermittent vs Continuous Supply 122
7 Conclusion 125
7.1 Critical engineering assessment 125
7.2 Future developments 127
Bibliography 129
Acknowledgments 137

List of Figures

Figure 1: Scheme of major offshore platform [4] 3
Figure 2: Annual offshore natural gas production (2015-2019) [8] 5
Figure 3: Capacity factor (in percent) ranges reported for various renewable energy sources [14] 12
Figure 4: Shares of clean energy technologies in total energy demand, 2023 13
Figure 5: Geothermal Heat Flow Map of Italy 17
Figure 6: Gas, oil and water distribution in an O&G reservoir 19
Figure 7: Temperature-Depth plot 23
Figure 8: Distribution of platforms by geothermal heat potential 24
Figure 9: The continuum of geothermal energy technology applications and uses [28] 24
Figure 10: Illustrations of commonly used closed-loop and open-loop ground heat exchangers [28] 27
Figure 11: Geothermal water disposal [12], AI generated image 31
Figure 12: Configuration of ex-situ trickle bed reactor [30], [32] AI generated image 37
Figure 13: Schematic representation of the LOHC cycle hydrogenation (a) and dehydrogenation (b) [34] 39
Figure 14: Schematic layout of a modular Fixed-Bed Reactor for DBT hydrogenation [34][35][37][38] AI generated image 40
Figure 15: Heat pump theoretical operation cycle in heating mode [41] 43
Figure 16: Schematic of (a) osmosis (b) osmotic equilibrium (c) RO [45] 46
Figure 17: Specific energy consumption for thermal and membrane desalination processes and greenhouse gas emissions for unit freshwater production [14] 48
Figure 18: Production capacity of the desalination units as a function of the heating medium inlet temperature [47] 51
Figure 19: Internal configuration of the Alfa Laval AQUA Blue plate pack [47] 51
Figure 20: External configuration of the Alfa Laval AQUA Blue plate pack [47] 52
Figure 21: Membrane Distillation principles [49] 53
Figure 22: VMD configuration [49] 54
Figure 23: Offshore platform artificial reef conversion methods [64], AI generated image 62
Figure 24: Overall block diagram of the platform plant configuration 70
Figure 25: Simplified process flow diagram of the biological methanation scenario 74
Figure 26: LOHC hydrogenation simplified process flow diagram 77

Figure 27: NH_3 production simplified process flow diagram.....80
Figure 28: Representation of the two main operational phases of the plant.....87
Figure 29: Comparison of nominal thermal power capacities (heating demand vs. exothermic heat production) for the three synthesis pathways under steady-state conditions.....89
Figure 30: Total annual thermal energy produced by the exothermic reactions – comparison between Case 1 (intermittent supply) and Case 2 (continuous supply).....90
Figure 31: Annual thermal energy required for transient start-up phases across the three chemical technologies under Case 1 operating conditions.....91
Figure 32: Total annual thermal energy required by the desalinations units: comparison between Case 1 (intermittent supply) and Case 2 (continuous supply).....100
Figure 33: Working methodology for MCDA.....106
Figure 34: Adaptability percentage of different scenarios 120
Figure 35: Sensitivity analysis – Comparison between Simos Weights and Equal Weights Scenario 121
Figure 36: Sensitivity analysis – Comparison between intermittent and continuous supply .124

List of Tables

Table 1: Difference between formation and produced water 20
Table 2: Comparison between biological and chemical methanation [30] 34
Table 3: Comparison reaction enthalpies and specific waste heat production for different exothermic synthesis processes 45
Table 4: Comparison between different technologies for thermal distillation 56
Table 5: Quantitative summary of the mass, thermal, and electrical results for the biologic methanation system 75
Table 6: Quantitative summary of the mass, thermal, and electrical results for the LOHC (DBT) hydrogenation system 78
Table 7: Outlet temperatures and thermal cooling duties for each compression stage 81
Table 8: Quantitative summary of the mass, thermal, and electrical results for the ammonia synthesis using Haber Bosch process 82
Table 9: Thermodynamic and electrical utility requirements for the analysed Power-to-X technologies (referenced to a baseline H_2 flow rate of 9.09 kg/h) 84
Table 10: Operational times of Case 1 and Case 2 88
Table 11: Integrated annual mass and energy balances for biological methanation, LOHC hydrogenation, and ammonia synthesis under Case 1 (intermittent supply) and Case 2 (continuous supply) operating conditions. 88
Table 12: Quantitative mass, thermal, and electrical metrics for the Reverse Osmosis (RO) desalination system under cold and geothermally-preheated operation 93
Table 13: Thermodynamic and electrical utility requirements for the analysed desalination technologies (referenced to a baseline permeate production flow rate of 310 kg/h) 99
Table 14: Integrated annual mass and energy balances for geothermal optimized Reverse Osmosis, Vacuum Thermal Distillation, and membrane distillation under Case 1 (intermittent supply) and Case 2 (continuous supply) operating conditions 100
Table 15: Daily electrical demand breakdown and operational assumptions for a 10-cage thermally assisted fish farming module (adapted from [58]) 102
Table 16: Evaluation matrix 107
Table 17: Binding criteria 110
Table 18: Multi-criteria evaluation matrix and boundary conditions for index assignment 112
Table 19: Weight assigned to each macro-category 114
Table 20: Results obtained from the evaluation matrix 116

1 Introduction

1.1 Project context

This research involves studying the conversion of offshore oil and gas production platforms that have reached the end of their lifespan due to the depletion of the reservoir on which they operate, identifying their alternative uses to support the ongoing energy transition.

In recent years, several reconversion alternatives have been evaluated for Italian offshore platforms. The main options include renewable energy production, aquaculture and marine laboratories and the use of depleted reservoir as storage systems [1].

In particular, a strategic collaboration between the Politecnico of Torino and the Italian Ministry of Environment and Energy Security (MASE), led to the detailed assessment of three main repurposing options. All these options have the purpose of valorising the existing structures, reducing the environmental impacts and the costs linked to the complete decommissioning of offshore structures [2]:

- Option 1 – **Photovoltaic Power Generation and Desalination**: this configuration involves the installation of a photovoltaic (PV) plant on the platform deck to feed a desalinization system of sea water based on Reverse Osmosis (RO). The objective is the production of freshwater that can be distributed to nearby maritime facilities or sent onshore for civil or industrial purposes.

- Option 2 – **Seasonal Energy Storage (CH_4/H_2 mixture)**: this variant explores reusing the platform and its wells for the injection of a blend, typically composed of 90% Natural Gas (CH_4) and 10% Hydrogen (H_2), into the depleted reservoir. The system acts as seasonal storage hub, absorbing the mixture from the national grid and releasing it during peak demand periods.

- Option 3 – **Permanent Carbon Capture and Storage (CCS)**: this scenario converts the facility into a CO_2 injection station. Carbon dioxide, captured from industrial clusters, is

injected into the underlying geological formations for permanent sequestration, followed by a rigorous long-term monitoring phase.

In this research another option (Option 4) that involves the exploitation of the geothermal potential of the reservoir will be analysed. For geothermal energy, a large portion of the implementation cost comes from drilling [3]. Thus, research efforts to repurpose oil and gas wells to geothermal wells are increasing.

Various types of offshore installations are present in the Italian seas, particularly in the Adriatic area. These structures can be classified primarily based on their structural complexity [2]:

- Mono-tubular and bi-tubular platforms: characterized by one or two main steel columns driven into the seabed supporting a small topside deck. They typically feature an emerged surface area of less than 100 m^2 (with a few exceptions, such as the *Davide* platform at 252 m^2 and *Guendalina* at 270 m^2).

- Reticular-structure (jacket) platforms: characterized by a lattice frame structure and a significantly larger deck area, which allows for the installation of surface equipment and processing facilities.

- Subsea wellheads: underwater wellhead systems installed directly on the seabed without any emerged surface structure.

- Platform clusters: groups of operating within the same offshore field, where a primary host platform can serve neighbouring facilities via subsea umbilicals and pipelines.

For the purposes of this preliminary study, all marine infrastructures are evaluated independently of their surface area.

In order to better explain and understand the various decommissioning options, a general scheme of a typical platform structure is reported in Figure 1.

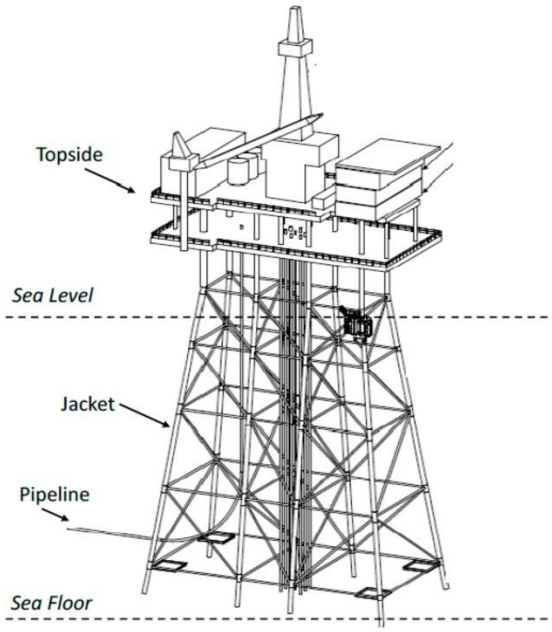


Figure 1: Scheme of major offshore platform [4]

An offshore platform operates over a specific hydrocarbon field; however, its multiple production or injection wells are frequently completed across different geological layers and strata within the reservoir, thereby tapping into distinct temperature and pressure gradients. Depending on the asset architecture, a typical offshore platform can be composed of [4]:

- a topside, the above-water structure, including oil and gas processing equipment, where the offshore activities take place, including drilling rigs, helidecks, cranes;
- a jacket, which supports the topside and is composed of the parts of the structure that are anchored in the bottom;
- footings, the lowest and heaviest section of the jacket, which include pile clusters to aid piling of the structure into the seabed, and a drilling template, through which the wells are drilled;
- a pile of drill cuttings consisting of drilled rock particles and drilling fluids arising from drilling the wells;
- pipelines and subsea lines, traditionally used for the export of oil and gas, which may also include electrical power cables and umbilicals for power transmission with the mainland or other facilities.

Furthermore, offshore assets do not always operate in isolation; while some platforms are standalone units, they are frequently arranged in interconnected clusters, linked to one another via complex networks of subsea pipelines and power lines to optimize production and logistics.

1.1.1 Overview of the Italian offshore infrastructure

According to official reports from the Italian Ministry of Environment and Energy Security (MASE) [5], the Italian offshore landscape comprises 139 structures (Status as of December 31, 2025). Based on their type and use, they are divided into:

- 109 production units (including 15 subsea wellheads);
- 10 production support platforms (compression or connection);
- 20 non-operational structures, 16 of them are awaiting decommissioning.

As specified in the Ministerial Press Release of June 30, 2026 [6], 15 of the inactive structures are slated for total removal without the possibility of repurposing. To date, only two platforms (SQUALO and PENNINA) have been officially designated for reuse in non-hydrocarbon activities [6]. It is crucial to note that for many platforms awaiting decommissioning, the mineral closure (plug and abandonment) procedures have already been initiated, effectively precluding any further exploitation of the reservoir for storage or geothermal purposes.

Considering that the standard operational lifespan of an Offshore Oil & Gas Platform (OOGP) ranges between 30 and 40 years [7], and given that the average installation year for Italian facilities is 1990 [5], a significant number of structures will require critical assessment and potential intervention within the 2020–2030 decade.

To fully understand the current status of the Italian offshore network, it is essential to analyse its recent production trends. As illustrated in Figure 2, the annual offshore natural gas production in Italy has experienced a progressive and significant decline over the last decade (2015–2025), dropping from approximately $4.5 \cdot 10^9\ Smc$ in 2015 to below $2.0 \cdot 10^9\ Smc$ in recent years.

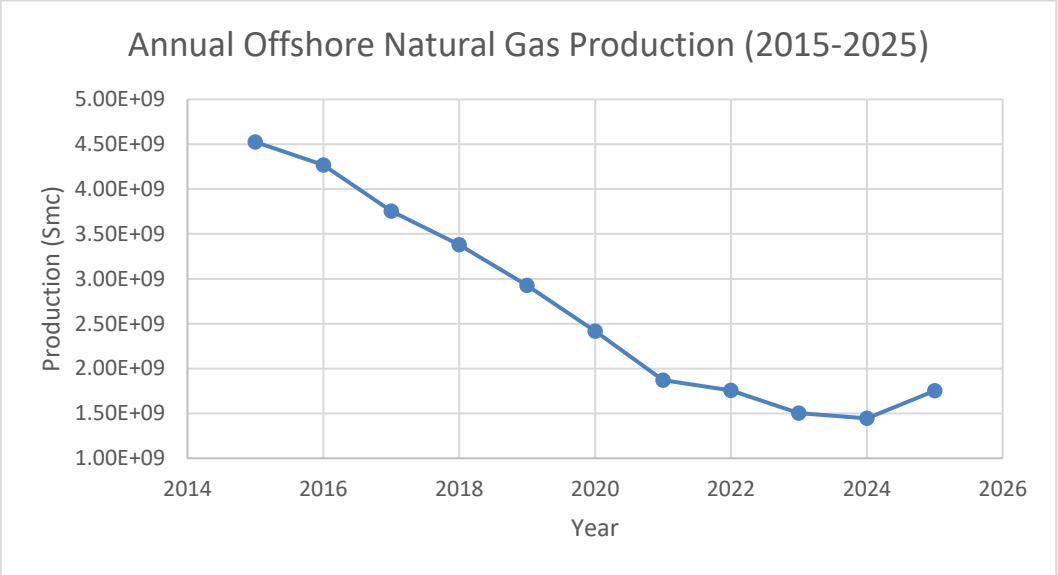


Figure 2: Annual offshore natural gas production (2015-2019) [8]

This downward trend is driven by two main factors: the natural depletion of historical marine reservoirs and a strategic shift in national energy policies. In accordance with European decarbonization goals, Italy has steadily oriented its long-term strategies toward the energy transition, discouraging the development of new fossil fuel extractions while promoting green alternatives. However, this steady decline in gas production brings to light a critical industrial challenge: a massive number of offshore platforms are reaching the end of their economic life, transitioning into an idle or depleted status. This industrial shift underscores the significance of the present research; rather than viewing asset depletion as a liability, this work investigates how these declining infrastructures can be repurposed into valuable hubs for low-carbon energy transition.

1.1.2 The decommissioning process: challenges and economics

Decommissioning is the final step of life cycle of asset belonging to Oil & Gas sector and, in general, of industrial plants. It's necessary to consider it as fundamental part of investment process and it can have important economic, social, and environmental implications in the context in which it's realized. In recent years, the interest of stakeholders in decommissioning has progressively increased. The goal is to make the system efficient based on circular economy and sustainability concepts.

While the Oil & Gas sector currently dominates the decommissioning landscape, it is not the only industry affected. With the rapid expansion of offshore wind energy, decommissioning activities will increasingly involve renewable energy infrastructures. Every offshore infrastructure is characterized by a specific design life. Upon reaching the end of this nominal operational period, a structural integrity assessment can determine whether a life extension is technically feasible.

For Oil & Gas offshore platform, the process is inherently complex, far exceeding a simple "reversal" of the installation phase. Over decades, these structures facilitate the development of complex marine ecosystems (such as artificial reefs) that must be carefully managed. Due to the relative novelty of the decommissioning industry, assessing costs, durations, and operational scopes remains challenging due to limited historical benchmarks.

The Bureau of Safety and Environmental Enforcement (BSEE) [9] has monitored decommissioning expenditure data from operators in the US Gulf of Mexico since 2016 to estimate federal decommissioning liabilities. Fixed platform removals are expected to cost on average $977,000 in shallow water (depth < 30 m) rising to $3.6 million for depths between 61 and 122 m. However, it must be emphasized that over the past decade, severe macroeconomic inflation, supply chain constraints, and rising vessel charter rates in the offshore sector have caused real-world decommissioning costs to escalate significantly worldwide. While these costs serve as global indicators, the shallow bathymetry of the Adriatic Sea suggests that costs for the Italian platforms may be lower than those recorded in deepwater environments yet still represent a significant financial burden for operators.

1.2 Purpose of the project

The primary objective of this thesis is to evaluate whether end-of-life offshore oil and gas facilities can represent a strategic potential for harvesting the geothermal energy trapped within depleted hydrocarbon reservoirs. This research first aims to determine the technical feasibility of exploiting these structures as geothermal assets, identifying the most suitable industrial end-uses based on reservoir thermal characteristics and localized low-enthalpy gradients. Subsequently, the thesis evaluates and compares different technological configurations to determine their practical integration, deployment maturity, and overall adaptability within the

Mediterranean context. To achieve this, the research is structured around the following specific objectives:

- **Assessment of offshore geothermal potential**: to evaluate the low-enthalpy geothermal energy available in Italian offshore fields, cross-referencing subsoil data with the location of existing production platforms.

- **Identification of suitable technologies**: to screen and identify surface technologies (e.g., energy vectors production, membrane distillation, aquaculture) capable of efficiently exploiting low-temperature geothermal fluids, while ensuring strict compatibility with the demanding offshore environment and the severe spatial and footprint constraints typical of these marine infrastructures.

- **Quantification of energy capabilities**: to estimate the thermal and electrical needs, the available geothermal power, and mass flow rates of harvestable geofluid for each scenario, thereby assessing whether the projected energy yield justifies the required technical deployment or if the practical utility remains negligible.

- **Development of a multi-criteria decision framework**: to implement a rigorous engineering methodology for ranking and selecting the optimal technology tailored to offshore constraints, explicitly evaluating whether the technical and economic effort of retrofitting is balanced by real-world operational benefits.

As highlighted in the IEA Geothermal Report 2024 [10], the oil and gas industry could play a central role in accelerating geothermal development. This sector has extensive know-how in handling liquids and gases, large financial resources, substantial research and development expertise, technical and operational knowledge, and proficiency in executing and managing large, capital-intensive projects. Applying the oil and gas industry's expertise and resources more widely to geothermal technologies could therefore expand their potential and reduce their costs significantly. Consequently, the synergy between the Oil & Gas and geothermal industries – which serves as the starting point for this research – is a subject of increasing international relevance, further validating the coherence of this study. Moreover, the repurposing of abandoned wells avoids the prohibitive upfront drilling costs and the risks associated

with non-transmissive reservoirs, which currently represent major obstacles to geothermal expansion. In geothermal engineering, reservoir transmissivity defines the ability of the formation to transmit fluids. High upfront investments in new wells carry the risk of targeting formations with insufficient permeability or thickness, leading to inadequate fluid flow rates. Utilizing existing operational data from oil and gas wells eliminates this subsurface uncertainty, as the hydraulic connectivity of the reservoir has already been proven during past production phases.

The geothermal potential in Italy has already been extensively evaluated, with key findings published in the study *"Looking forward to a decarbonized era: Geothermal potential assessment for oil & gas fields in Italy"* [11]. The primary distinction between that work and the current study lies in the exclusion of offshore reservoirs in the former, driven by the limited feasibility of direct heat exploitation at sea. Indeed, focusing on onshore wells aligned with their objective of assessing direct thermal applications – such as district heating or agricultural use (e.g., greenhouses) – which inherently require close proximity to mainland urban centres or industrial hubs. Interestingly, the main technical challenges identified for onshore repurposing closely parallel those encountered offshore, specifically regarding reservoir characterization, data uncertainty, and the optimization of existing infrastructures.

1.3 Thesis structure

To address the challenge of offshore platform decommissioning through geothermal repurposing, this thesis unfolds as a progressive engineering evaluation – moving from foundational geological and technical constraints to quantitative thermodynamic modelling, ultimately culminating in a multi-criteria decision framework.

The work is structured as follows:

- Chapter 2 **("Geothermal energy")** establishes the physical and geographical boundary conditions of the study. It provides a comprehensive overview of geothermal system configurations, evaluates the synergies between the Oil & Gas sector and geothermal exploitation, and characterizes the Italian offshore geothermal landscape – specifically defining target reservoir temperatures and hydrochemical conditions.

- Chapter 3 **("Prefeasibility study of reconversion scenarios")** builds upon these baseline boundary conditions by performing a qualitative screening of seven potential platform repurposing pathways. Divided into chemical synthesis processes (Power-to-X), water desalination technologies (Seawater-to-X), and biological applications, this chapter analyses the core chemical/physical processes, equipment requirements, offshore logistical constraints, and safety implications for each candidate scenario.

- Chapter 4 **("Thermodynamic performance and energy assessment of reconversion scenarios")** translates the qualitative concepts from Chapter 3 into rigorous engineering models. By formulating comprehensive mass and energy balances, this chapter quantifies the net energy consumption/production, evaluates thermal integration during steady-state and transient operations, and determines the actual exploitation rate of the available low-enthalpy geothermal source.

- Chapter 5 **("Guidelines: definition of the methodology")** addresses the decision-making challenge arising from the complex trade-offs identified in Chapter 4. It introduces a structured Multi-Criteria Decision Analysis (MCDA) methodology based on the Weighted Sum Method, defining a balanced hierarchy of technical, structural, logistical, economic, and environmental criteria tailored to the offshore environment.

- Chapter 6 **("Elaboration of the final results")** applies the decision-making framework to a specific case study in the Adriatic Sea. It delivers the final adaptability ranking of the seven scenarios and subjects the model to sensitivity analyses – testing the impact of weight distribution and continuous versus intermittent renewable power supply to ensure the robustness of the strategic recommendations.

- Chapter 7 **("Conclusion")** synthesizes the main achievements of the research, highlighting critical technical insights, practical limitations encountered during the study, and pathways for future research.

2 Geothermal energy

This chapter sets the technical and geographical boundary conditions for evaluating geothermal heat recovery in offshore environments. First, Section 2.1 examines the strategic synergies between the Oil & Gas sector and geothermal energy exploitation. Section 2.2 explores the Italian geothermal landscape and presents the methodology used to construct the national geothermal map. In this context, a robust resource assessment must extend beyond broad heat-flow mapping. To establish true engineering feasibility, the assessment framework must integrate deep reservoir temperatures, effective permeability, fluid chemistry and well mechanical conditions. Accordingly, Section 2.3 describes the reservoir characterization framework, providing the mathematical models used to translate surface data into deep reservoir temperatures and hydrochemical conditions. Finally, Section 2.4 introduces the primary technical configurations for geothermal recovery – comparing closed-loop and open-loop systems – establishing the engineering basis for the prefeasibility scenarios analysed in Chapter 3.

Geothermal energy is an important key resource for the global energy transition because it provides baseload electricity generation, heat production and storage. Depending on the enthalpy of the geothermal fluid the thermal energy can either be converted into electricity – typically via Organic Rankine Cycles (ORC) for low-to-medium temperatures – or utilized directly for heat production. Additionally, when integrated into Geothermal Energy Storage (GES) systems, these reservoirs can act as underground thermal batteries, storing excess heat to support grid stability. GES technologies can provide efficient energy solutions for heating and cooling applications [12].

Unlike variable renewable energy (VRE) sources, such as solar and wind, geothermal power plants operate continuously, maintaining maximum capacity during the year. Capacity factor[1] is an important variable to be considered for scalability and operation of a technology. When compared with other renewable energy sources such as solar, wind, and biomass sources, the

[1] Capacity factor: the ratio of the electrical energy produced by a generating unit for the period of time considered to the electrical energy that could have been produced at continuous full power operation during the same period.

capacity factor for geothermal sources is very high. Figure 3 illustrates the capacity factors of different renewable energy sources. The capacity factor for a resource can be influenced by resource availability, processing equipment or transmission variability, and other external factors such as power market fluctuations [13], [14].

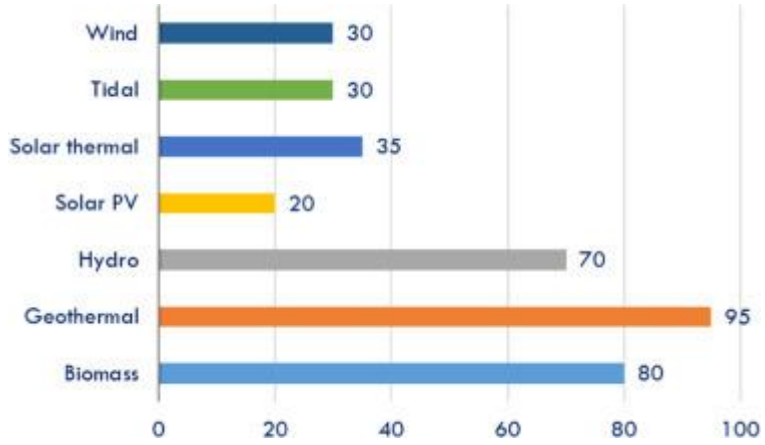


Figure 3: Capacity factor (in percent) ranges reported for various renewable energy sources [14]

From the economic point of view, it is possible to compare different sources of energy to understand which is less expensive by using a parameter called Levelized Cost of Energy (LCOE) that represents the life-cycle cost for each unit of energy produced in the lifetime of a project. From this evaluation for geothermal energy, it emerges that this cost ranging from 40 $/MWh to over 240 $/MWh. Costs are highly dependent on the quality of the geothermal resource (i.e. its depth, temperature and flow rate) and rock permeability. This value exceeds the LCOE of most solar PV and wind installations. However, geothermal power is a dispatchable technology that can provide many additional services to the energy system, which is not captured in the LCOE methodology.

In addition to its stability, geothermal energy is highly dispatchable and helps the resilience of electricity grids by balancing the fluctuations of solar and wind energy. Moreover, geothermal facilities have a relatively small physical footprint per unit of energy generated and show low lifecycle greenhouse gas emissions. Despite these benefits, geothermal is one of the least used clean energy sources (Figure 4), primarily due to high upfront drilling costs, geological risks associated with the exploration phase, and social acceptance challenges [15]. However,

the International Energy Agency (IEA) projects that, with continued technological advancements and cost reductions, geothermal energy could account for up to 15% of the global electricity demand growth by 2050 [13].

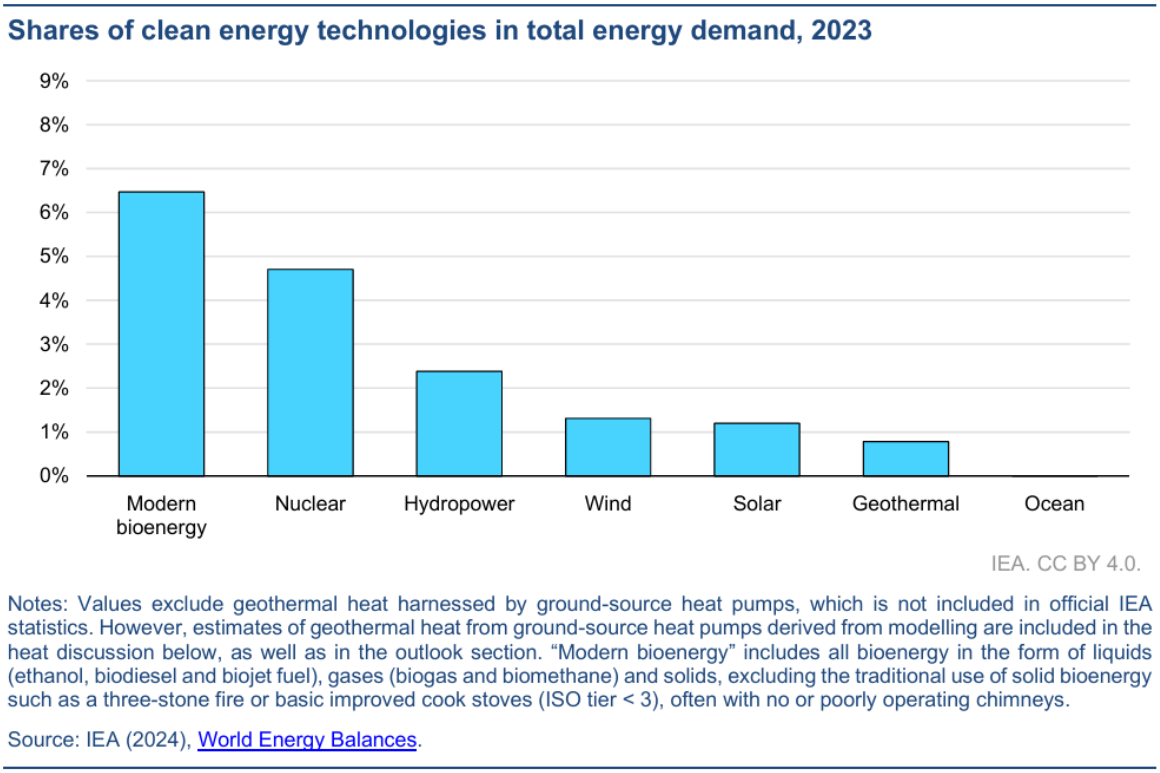


Figure 4: Shares of clean energy technologies in total energy demand, 2023

Historically, geothermal exploitation has focused on high-temperature resources (>180°C) where wells around 1000-2000 m deep are drilled into hot aquifers to produce steam or a two-phase water-steam mixture. These resources are restricted to areas with high thermal gradients at tectonic-plate boundaries (such as the US Geysers, Indonesia, and Iceland) where tectonic deformations provide high permeability. Because these hydrothermal systems are geographically limited and already heavily exploited, the industry is shifting its focus toward low-to-medium temperature systems [3].

These lower-temperature resources are commonly found in deep sedimentary basins, geological formations characterized by thick sequences of sedimentary rocks. Crucially, these basins frequently host mature or depleted hydrocarbon reservoirs. This overlap represents a strategic opportunity for the geothermal sector: the extensive geological data, existing infrastructure,

and operational wells from oil and gas exploitation can be repurposed to extract low-enthalpy geothermal fluids, eliminating exploration risks and upfront drilling costs [16].

Globally, driven by direct-use applications like district heating and industrial processes, the total installed capacity for direct geothermal heat utilization has surpassed 170 GWt, according to the International Geothermal Association (IGA) [17]. The leading nations and regions in this sector include [18]:

- China: the global leader in geothermal direct-use and district heating, with an installed capacity exceeding 40 GWt.

- The United States: featuring approximately 20 GWt of installed capacity. Applications are highly diversified, ranging from geothermal heat pumps to space and greenhouse heating, agricultural drying and animal farming.

- Europe: is one of the leading regions in the direct use of geothermal energy worldwide. With 34 countries reporting geothermal use, Europe accounts for 31.9% of the world's installed capacity (MWt).

    - The Paris Basin *(France):* this area hosts deep aquifers (between 1.5 and 2 km depth), most notably the Dogger formation. It represents one of the largest concentrations of low-enthalpy geothermal operations globally, with dozens of active plants providing heating to approximately 6–7% of the Paris metropolitan area.

    - The Molasse Basin (Germany/Austria): a major European hub for low-enthalpy geothermal energy, powering extensive district heating networks in urban areas such as Munich.

    - National leaders: countries like Sweden (via extensive geothermal heat pump deployment) and Turkey (via direct heating and greenhouse applications) represent the highest statistical shares of geothermal direct utilization in the European region.

2.1 Synergies with the Oil and Gas industry

Approximately 80% of the investment required in a geothermal project involves capacity and skills that are common in the Oil and Gas (O&G) industry [10]. The sector has transferable skills, data, technologies and supply chains that make it central to the prospects for next-generation geothermal.

Diversifying into geothermal energy could be of great benefit to the O&G operators, providing opportunities to develop new business lines in the fast-growing clean energy economy, as well as a hedge against commercial risks arising from projected future declines in fossil fuel demand [13]. International examples, such as the EnergyX project in Norway, demonstrate this trend; leading operators (e.g., TotalEnergies, OMV, and Reelwell) are currently developing solutions to reuse abandoned petroleum wells for heat and electricity production, particularly in sensitive environments like in the high Arctic Archipelago of Svalbard [10].

Indeed, following the closure of the local coal mine in Longyearbyen – the administrative centre and largest settlement in Svalbard – there is an urgent need for a new, reliable energy source. The strategy to identify the best post-coal energy mix aims to maximize the renewable energy share, thereby minimizing carbon emissions. Because Longyearbyen operates an off-grid energy system with no electrical or heating connections to neighbouring communities, diesel has been introduced as a temporary bridge solution. However, the ultimate goal remains the implementation of a fully sustainable energy system by 2030.

In this context, the primary technological solution under investigation is the deployment of an Advanced Closed-Loop system for deep geothermal energy extraction, designed to provide baseload heat and optional electric power to the community [19]. This configuration, which is currently at the stage of a feasibility study, involves the installation of a coaxial Deep Borehole Heat Exchanger (DBHE). At present, the existing onshore petroleum exploration wells are being utilized to derive the thermal properties of the subsurface formations [20].

It is relevant to note that a closed-loop configuration was specifically selected for this Arctic location due to the low probability of encountering a suitable hydrothermal reservoir with sufficient permeability to implement a conventional open-loop geothermal system [19].

Conversely, in the Mediterranean context evaluated in this study, the proven availability of reservoir brine and adequate geological conditions make open-loop configurations far more favourable for maximizing energy recovery.

It must be stressed that platform repurposing is not a universally applicable solution: not every offshore asset is suitable for geothermal conversion. Rather, a successful offshore geothermal assessment must be established at the physical intersection of fluid temperature, reservoir performance, structural well integrity, and platform accessibility [21].

2.2 The Italian geothermal landscape

Italy holds a historic leadership position in geothermal energy, primarily focused on electricity generation. All the operational plants are currently located in Tuscany, in the Larderello – Travale and Mount Amiata fields. At the end of 2022, Italy reached an installed capacity of 915 MWe (with an operational running capacity 774 MWe) producing approximately 6 TWh per year, representing 2.1% of the total domestic generation, and meeting more than 30% of the electricity demand in the Tuscany region [10].

In addition to power generation, geothermal fluids are used as heat sources directly, mainly for spas, space and district heating, greenhouses and aquaculture. In 2020, the direct use capacity was estimated at 1316 MWth with annual thermal energy supply totalling some 9.7 PJ [10].

This section explores the regional distribution of geothermal resources across the Italian territory, aiming to cross-reference subsurface thermal data with the locations of existing offshore hydrocarbon platforms to identify the most suitable assets for reconversion.

The primary indicator used to define the geothermal potential of an area is the **heat flow**. It is defined as the amount of thermal energy escaping from the Earth's interior to the surface per unit area and measured in milliwatts per square meter (mW/m^2). As illustrated in the map in Figure 5, the Italian offshore presents significant thermal heterogeneity. Notably, the Adriatic Sea is characterized by a low heat flow, with values generally remaining below $40 - 60 \frac{mW}{m^2}$. Consider that large parts of Tuscany and Latium, are affected by regional anomaly and the average heat flow is $80 \frac{mW}{m^2}$ but it may locally rise up to $200 - 400 \frac{mW}{m^2}$ [22].

This thermal depression is primarily a consequence of the geological history of the Adriatic foredeep belt, which encompasses the Po Plain and the Adriatic and Southern Apennines troughs. This region has been affected by rapid and intense sediment deposition during recent geological eras, which acted as a thermal blanket, temporarily lowering the shallow heat flow values [23].

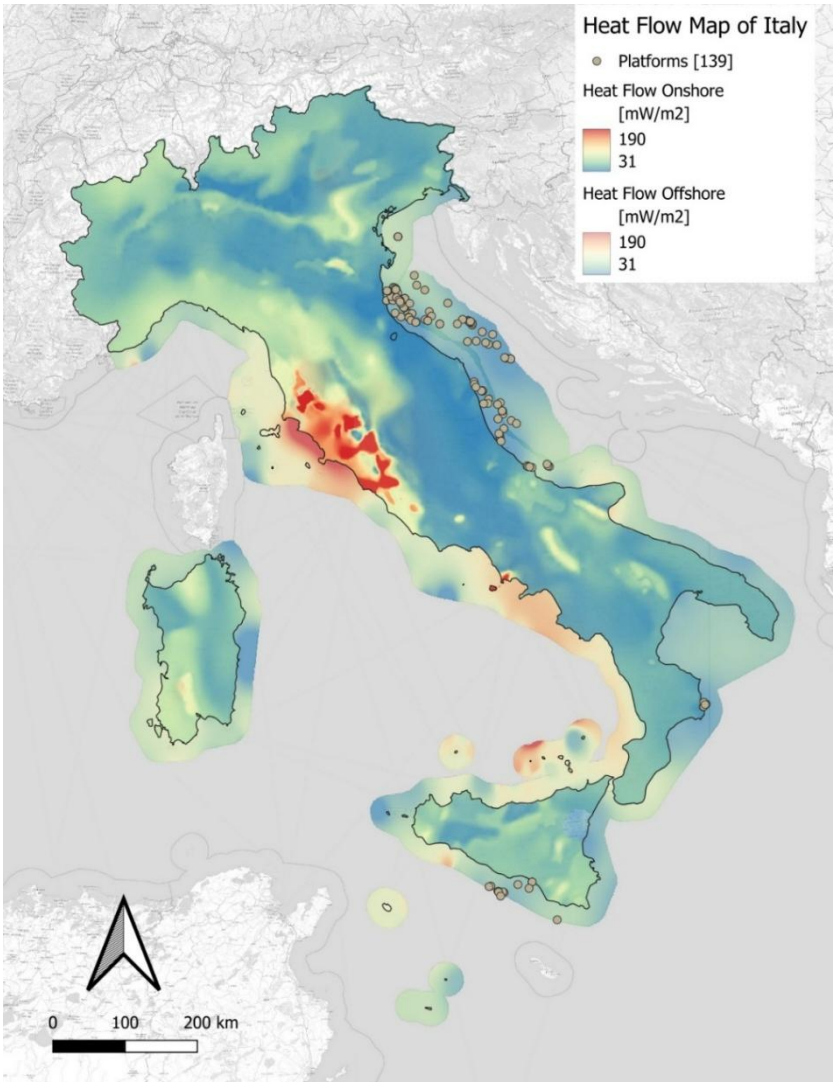


Figure 5: Geothermal Heat Flow Map of Italy

However, a critical paradox emerges when cross-referencing this thermal data with the industrial landscape: while the Adriatic Sea displays the lowest heat flow regional values, it simultaneously hosts the highest concentration of offshore platforms in Italy. Starting from this geological constraint, the engineering challenge of this study is to turn a low-potential scenario into a viable opportunity by identifying surface reconversion solutions capable of maximizing energy recovery from the area.

To address this challenge, the following subsections will present the step-by-step methodology used to construct the Italian geothermal map (Sections 2.2.1 through 2.2.3), detailing the data integration and statistical refinement required to bridge the gap between macro-regional data and asset-specific applications.

2.2.1 Methodological framework for the realization of the Italian geothermal map

The spatial distribution of geothermal resources was modelled using QGIS 3.40.4 to establish a robust analytical baseline for the project. In this study, the geothermal map is not merely a representational tool but the essential starting point for estimating the reservoir temperature ($T_{reservoir}$) at the specific depth of each offshore platform. This thermal characterization is critical as the available temperature dictates the technical feasibility and the efficiency of the different technological scenarios proposed for platform repurposing.

2.2.2 Data integration and spatial domain

The construction of the heat flow map integrated two distinct datasets to ensure a continuous analysis across both terrestrial and marine domains. Initially, high-resolution data from the MASE (Italian Ministry of Environment and Energy Security) were utilized for the Italian onshore territory, including the mainland and the major islands (Sicily and Sardinia) [24]. However, since the core objective of this research is to evaluate the conversion of offshore assets located in the Mediterranean seas, these subaerial data were integrated with a Global Heat Flow Database to extend the thermal characterization to the marine basins [25]. As expected, a discrepancy in data density was observed: the onshore representation exhibits higher spatial precision, while the offshore map relies on the interpolation of marine measurement points.

2.2.3 Statistical refinement and practical application

To enhance the legibility of the regional thermal trends, a 2%-98% Cumulative Count Cut was applied, filtering out isolated anomalies to define a more representative range between 31 and 190 $\frac{mW}{m^2}$. This refined heat flow dataset allows for the subsequent calculation of the geothermal gradient. By crossing these data with the depth of the wells and the thermal conductivity of the subsoil, it becomes possible to estimate the reservoir temperature. This final parameter ultimately serves as the primary selection criterion for identifying the most suitable technology for each specific offshore site.

2.3 Reservoir characterization

While macro-regional mapping identifies areas of geothermal interest, fluid extraction requires a high-resolution understanding of the target formation. This section details the reservoir characterization framework, examining the key hydrodynamic, thermal, and chemical properties – such as porosity, permeability, temperature, and fluid salinity – that dictate the actual energy capacity of the subsurface and its chemical compatibility with engineering materials.

In geology, a reservoir is a subsurface body of rock having sufficient porosity and permeability to store and transmit fluids. Commonly, reservoirs exhibit a stratification of gas, oil, and water (moving from top to bottom) (Figure 6). The majority of Italian reservoirs are gaseous hydrocarbon deposits [5]; therefore, the water is located immediately below the gas zone.

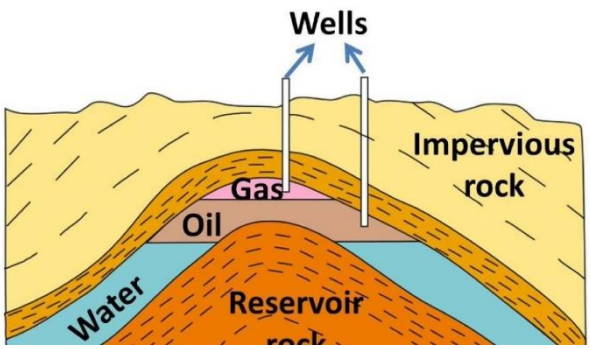


Figure 6: Gas, oil and water distribution in an O&G reservoir

The main parameters to consider for a reservoir are:

- **Porosity**: the percentage of pore volume or void space within a rock that can contain fluids [26]. It is calculated as the ratio of pore volume to total bulk volume:

$$n = \frac{V_{void}}{V_{tot}} \cdot 100 \quad [\%]$$

  It's possible to distinguish between primary and secondary porosity depending on the nature of the space between the grains: the former is a relic of deposition (the space between grains that were not completely compacted), while the latter develops through the subsequent alteration of the rock.

  For geothermal purposes, the reference is usually effective porosity, which is the interconnected pore volume that contributes to fluid flow, excluding isolated pores. In simple terms, the porosity of a rock is a measure of its ability to hold a fluid.

- **Permeability**: a measure of rock's ability to transmit fluids, typically measured in darcies or millidarcies [26]. It's possible to distinguish between absolute permeability measured when a single fluid (or phase) is present and effective permeability, which is the ability to preferentially transmit a particular fluid when other immiscible fluids are present (for example, the effective permeability of gas in a gas-water reservoir).

In the context of geothermal repurposing, it is necessary to distinguish between **Formation Water** and **Oilfield Produced Water (OFPW)**. According to the Schlumberger Energy Glossary [26], formation water is the water that occurs naturally within the pores of rock. Formation water, or interstitial water, might not have been the water present when the rock originally formed. In contrast, connate water is water trapped in the pores of a rock during its original formation, and it's often called "fossil water".

On the other side, Oilfield Produced Water is a combination of underground water from the underground formation, chemicals used during drilling and production operations, and potentially rainwater accumulated at the production sites [27].

The table below summarizes the main differences:

Table 1: Difference between formation and produced water

Concept	Core definition	Reference context
Formation water	Water naturally present in rock pores from geological times	Studied to understand reservoir properties (salinity, pressure, temperature, resistivity)
Produced water	The fluid that reaches the surface	Includes formation water and chemical additives

In simple terms, formation water is the starting point, which becomes produced water after interacting with substances and equipment during extraction. For this study, the latter is more relevant as it is the fluid that reaches the platform and can cause problems such as scaling, fouling, and clogging.

Chemical and physical data, related to the water allows the estimation of the type and intensity of corrosion of equipment and to establish the possibility of formation of dangerous incrustations. It's possible in this way to act with chemicals or physical treatments in the well and eventually to substitute production equipment with a more adapted one.

Another important parameter is **salinity**. Initially, this value can be estimated qualitatively using the concept of resistivity. Before the production phase, logging methods estimate reservoir stratification based on the resistivity of different fluids. Oil and gas have low electrical conductivity and thus high resistivity. For water, resistivity depends on salinity: a high salt concentration results in low resistivity. For more precise chemical characterization, it is necessary to rely on data from physical water sampling.

Finally, during the abstraction phase, it's necessary to know the reservoir pressure to quantify the electrical consumptions of the pumps used for artificial lift. Reservoir pressure is the pressure of fluids within the pores, usually hydrostatic (the pressure exerted by a column of water from the formation's depth to sea level). Because reservoir pressure changes as fluids are produced, it should be described as measured at a specific time (e.g. initial reservoir pressure). If a reservoir is depleted after years of gas extraction, pumps are required to extract the water.

2.3.1 Reservoir temperature

The temperature of the reservoir plays a fundamental role in selecting the most suitable technology for the platform's repurposing.

The temperature in the Earth's crust increases with depth due to the conductive heat flux originating from the Earth's core and directed toward the surface. The Fourier's law for heat conduction fixes that with the increasing of the depth, the temperature typically increases in a range between 15 and 50°C/km in the first 3 km of the crust. This variation is known as the geothermal gradient. Below a depth of approximately 15 m from the seabed, the temperature is no longer influenced by seasonal atmospheric fluctuations and, at around 15 m, it's constant and equal to the average annual value of the reference site and then starts to increase downwards. The temperature at a specific depth (z) can be calculated as follows:

$$T(z) = T_{seabed} + \frac{q}{\lambda} z$$

Where:

- T_{seabed} : average seabed temperature, assumed to be 15°C (consistent with the Mediterranean annual average [2]).
- q : geothermal heat flow (W/m^2).

- λ : thermal conductivity of the reservoir $(W/m \cdot K)$.
- z : vertical distance from the seabed to the target depth (m).

Defining a unique value for thermal conductivity in the Adriatic Sea is challenging, since the subsoil is composed of several overlapping layers that have different thickness and thermal properties. For this preliminary study, the representative average values of thermal conductivity $\lambda = 2.2\ \frac{W}{m \cdot K}$ and depth $z = 2000\ m$ were assumed. The average thermal conductivity was estimated based on lithostratigraphic descriptions of the Central-Northern Adriatic foreland [23], which is dominated by water-saturated siliciclastic sediments (clays and sands). Since these reservoirs have already undergone extensive exploration before commercial exploitation detailed information is typically available within the operator's internal databases. Consequently, for any future site-specific development, these preliminary assumptions can be replaced with precise local measurements or with the actual Bottom Hole Temperature (BHT).

To translate these regional surface heat flow data into operational subsurface insights, the thermal gradient must be evaluated as a function of depth. Figure 7 illustrates the temperature-depth profile modelled for the target offshore area. To ensure a representative yet computationally efficient evaluation of the entire asset cluster, the local heat flow was computed as the arithmetic mean of the individual heat flow values extracted beneath each platform. This averaged heat flow establishes a generalized geothermal baseline, allowing for a preliminary estimation of reservoir temperatures at various target operational depths.

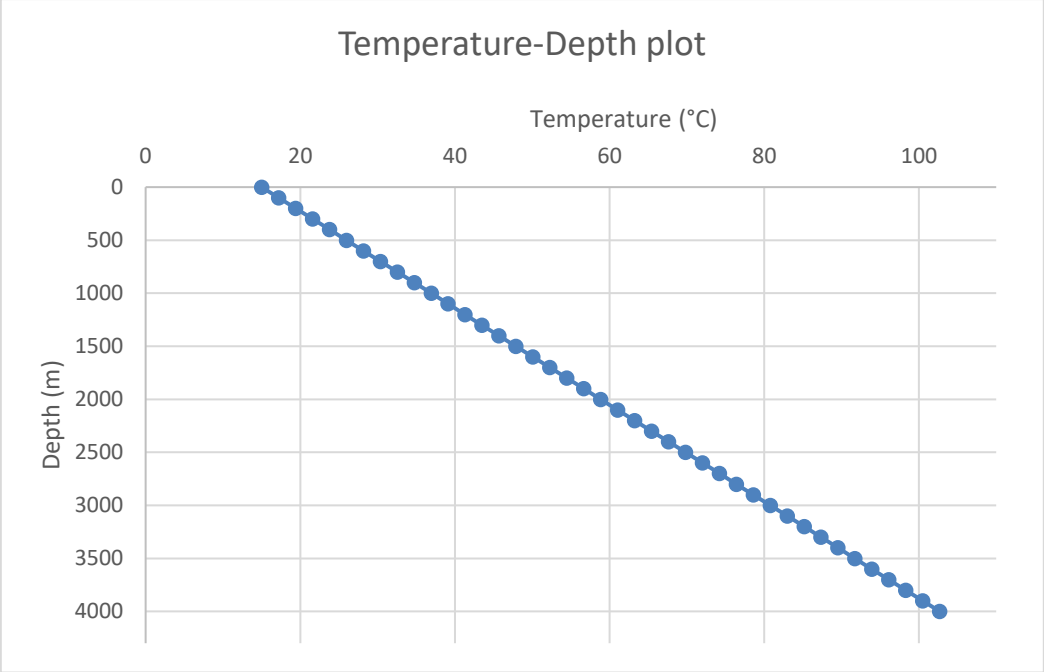


Figure 7: Temperature-Depth plot

For a geothermal reservoir this general classification depending on its temperature is valid [12]:

$$\begin{cases} \text{Low enthaply} \rightarrow T < 90°C \\ \text{Medium enthalphy} \rightarrow 90°C < T < 150°C \\ \text{High enthalpy} \rightarrow T > 150°C \end{cases}$$

By analysing the 139 offshore structures in the Mediterranean Sea, it was observed that most reservoirs exhibit temperatures ranging from 47°C to 67°C. According to the general geothermal classification, these reservoirs are categorized as low-enthalpy resources (temperatures lower than 90°C). Further details can be found in the figure below (Figure 8).

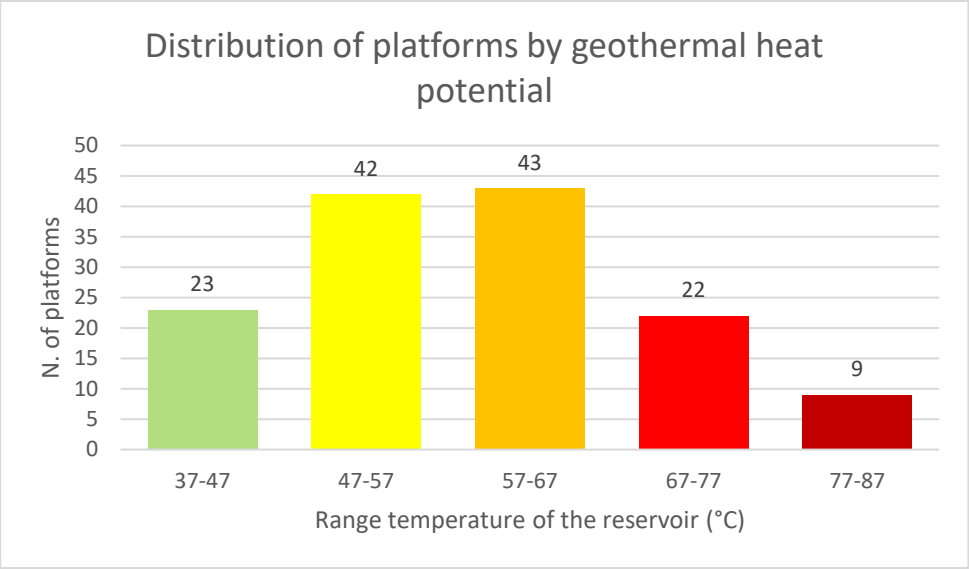


Figure 8: Distribution of platforms by geothermal heat potential

As shown in the Lindal Diagram (Figure 9), the most efficient way to exploit this thermal energy is through direct use. In the following chapter, several scenarios will be analysed, focusing on the specific constraints of the offshore environment.

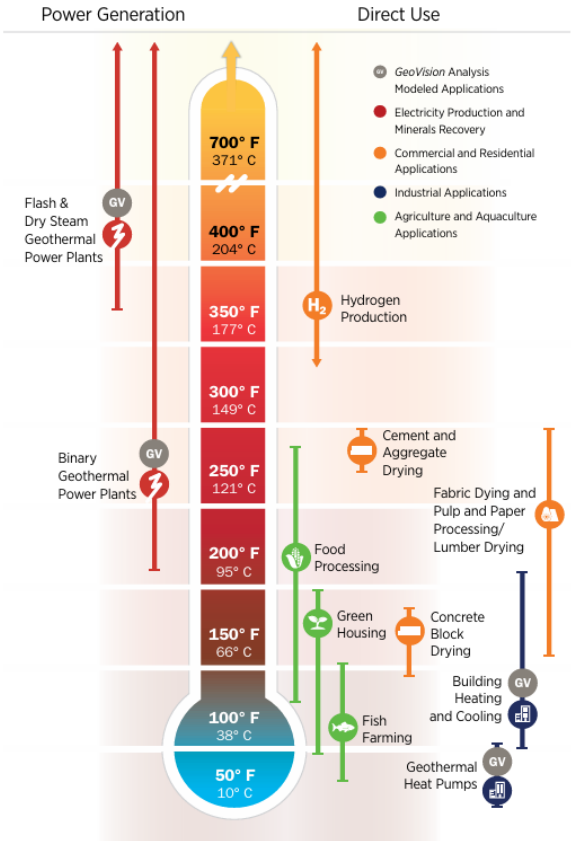


Figure 9: The continuum of geothermal energy technology applications and uses [28]

2.3.2 Geothermal fluid chemistry & scaling mitigation

Geothermal water composition is characterized by the macro-elements of the reservoir rock and the subsurface environment to which it is exposed over geological time. The most frequently observed elements with high concentrations are $Na^+, K^+, Ca^{2+}, Mg^{2+}, HCO_3^-$, CO_3^{2-}, SO_4^{2-}, and CO_2. Other micropollutants may include heavy metals such as mercury, copper, lead, silver, iron, zinc, arsenic, manganese, chromium, beryllium, selenium, vanadium, cadmium, nickel, strontium, uranium, cobalt, gallium, and antimony. Additionally, elements like Boron, and Silica may be present in geothermal waters. High concentrations of Silica are particularly problematic as they can lead to the formation of deposits that block the pipelines responsible for water transport. Moreover, dissolved gases are present in the water, and their concentration can be affected by various factors such as temperature or pressure [14].

Scaling from geothermal fluids has been recognized as a major obstacle in the development of geothermal energy [29]. The term "scaling" or scale formation is commonly used when the precipitate forms a hard deposit. The formation of scale on equipment surfaces exposed to geothermal fluids can have serious economic consequences, arising from energy losses, increased capital costs due to equipment oversizing, higher pumping costs, and increased expenses for cleaning and maintenance. In severe cases, it can lead to a loss of production or even the abandonment of production or reinjection wells due to clogging. The composition of the scale in geothermal plants is typically very complex and depends on many parameters, such as the temperature and pressure of the fluid, the history of water-rock interactions and the operating conditions. To mitigate this problem, scaling inhibitors are usually employed. It's important to underline that scaling acts as a major operational obstacle only for open-loop technologies that directly pump reservoir brine to the surface. Furthermore, scales can also precipitate inside chokes and safety valves; such a phenomenon increases the operational risk profile, as it can impair component mobility and potentially compromise the reliability and integrity of well control systems.

Furthermore, the combination of geothermal fluid aggressive chemistry with harsh marine conditions significantly amplifies operational risks. Offshore environments expose topside and subsea infrastructure to atmospheric salt spray, high humidity, continuous vibration, and

wave-induced dynamic loads [21]. When geothermal fluid aggressiveness, aging well materials, and marine exposure act simultaneously, the resulting risk profile becomes considerably more complex than that of conventional onshore geothermal installations.

2.4 Technical configurations for geothermal energy recovery

Following the thermodynamic and chemical characterization of the reservoir, the challenge shifts from resource mapping to energy extraction. Extracting heat from a depleted hydrocarbon reservoir requires choosing the most efficient thermodynamic interface between the subsurface and the platform. This section analyses the two main technical configurations for geothermal recovery: Closed-loop (Section 2.4.1) and Open-loop (Section 2.4.2) evaluating their operational profiles, engineering feasibility, and fluid-dynamics constraints within an offshore environment. Additionally, the logistic options for wastewater management are addressed.

2.4.1 Closed-loop geothermal systems

Closed-Loop Geothermal Systems (CLGSs) – also referred to as Advanced Geothermal Systems (AGSs) – require the drilling and sealing of deep, large, artificial closed-loop circuits. These systems act as underground heat exchangers in which a fluid is circulated and heated by surrounding hot rocks (without chemically interacting with them) through conductive heat transfer [13].

Various designs are under research, including deep vertical doublets with laterals, horizontal configurations and single vertical boreholes with concentric isolated pipes [28]. One advantage of CLGSs is that they have very few site-specific requirements, enabling their application virtually everywhere and limiting development risks related to resource availability. They also offer high predictability and low water and pumping energy consumption; however, their main drawback is a generally lower thermal efficiency compared to open systems [12].

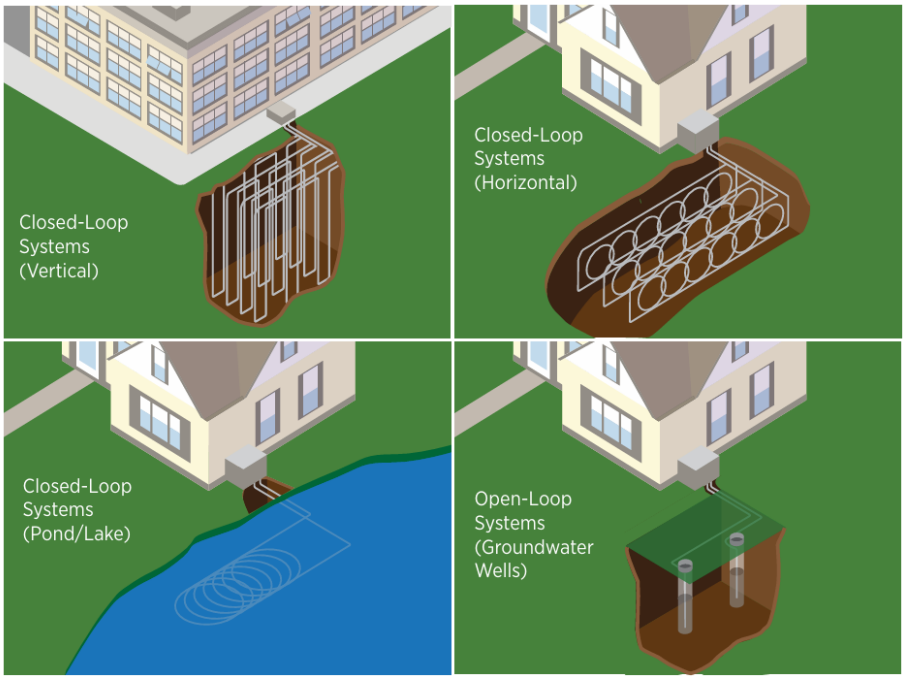


Figure 10: Illustrations of commonly used closed-loop and open-loop ground heat exchangers [28]

2.4.2 Open-loop geothermal systems

Open-loop systems exploit the physical abstraction of groundwater from an aquifer, relying on forced convection. This method offers several advantages: it uses a natural medium with a high specific heat capacity and extracts more heat per well than closed-loop systems. Moreover, these systems can operate with saline groundwaters, meaning water quality is often not a limiting factor for cooling and heating schemes.

On the other hand, open-loop configurations are highly geologically dependent, because they need to be in proximity of an aquifer able to provide an adequate yield. Operational challenges include the cost of pumping and the risk of fouling or clogging of heat exchangers and reinjection wells due to particulates, mineral precipitates, or biofilms. For this reason, water characteristics, like turbidity, chemistry and microbiology must be strictly monitored. Additionally, the design must carefully account for thermal and hydraulic feedback by ensuring sufficient distance between abstraction and injection points to prevent efficiency losses [12].

2.4.3 Comparison in the offshore context

In the offshore context, abandoned reservoirs often contain a significant amount of hot brine and residual gas, making open-loop technology a viable option. It's important to underline that,

in this configuration, the geothermal fluid is pumped to the platform and separated from the residual gas. The volume of produced water increases with the maturity of the assets, so when the hydrocarbons wells are going to be depleted, the conversion into geothermal wells could be a reasonable alternative to the mining closure [11].

While open-loop technology provides higher mass flow rates and temperatures at the platform level, the closed-loop alternative offers a simpler operational profile. Moreover, the working fluid is isolated inside the pipe, there's no risk of contamination or corrosion from the reservoir brine. Despite CLGS consumes less pumping energy, it has a limited amount of thermal energy exploitable.

Focusing on the specific reservoir depth, the closed-loop option can be excluded. Since the reservoir is located at a depth of approximately 2 km, the installation of a downhole heat exchanger is unfeasible from both an economic and engineering perspective, as the capital expenditures (CAPEX) would be excessively high.

In conclusion, for deep offshore reservoirs, the **open-loop** configuration is the most effective choice. However, it presents specific technical challenges, such as fluid availability and chemical compatibility.

2.4.4 Water disposal and reinjection

In the open loop configuration, after passing groundwater through the heat exchangers, pumps on the platform, there's the challenge of disposing of it. Coherently groundwater temperature will be lower, and the variation of temperature depends on the reconversion scenario chosen. There're typically several options for groundwater disposal [12]:

1. **Disposal to a surface water body**

This involves discharging the water into the sea. A risk assessment must be performed to consider how the warm temperature of the discharged water will affect the ecology of the surface water body. Warm water is usually more environmentally problematic to discharge than cold water, as the solubility of dissolved gases, such as oxygen, decreases as temperature increases. Additionally, the geochemical compatibility of the discharged groundwater with the

recipient water must be assessed. Groundwater may be poor in dissolved oxygen, rich in dissolved iron, or somewhat saline, all of which could significantly impact aquatic life. Permission from an authority responsible for regulating the water environment is usually required, and a discharge fee may have to be paid.

2. Re-injection to the abstracted aquifer (well doublet)

This method involves returning the water to the same aquifer from which it was extracted. This is attractive because it has few or no water resource implications (there is no net abstraction of water from the aquifer) and often minimizes the risk of ground settlement that can occur in some soils due to prolonged net abstraction of groundwater. The re-injection of limited quantities of water may be feasible via a soakaway structure, while larger quantities usually require the use of re-injection wells. The injected water may need to be sterilized to hinder bacterial clogging of the well screen or the aquifer. It must have a very low particle content, and the water pressure and gas content must be controlled to prevent exsolving gas bubbles from clogging the aquifer and decreasing its permeability. Care must be taken to avoid re-injecting groundwater too close to the abstraction well to prevent 'short-circuiting,' where re-injected groundwater breaks through into the abstraction well, compromising system efficiency.

A well doublet may lead to issues such as the cone of depression and the cone of reinjection. If we re-inject in the same body, we might lower the water table around the extraction well and increase the water table near the pond. Inducing a local flow increases velocity and turbulence, preventing particles from settling and increasing the extraction of particulate matter. This flow of small particles increases porosity and sediment settlement, potentially causing abrasion of submerged pumps and reducing their working life, leading to more maintenance.

3. Disposal to another aquifer

If there is more than one aquifer below the site, groundwater can be abstracted from one aquifer horizon and disposed of by re-injection or re-infiltration into another hydraulically distinct aquifer. This method involves consuming water from one body and re-injecting it into another. The injection of water must not cause an unacceptable rise in groundwater levels in the second aquifer, and the injected water must be geochemically compatible with the natural water of the

second aquifer. Any heat plume (i.e., body of warm or cold injected groundwater migrating with natural groundwater flow) must not constitute unacceptable heat pollution or adversely impact any users. Therefore, to ensure this method is viable, it must be guaranteed that abstraction from the first aquifer does not unacceptably compromise its resources or negatively impact other users or environmental features.

4. Disposal of wastewater to the abstraction well

In a standing column well system, a proportion of the waste groundwater, having served the heating scheme, may be re-injected back into the upper part of the abstraction well. The cool re-injected water takes time to flow down the well to the pump, and its temperature will re-equilibrate on the way down by conductive transfer of heat from the borehole walls. In the well, it will mix with a percentage of 'new' groundwater entering from the aquifer, eventually establishing an equilibrium situation.

In this configuration the main problem is related to the short circuit that might be produced between the submerged pump and the reinjection. Since both processes occur in the same location, a small percentage of injected water may enter the abstraction phase, mixing with the recirculating water and reducing its temperature. If the operating time of the plant is not balanced well, the efficiency of the open loop system will decrease over time.

The possibilities described are illustrated in Figure 11:

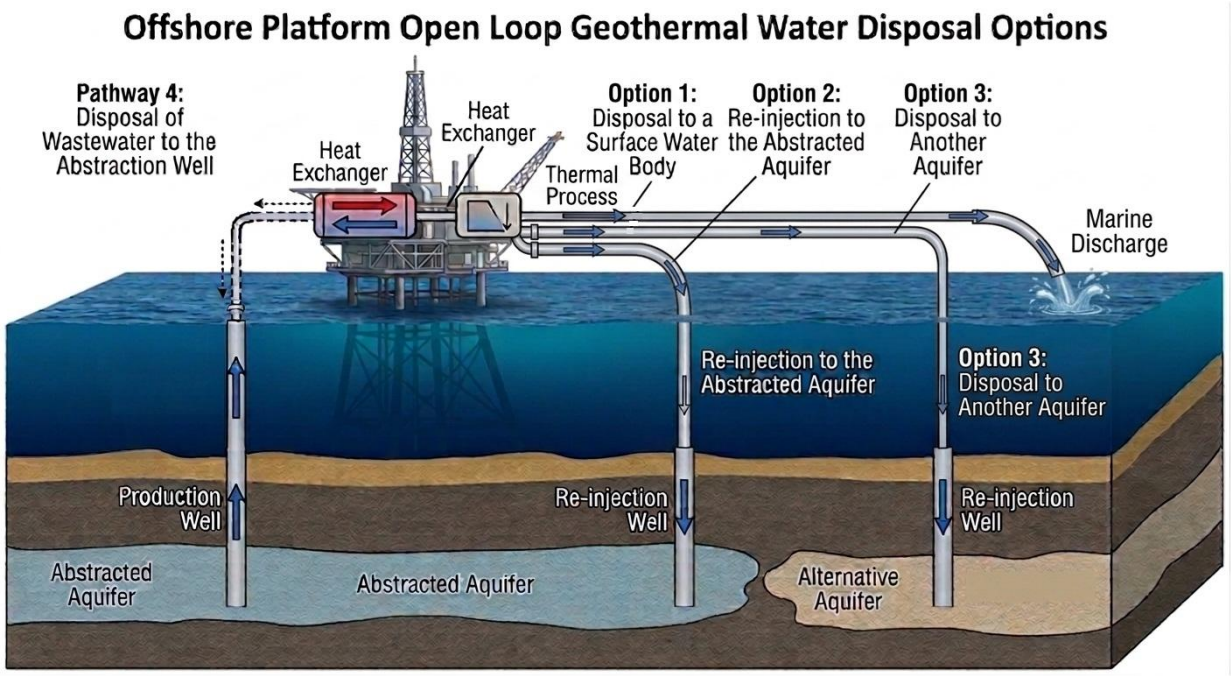


Figure 11: Geothermal water disposal [12], AI generated image

It is worth noting that while Figure 11 illustrates a simplified operational layout, a single offshore platform typically manages multiple wells extending to varying depths and trajectories. Consequently, these wells often operate across different geological layers and reservoir strata that are hydraulically disconnected from one another, meaning that abstraction and re-injection activities may involve separate underground horizons with distinct thermal properties.

3 Prefeasibility study of reconversion scenarios

Following the comprehensive overview of the offshore decommissioning context and geothermal principles presented in the previous chapters, the immediate challenge is to identify which technologies can practically adapt to an isolated marine environment. When geothermal heat is analysed onshore, two main configurations are typically proposed depending on the reservoir temperature: Organic Ranking Cycle (ORC) for electricity production in high enthalpy systems, or district heating for low to medium enthalpy systems. In an offshore context, the situation is fundamentally different. District heating is technically unfeasible due to the distance of the platforms from the coast (on average 24 km [5]). For this reason, this study focuses on low enthalpy processes that traditionally rely on waste heat recovery but are here powered by geothermal energy.

Some of these processes are thermally driven (such as Membrane Distillation) while in others, heat is used to increase overall efficiency (Reverse Osmosis), or to provide the necessary thermal conditions for exothermic reactions (Biological Methanation, LOHC and NH_3 production). Conversely, artificial reef conversion does not exploit the geothermal potential itself but it represents a valid alternative for mono-tubular and bi-tubular platforms with limited deck space. Finally, for the geothermal assisted aquaculture, reservoir with low temperatures (between 40 and 50°C) can be used because their role is just to increase the temperatures of the fish tanks.

The proposed scenarios will be evaluated through a multi-disciplinary approach. Each technology is analysed focusing on its operational requirements (such as temperature and energy demand), logistical constraints (area footprint and raw materials), and environmental integration. While some sections emphasize chemical and thermal aspects, others focus on structural feasibility and circular economy principles. To conclude the chapter, a comprehensive comparison table will be provided to highlight the strengths and weaknesses of each scenario for offshore repurposing, providing the qualitative foundation required to transition toward the rigorous quantitative sizing of the plants.

3.1 Biological methanation

3.1.1 Process fundamentals

In biological methanation, CO_2 and H_2 (typically in a stoichiometric molar ratio of 1:4) are converted into CH_4 by hydrogenotrophic methanogenic archaea. These microorganisms consume H_2 and CO_2 to produce methane as their primary metabolic product according to the following exothermic reaction:

$$CO_2 + 4H_2 \rightarrow CH_4 + 2H_2O \qquad \Delta H^0 = -165 \frac{kJ}{mol\ CO_2}$$

While both chemical (Sabatier) and biological methanation aim to produce methane, they differ significantly in operating conditions. Chemical methanation requires high temperatures (300-500°C) and metal catalyst (Nickel or Ruthenium). In contrast, the biological process occurs at lower temperatures (25-65°C) and ambient pressures, making it a more suitable candidate for integration with low-grade geothermal heat [30]. In Table 2 a comparison between biological and chemical methanation is presented. For this research, only biological methanation is considered since it occurs at lower temperatures.

Table 2: Comparison between biological and chemical methanation [30]

Parameter	Biological methanation	Chemical methanation
Reaction temperature	25-65°C	300-500°C
Reaction pressure	Atmospheric to 10 bar	1-30 bar
Catalyst	Microbial consortia or pure cultures	Metal catalyst (e.g. Ni, Ru)
Methane yield	Up to 100%	Up to 80%
Methane purity	Up to 99%	Up to 97%
By-products	None or minimal	Water and trace amounts of CO
Energy consumption	Low	High
Environmental impact	Low carbon footprint	High carbon footprint

3.1.2 Comparison of process configurations

Biological methanation can be conducted through three approaches [31]:

- In-situ: H_2 is directly injected into an existing anaerobic digestion (AD) reactor.
- Ex-situ: CO_2 and H_2 are fed into a dedicated external reactor containing the microbial culture.
- Microbial Electrosynthesis (MES): CO_2 is reduced to CH_4 via electroactive microorganisms under an applied voltage.

For the purpose of this offshore repurposing study, only the ex-situ configuration has been selected. In-situ methanation is unfeasible as it requires a constant supply of organic biomass (sewage or agricultural waste) which is not available on an offshore platform. Transporting biomass from mainland would be logistically and economically unsustainable. MES was also excluded due to its low Technology Readiness Level (TRL), as it remains largely a laboratory-scale technology too risky for the harsh and corrosive marine environment.

3.1.3 Technical parameters and reactor design

The ex-situ configuration, particularly using Trickle Bed Reactors (TBR), offers high methane purity (95-99%) and better scalability. However, the main technical challenge remains the low gas-liquid mass transfer, as H_2 has very low solubility in water (1.6 mg/L at 25°C) [31]. The TBR configuration for ex-situ BM is based on the hydrogenotrophic methanogens activity that are immobilized as a biofilm on the packing material; this arrangement results in a large contact area between the biofilm and the fed gases [32]. Since the TBR has only recently applied to ex-situ BM, the understanding of the process is still evolving specifically regarding optimal conditions and maximum performance. Currently, this technology is primarily in the experimental phase, largely due to the high costs associated with H_2 production.

To address the technical requirements of an offshore installation, the following parameters are considered:

- Dimensions: these vary significantly depending on the application scale. While this technology is currently at a laboratory scale with operative volumes ranging from < 1 l to 61 l [32], offshore repurposing would require modular scaling. To meet the technical

and productive requirements of the investigated asset, a benchmark working volume of 2 m^3 has been assumed for the quantitative sizing of the reactor unit (Section 4.2.1). This upscaling allows transitioning the biological methanation process toward a representative pre-commercial scenario compatible with offshore utility flows.

- Operating temperature: the process distinguishes between mesophilic (30-40°C) and thermophilic (55-65°C) regimes [31]. The thermophilic range is preferred for this study as it increases reaction rates and perfectly matches the available geothermal brine temperature (60-70°C).

- Mass flow and water demand: the mass flow of reagents follows the 4:1 H_2/CO_2 ratio. While water is a by-product of the reaction itself, a steady supply of fresh water is necessary to prepare and replenish the nutrient solution (mineral salts, nitrogen, and phosphorus) [30].

- Offshore resilience: studies investigating the effect of feedstock limitation have shown that hydrogenotrophic methanogens are highly resistant to starvation [30]. Consequently, biological methanation efficiency could be recovered even if the substrate gases remain unavailable and the bioprocess is suspended for several days. Furthermore, the system can be highly automated, meaning 24/7 on-site personnel are not required; the process can be monitored remotely, with periodic maintenance for nutrient replenishment and sensor calibration.

As shown in Figure 12, the TBR is the most suitable configuration for the offshore context because it does not require high energy input for continuous mixing or bubbling; instead, it exploits gravitational force for liquid distribution [32]. Moreover, it's important to highlight the dual function of the thermal jacket during different reactor phases. Initially, during start-up, the geothermal fluid acts as a heat source to reach the thermophile regime (55-65°C) and activate the archaea metabolism. During the steady-state phase, the exothermic reaction releases a considerable amount of energy. In this stage, the jacket serves to remove excess heat, maintaining the reactor stable between 55-60°C.

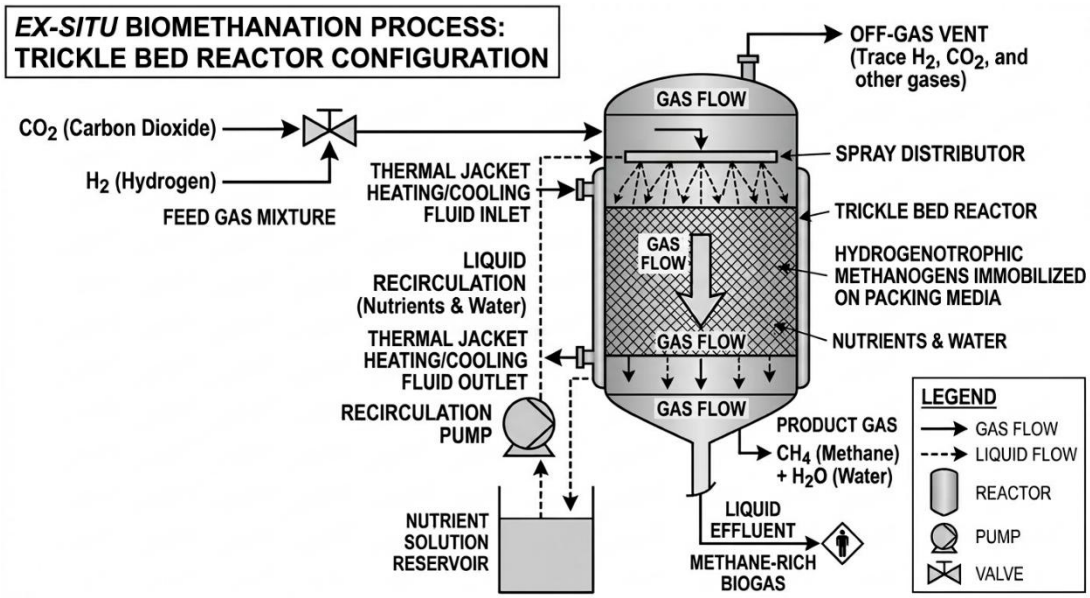


Figure 12: Configuration of ex-situ trickle bed reactor [30], [32] AI generated image

3.1.4 Infrastructure and logistics

The location of the reactor is critical for cost-efficiency. An ideal site would simultaneously combine low-cost and renewable electricity for H_2 production, a sustainable CO_2 source, adequate space for facilities, water supply, process heat integration opportunities, as well as access to gas market [31]. On a repurposed platform, the ideal synergy is achieved by combining:

- Local H_2 production via electrolysis or use of H_2 transported via pipeline.
- CO_2 supply via pipeline or local reservoir sources, creating a strong alignment with Carbon Capture, Utilization, and Storage (CCUS) strategies by enabling permanent CO_2 sequestration directly into the depleted reservoir.
- Geothermal heat integration for temperature control.
- Subsea pipelines for the transport of the final biomethane to the mainland grid.

Despite its high potential, offshore biological methanation faces specific challenges: (i) the logistics of CO_2 supply and storage, (ii) the management of nutrient-rich wastewater to prevent marine eutrofization, and (iii) the need for precise liquid distribution within the TBR to avoid channelling effects caused by platform motions (only if the platform is not bottom fixed).

In the Italian context, most of the offshore structures (129 out of 139 [5]) are already utilized for gas extraction. This represents a significant advantage, as the infrastructure for managing and transporting the methane produced is already in place.

3.1.5 Conclusion

By utilizing geothermal heat to maintain thermophilic conditions and repurposing existing O&G infrastructure for gas transport, the process overcomes the typical barriers of "Power-to-Gas" technologies. The choice of a biological pathway over a chemical one ensures lower energy consumption, increased safety, and high resilience to the typical constraints of the marine environment. However, the system's growth is currently limited by the availability of green hydrogen, as global production still relies on fossil fuels for >98% of the total supply [33].

3.2 Liquid Organic Hydrogen Carriers (LOHC) system

3.2.1 Process fundamentals

Hydrogen storage is critical for the efficient and safe utilization of hydrogen as an energy carrier. Among several developed systems, such as compressed gas (CH2), liquid gas (LH2), metal hydrides, chemical hydrides and carbon material hydrogen storage (CMH2), liquid organic hydrogen carriers (LOHCs) stand out as an innovative technology. LOHCs chemically bind hydrogen in liquid organic compounds under atmospheric conditions, making them non-explosive, non-volatile, and significantly safer than conventional high-pressure or cryogenic system [34].

The system operates through a reversible cycle of hydrogenation (storage/charging) and dehydrogenation (release/discharging). Hydrogen-rich (Hx–LOHC) and hydrogen-poor (H0–LOHC) states form a cyclic process where catalysts are used to manage the chemical bonds. This study focuses exclusively on the hydrogenation process, which is an exothermic catalytic reaction that occurs inside a reactor whose temperature can be maintained by the integration between geothermal heat and an auxiliary system. During this phase, unsaturated bonds in the organic carrier are converted into saturated ones at temperatures typically ranging from 80°C to 150°C and pressures of 10-50 bar, utilizing noble metal catalysts such as Pd, Pt, or Ru. A schematic representation of the reaction during both the phases is illustrated in Figure 13.

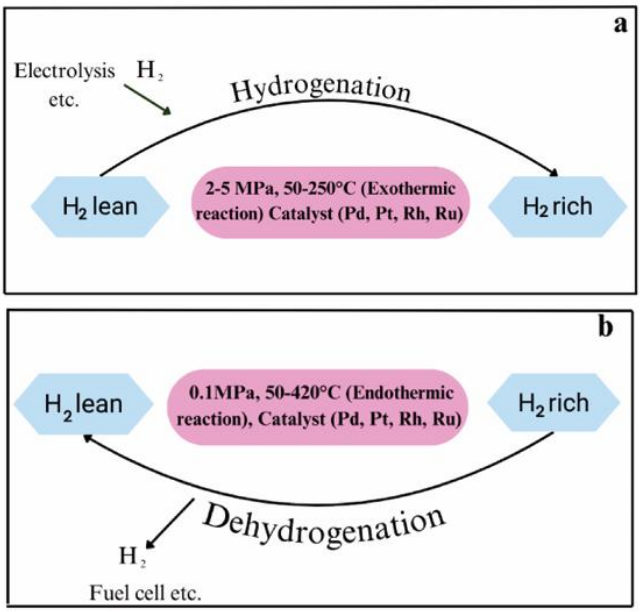


Figure 13: Schematic representation of the LOHC cycle hydrogenation (a) and dehydrogenation (b) [34]

3.2.2 Dibenzyltoluene (DBT) systems

Among available LOHC compounds, Dibenzyltoluene (DBT) and its fully hydrogenated form, Perhydrodibenzyltoluene (H_{18}-DBT) are the most prominent for industrial-scale applications. DBT is particularly suitable for offshore environments due to its superior properties [34]:

- Stability: high thermal and chemical stability with a high boiling point (~390 °C) and low vapor pressure.
- Safety: low toxicity and low environmental risk, as it is already widely used as an industrial heat transfer fluid.
- Capacity: a hydrogen storage capacity of approximately 6.2% in weight (within the general LOHC range of < 8%).

The hydrogenation reaction of DBT (hydrogen charging) can be written as follows [35] [36]:

$$C_{21}H_{20} + 9H_2 \rightarrow C_{21}H_{38} \qquad \Delta H = -65.4\ \frac{kJ}{mol\ H_2}$$

This exothermic reaction typically requires elevated hydrogen pressures (10–50 bar) and moderate temperatures (150–200°C) to ensure high conversion and selectivity. Crucially, while the reaction is net-exothermic at steady-state conditions, external geothermal heat remains essential during the initial start-up phase to trigger the catalytic process and to continuously pre-

heat the incoming cold reactants up to the required activation threshold. The selection of catalysts (supported on alumina) is vital to provide high selectivity and activity, allowing the reaction to proceed with a relatively low activation energy required to be compatible with the potential of a geothermal reservoir [34].

The reaction is normally conducted in fixed-bed reactors operating under a trickle-bed regime (TBR), in which gas (H_2) and liquid (H0-DBT) streams flow downward through a solid catalyst bed where the reaction takes place [37]. In this specific case, the catalyst is usually Ru/Al2O3 [38]. To ensure performance, the gas-liquid mixture must be distributed homogeneously over the catalyst bed by means of a high-efficiency distributor tray. This is essential to achieve complete wetting of the catalyst, avoiding the formation of hot spots or channelling [37]. As shown in Figure 14, the system includes a gas-liquid separator at the reactor outlet to recover unreacted hydrogen for recycling.

Similar to biological methanation, the reactor temperature is regulated by a thermal jacket. Furthermore, catalyst deactivation must be considered; factors contributing to degradation include ineffective catalyst utilization, poor liquid distribution, and radial temperature gradients within the catalytic bed.

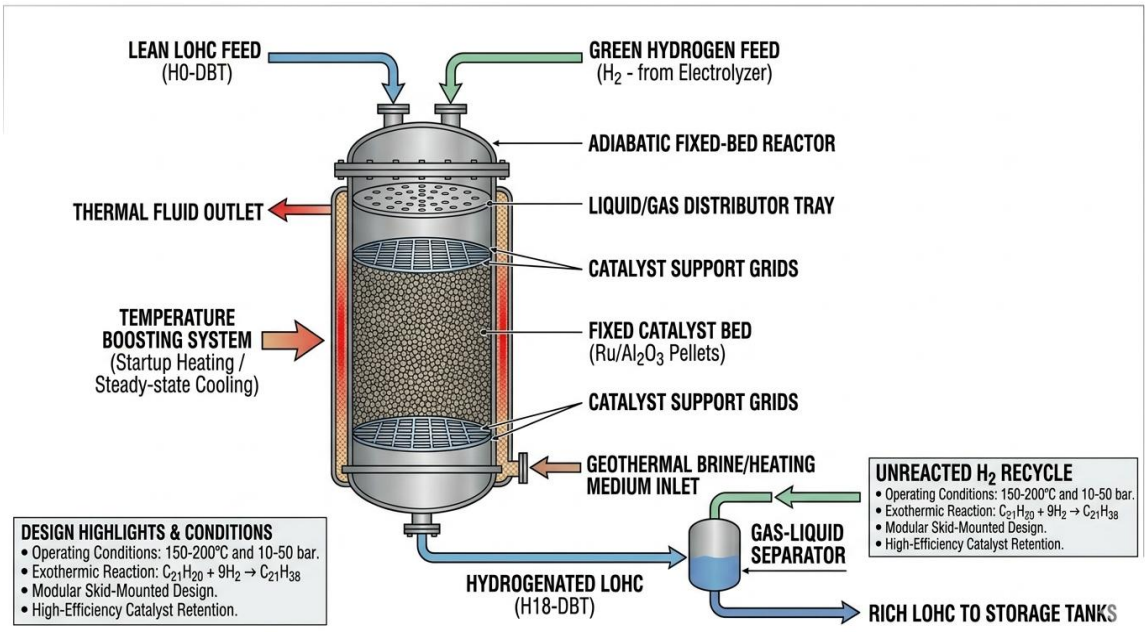


Figure 14: Schematic layout of a modular Fixed-Bed Reactor for DBT hydrogenation [34][35][37][38] AI generated image

3.2.3 Infrastructure and logistics

LOHC technology was primarily developed to solve the lack of infrastructure for large-scale hydrogen distribution. Traditional hydrogen transport faces "stress corrosion" in metal pipelines and high power consumption for liquefaction (the density of LH_2 is 5.9 times lower than LNG, leading to significant storage losses) [39].

In a repurposed offshore scenario, LOHC offers strategic advantages:

- Infrastructure reuse: the “rich” LOHC can be stored in conventional fuel tanks or transported via existing Oil & Gas logistics chains (standard tankers and pipelines).
- Offshore reliability: these chemical plants are designed for continuous, highly automated operation with minimal human intervention.
- Storage synergy: the offshore reservoir itself could potentially be used for hydrogen storage prior to LOHC formation, provided appropriate purification is performed.

However, some limitations remain, such as the high energy consumption in LOHC technology, the difficulty of catalyst development in hydrogenation and dehydrogenation systems, and the decrease in hydrogen storage performance as the number of cycles increases. Focusing on the offshore context, there are additional issues related to weight and balance, as well as bunkering. Furthermore, charging operations can only take place in calm seas. If the sea remains rough for weeks, the platform's tanks fill up, forcing a production shutdown.

3.2.4 Thermal integration

Since the hydrogenation of DBT requires temperatures between 150 and 200°C and the geothermal fluid reaches the platform at approximately 65-70°C, a thermal boosting is necessary. Two main technologies can be employed to bridge this temperature gap: gas-fired boilers and industrial heat pumps. It is important to note that once the hydrogenation reaction is initiated, its exothermic nature helps maintain the operating temperature, reducing the external energy demand.

Boiler integration

Residual natural gas often remains in depleted reservoirs, either located in the "gas cap" or dissolved in the brine under pressure. In an open-loop configuration, the geothermal fluid

(brine and gas) is extracted and processed through a two-phase separator to decouple the liquid from the gaseous phase. The separated gas can then be utilized to power a boiler. However, since residual gas is a finite resource, the system must be designed for future transition: as the gas is depleted, the gas boiler can be replaced by an electric boiler powered by offshore renewable sources, ensuring the long-term continuity of the platform's operations.

Although utilizing residual gas generates CO_2 emissions, it remains a compelling transition solution. This approach recovers energy from gas that would otherwise remain unexploited in the reservoir or, in some cases, be subject to flaring. By repurposing this existing chemical energy for thermal boosting, the platform reduces its immediate dependence on external power during the early stages of the energy transition.

Industrial heat pump

A heat pump is a thermodynamic device that utilizes mechanical energy to transfer heat from a low temperature source to a high temperature medium. The cycle consists of four principal phases [40]:

1. Evaporation: the refrigerant absorbs thermal energy from the geothermal source and evaporates.
2. Compression: an electric compressor compresses the gas, increasing both its pressure and temperature.
3. Condensation: the high temperature gas releases heat to the process fluid (the LOHC medium) in the condenser, returning to a liquid state.
4. Expansion: the liquid passes through an expansion valve, reducing its pressure and temperature before restarting the cycle.

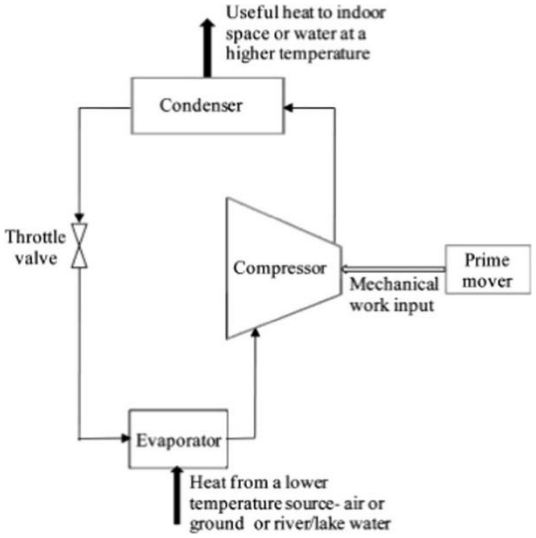


Figure 15: Heat pump theoretical operation cycle in heating mode [41]

While residential heat pumps typically reach maximum temperatures of 80°C, industrial heat pumps can achieve temperatures up to 200°C [42]. These units are specifically engineered to withstand high-stress environments and corrosive conditions typical of offshore platforms.

In this specific application, the industrial heat pump is particularly advantageous due to the high temperature of the thermal source (70°C) compared to standard ambient air. The efficiency of a heat pump is defined by its Coefficient of Performance (COP), expressed as the ratio between the heat delivered to the high-temperature medium and the electrical work consumed:

$$COP = \frac{Q_{high}}{W_{net,in}}$$

Comparative analysis

Selecting the optimal auxiliary system involves trade-offs. Heat pumps offer higher efficiency and a longer lifespan but rely on electricity (which may need to be imported or generated via offshore wind/solar). Conversely, gas boilers utilize on-site residual gas, eliminating the need for external power during the initial phase; however, they produce carbon emissions and generally have a shorter operational life [43].

3.2.5 Conclusion

LOHC production valorises the offshore context by repurposing existing Oil & Gas infrastructure. However, the technology is currently limited by the high energy demand of the dehydrogenation phase (performed on shore) and the current costs of green hydrogen. Advances in catalyst research and improvements in electrolysis efficiency are expected to drive the large-scale adoption of LOHC systems as a safe and flexible hydrogen carrier [34].

3.3 Ammonia production

3.3.1 Process fundamentals

Ammonia is a carbon-free fuel with high hydrogen density (17.75 wt% of H content in the NH_3 molecule), which can be efficiently stored and transported exploiting existing infrastructures [44].

The Haber–Bosch process for NH_3 production remains one of the most impactful inventions in chemical engineering. It is based on the high temperature and high-pressure reaction between N_2 and H_2 in the presence of a suitable catalyst.

$$N_2 + 3H_2 \rightarrow 2NH_3 \qquad \Delta H = -92\ \frac{kJ}{mol\ N_2}$$

As a matter of fact, NH_3 formation requires a significant energy input, to achieve the activated state of the nitrogen molecule. Even with advanced catalysts, the reaction typically proceeds in a temperature range of 250–400°C and pressure range 100–200 bar [44].

Due to these extreme operating conditions, the Haber-Bosch process presents significant challenges for integration with low-to-medium enthalpy geothermal sources. The high temperature lift required exceeds the practical boosting capabilities of the 70°C reservoir analysed in this study. Consequently, while ammonia remains a key energy carrier, this scenario is considered less favourable compared to biological methanation and LOHC production, which operate under much milder conditions more compatible with geothermal potential.

3.3.2 Comparison between different exothermic reactions

Table 3 presents the enthalpy of reaction (ΔH) normalized per one mol of hydrogen consumed. This approach allows for a direct comparison of the "waste heat" generated by each process relative to the same unit of hydrogen input. The process that produces more heat is the hydrogenation of DBT, followed by biologic methanation and ammonia production.

Table 3: Comparison reaction enthalpies and specific waste heat production for different exothermic synthesis processes

Process	Chemical formula	$\Delta H\left(\frac{kJ}{mol\ product}\right)$	$\Delta H\left(\frac{kJ}{mol\ H_2}\right)$
Biologic methanation	$CO_2 + 4H_2 \rightarrow CH_4 + 2H_2O$	-165.0	-41.0
LOHC (DBT)	$C_{21}H_{20} + 9H_2 \rightarrow C_{21}H_{38}$	-588.6	-65.4
Ammonia (H-B)	$N_2 + 3H_2 \rightarrow 2NH_3$	-45.8	-30.5

3.4 Reverse Osmosis (RO) desalination

RO is currently the most reliable state-of-the-art technique for seawater and brackish water desalination. It is widely adopted to minimize desalination-associated costs and currently accounts for approximately 50% of the desalinated water produced globally. The efficiency of RO depends on several factors, including operational parameters, membrane type, and feed water characteristics [45].

3.4.1 Theoretical background

Osmosis is a natural process in which water molecules spontaneously move from a solution of low solute concentration (low osmotic pressure) to a solution of high solute concentration (high osmotic pressure) across a semi-permeable membrane (Figure 16 a). The membrane, being semi-permeable, rejects solutes and only allows water molecules to pass through. This flow continues until a state of osmotic equilibrium is reached, where the chemical potentials across the membrane become equal (Figure 16 b). This flow can be stopped or reversed by

applying external pressure to the higher concentration solution (feed). When the applied pressure exceeds the osmotic pressure, water molecules are forced to flow in the direction opposite to natural osmosis. This process is known as Reverse Osmosis (Figure 16 c) [45].

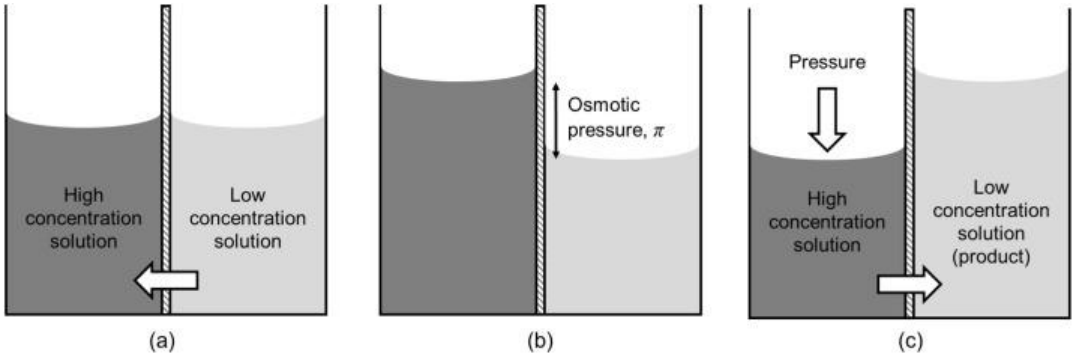


Figure 16: Schematic of (a) osmosis (b) osmotic equilibrium (c) RO [45]

3.4.2 Process phases

The RO system is not limited to the membrane passage, but it involves a complete operational cycle [2]:

1. Intake: seawater is aspirated at a specific depth (e.g. 15 m) to ensure stable physio-chemical characteristics and to limit the intake of suspended solids or the influence of surface currents.

2. Pre-treatment: a critical phase to protect the sensitive membranes. It includes chlorination (to eliminate bacteria), pH adjustment to approximately 7.5 (typically using sulfuric acid), coagulation, and flocculation (to remove organic and colloidal substances), followed by various filtrating stages.

3. High pressure section: the pre-treated water is pressurized to around 55-70 bar using high-pressure pumps to overcome the osmotic pressure and force the solvent through the membranes.

4. Post-treatment: the permeate (the exiting freshwater) is remineralized by passing through a calcite bed to reinsert essential mineral salts and adjust the pH to potable values (around 8) to human organism. A final disinfection is then performed.

3.4.3 Criticalities

Some criticalities include membrane scaling (inorganic fouling) and fouling (accumulation of organic and bacterial matter). To mitigate these issues periodic cleaning is needed with specific chemical solutions (acidic or alkaline depending on the deposit) to restore the original performance [2], [45].

3.4.4 Role of geothermal energy in Reverse Osmosis

In this study, geothermal heat is used to preheat the feedwater. Increasing the temperature in the range of 15°C to 40°C reduces water viscosity, enhancing membrane permeability. Consequently, the high-pressure pump requires less energy to overcome filtration resistance, leading to a reduction in the overall Specific Energy Consumption (SEC) of the desalination process.

The effect of temperature on the efficiency and related energy issues of the RO process has been the subject of many studies, and the main conclusions can be summarized as follows, for increasing feed temperature (T_f) in the range ~15°C to 40°C [46]:

- Improved flux: decreasing water viscosity leads to increasing membrane permeability and permeate fluxes; under specific conditions, the reported rate of change in permeate flux is approximately 3% per degree Celsius temperature increase.

- Permeate quality: increased solute diffusivity combined with reduced membrane solute-rejection results in a slightly higher salt passage (inferior permeate quality).

- Pressure requirements: the reduced membrane resistance to the filtration process allows for smaller feed-pressure requirements, which lead to smaller energy consumption for high-pressure pumps.

- Osmotic pressure trade-off: the significant increase of osmotic pressure with T_f is well known and tends to partially offset the aforementioned positive effects. However, withing the 15-40°C range, the viscosity-driven energy savings typically prevail.

3.5 Advanced thermal desalination scenarios

Thermal desalination is a process that utilizes evaporation and condensation to remove salt from water. Water is heated until it evaporates, leaving salts behind, and the vapor is then condensed to produce fresh water. The driving force of the process is the vapor pressure gradient.

The main thermal technologies include Multi-Effect Distillation (MED), Multi-Stage Flash (MSF), and Thermal Vapor Compression (TVC) [14]. This chapter focuses on two specific processes particularly suitable for geothermal integration: Vacuum Thermal Distillation (VTD) and Membrane Distillation (MD). Both are thermally driven and can efficiently exploit the low-to-medium grade heat (60-80°C) provided by geothermal fluids.

3.5.1 Energy requirements

Energy requirements for desalination vary from process to process. Thermal desalination processes require both thermal energy (for evaporation) and electrical energy (for pumping and vacuum maintenance). In general, Sea Water Reverse Osmosis (SWRO) is the preferred method globally due to its lower specific energy consumption and its inherent simplicity. However, when large quantities of low-cost thermal energy sources are available, thermal desalination becomes highly favourable and sustainable. Figure 17 shows the specific energy consumption for thermal and membrane desalination processes in terms of kJ of energy required for producing one unit of freshwater in kilograms.

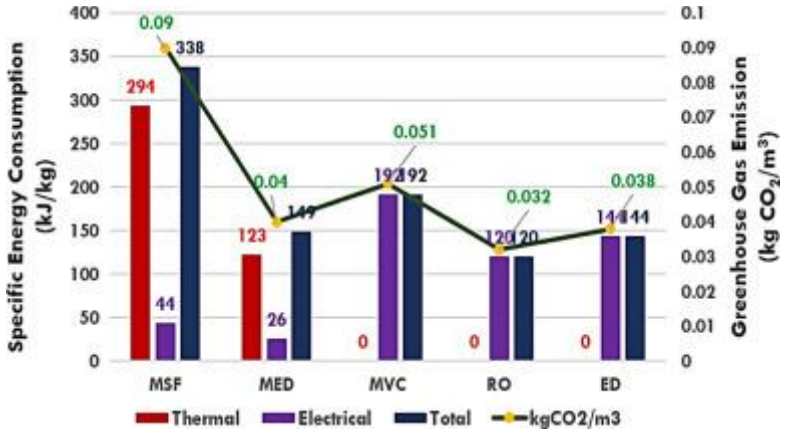


Figure 17: Specific energy consumption for thermal and membrane desalination processes and greenhouse gas emissions for unit freshwater production [14]

3.5.2 Selection criteria for geothermal integration

The selection of a desalination process for geothermal applications depends on several factors [14]:

1. Plant size: it depends on water demand, feed water concentrations, sources and water storage capacity.

2. Geothermal energy quality and quantity and other renewable energy sources: the chemical and physical characteristics of geothermal waters are critical in the design of a heat extraction and utilization scheme.

3. Desalination technology: the selection of the most appropriate process depends on the geothermal energy source characteristics such as temperature and flow capacities.

4. Feed water characteristics: the quality of the intake seawater must be evaluated to select the most suitable desalination process. When feedwater with relatively low Total Dissolved Solids (TDS) is available, membrane-based processes (such as Reverse Osmosis) are generally favoured. Rather than using the geothermal brine directly as feedwater – which would cause severe scaling, fouling, and corrosion – the geothermal fluid is kept in a closed loop to supply indirect heat. This thermal energy is used to preheat the seawater, thereby reducing its viscosity and lowering the specific energy consumption of the pumps, or to directly drive thermal desalination processes.

5. Product water: the desired product quality should be determined based on the end use. Agricultural and fish farm and animal feed operations may not require high quality potable waters. Desalination processes may prove to be cost-prohibitive for agricultural applications.

6. Brine disposal: brine disposal and management issues cannot be ignored for any desalination plant. It was shown that inland desalination has less environmental impacts when compared with seawater desalination. Disposal into oceans is a commonly practiced method for coastal desalination plants while evaporation ponds or sewer disposal is a better option for inland desalination plants.

7. Techno-economic requirements: energy source and the desalination energy requirements play a critical role in determining the desalination process.

3.5.3 The industrial benchmark: Vacuum Thermal Distillation (VTD)

Vacuum thermal distillation exploits reduced pressure to decrease the evaporation temperature of seawater. This is essential for geothermal applications, as it allows for boiling at temperatures significantly below 100°C, matching the thermal grade of the reservoir.

Case study: Alfa Laval AQUA Blue

A leader in this sector is Alfa Laval, a company specialized in the areas of heat transfer, separation and fluid management. It produces several models of vacuum distillation units and the most diffuse is AQUA Blue. The AQUA Blue E1 C-type utilizes a unique 3-in-1 titanium plate technology where evaporation, separation and condensation occur within a single plate pack [47]. The process and control system ensure fresh water with salinity levels below 2 ppm.

Technical sizing and performance analysis

The sizing of the desalination unit is based on the operational curves provided in the Alfa Laval AQUA Blue E1 C-type technical specifications (Figure 18). The performance of the system is strictly dependent on the thermal input provided by the geothermal fluid; as illustrated in the graph, a direct correlation exists between the heating water temperature and the freshwater production rate. The acronyms C80, C100, and C125 identify the different configurations of the plate pack, where a larger plate surface area corresponds to a higher nominal production capacity. A critical observation for the feasibility of this study is the minimum temperature threshold: the system is engineered to operate optimally at $T > 70°C$. This technical constraint is a key factor in the integration strategy. Since the geothermal reservoirs in the Adriatic Sea may exhibit lower temperatures, the gap between the available thermal grade and the required 70°C benchmark justifies the implementation of a thermal boosting system. By utilizing residual gas or other energy recoveries, it is possible to shift the operating point along these curves, ensuring a stable and significant mass flow of high-quality distilled water.

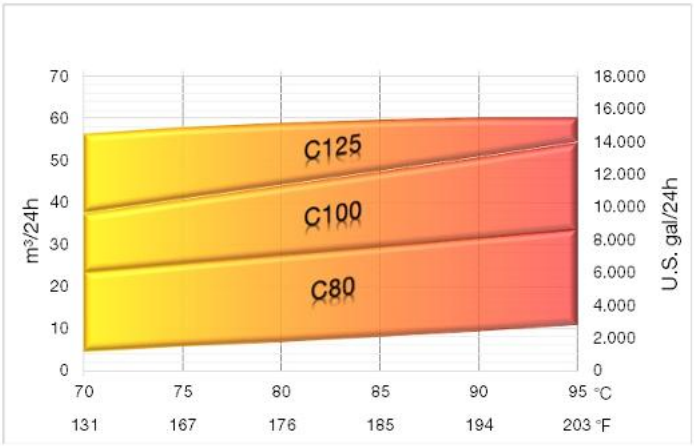


Figure 18: Production capacity of the desalination units as a function of the heating medium inlet temperature [47]

Working principle

An only type of plate in titanium is used. It manages all the 3 phases of the vacuum distillation that are evaporation, separation and condensation. The only difference is the configuration of the gaskets between the plates of process and service as it is possible to see in Figure 19. Since the vacuum of the process is inside the plate pack, no external mantle is required.

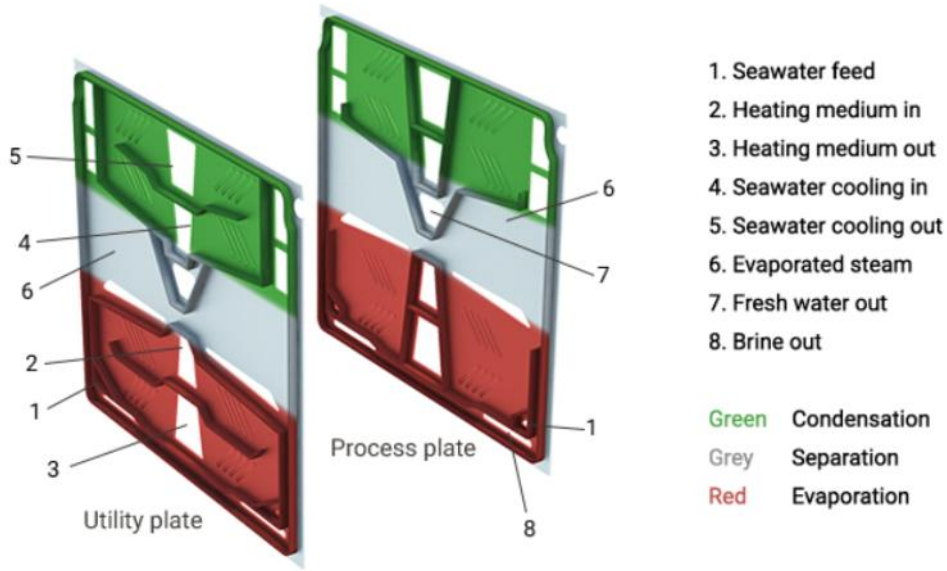


Figure 19: Internal configuration of the Alfa Laval AQUA Blue plate pack [47]

The AQUA Blue E1 C-type is heated by hot water, which enters the evaporator section, where it heats and evaporates a portion of the feedwater. The steam is condensed in the condenser. The feedwater is seawater, which is preheated by cooling the condenser. This cooling flow is also used as ejector motive flow. The evaporation occurs around 35-65 °C in a vacuum of 75-

99%, which is maintained by the brine/air ejector. The steam passes the separator section of the plate pack, where any droplets of entrained seawater hit the plate corrugations and fall back into the brine sump. Only clean steam reaches the condenser and is condensed into distillate, which is pumped out by the distillate pump. Figure 20 illustrates the process.

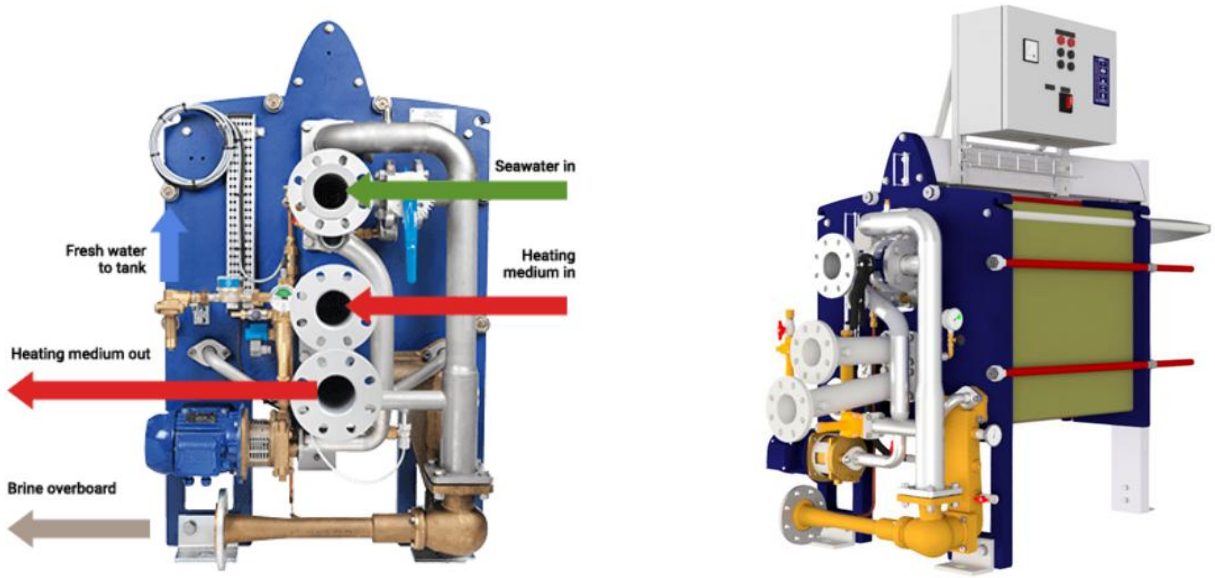


Figure 20: External configuration of the Alfa Laval AQUA Blue plate pack [47]

While the AQUA Blue represents a compact single-stage solution (total volume of a single unit is around 2.5 m^3, with a weight of approximately 1000 kg [47]), larger-scale applications can employ Multi-effect Evaporation Distillation (MED). For instance, a two-stage MED plant in Greece, using geothermal water with a wellhead temperature of only 61–62 °C from a borehole of 188 m deep, successfully produces 80 m^3/day, providing that vacuum-based thermal systems are highly effective even at very low temperatures [14].

3.5.4 The innovative frontier: Membrane Distillation (MD)

Membrane Distillation (MD) is a non-isothermal, thermally driven separation process where a hydrophobic microporous membrane acts as a physical barrier, allowing only volatile vapor molecules to pass through while retaining liquid water and dissolved salts [48].

Working principle

The Membrane Distillation process is recognized as a hybrid technology enjoying both thermal evaporation and membrane separation benefits in a single unit. The term MD originates from the fact that the procedure is analogous to conventional distillation, requiring energy to provide the latent heat of vaporization in order to accomplish separation under vapor-liquid equilibrium. The driving force for MD operation is provided by partial pressure gradient that is induced by a temperature gradient maintained across the two sides of a micro-porous membrane [49].

Figure 21 represents a schematic of MD principles. The feed solution (seawater) is preheated up to, for example, 65°C at one side of the membrane while the other side is maintained at a lower temperature, for example, 55°C. Since the hot (saline water feed) and cold (permeate or freshwater) streams are segregated by a membrane barrier, a very low temperature differential of 10°C is sufficient to generate the partial pressure required for producing freshwater through this process. Water vapor evaporates through the membrane pores and condenses on the side with lower temperature to form the distillate. A large temperature difference will result in a higher driving force and higher productivity at the cost of more thermal consumption and vice versa.

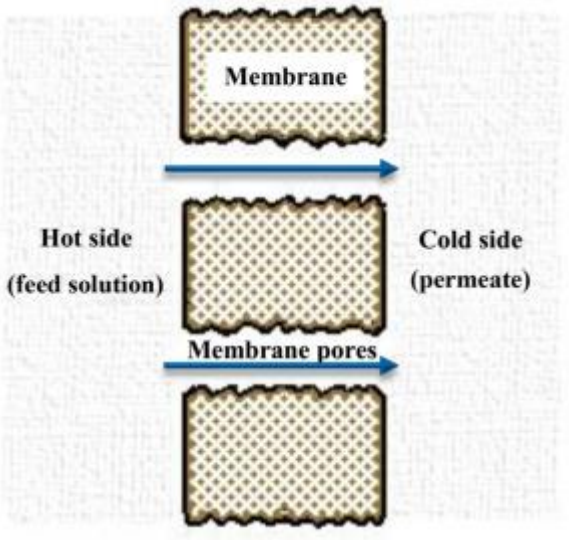


Figure 21: Membrane Distillation principles [49]

While MD can be operated under several basic configurations – such as Direct Contact Membrane Distillation (DCMD), where fluids touch both membrane sides – these standard

architectures suffer from severe sensible heat conduction losses through the thin polymeric layer [50]. To overcome this limitation and ensure industrial scalability, advanced commercial configurations evolve toward **Vacuum Membrane Distillation (VMD)**. In this process, the vapor is withdrawn by exerting a vacuum pressure to the permeate side of the membrane, which is kept as just lower than the saturation pressure of volatile components in the hot feed. In this case, the membrane is placed between the hot feed and a vacuum chamber. Vapor recovery takes place outside the membrane module by an external condenser. The existence of the vacuum on the permeate side allows higher partial pressure gradient and imposes an additional driving force for the process which in turn leads to higher distillation production rate compared to other MD configurations. Furthermore, the vacuum gap results in negligible heat loss by conduction which is a notable advantage of VMD. A schematic representation of this configuration is reported in Figure 22. It should be mentioned that supplementary electrical power is demanded by the operation of the vacuum pump [49].

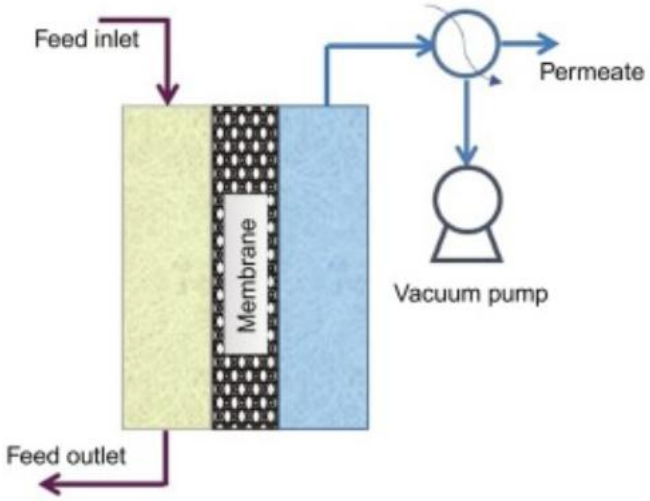


Figure 22: VMD configuration [49]

Advantages and drawbacks

MD is particularly attractive for offshore platforms because it's modular, lightweight and utilizes polymeric membranes that do not suffer from galvanic corrosion. The gentle operating conditions along with utilizing highly resistant membranes in MD, lowers the susceptibility to fouling and scaling – a major drawback of membrane-based operations – which reduces

maintenance costs. Also, due to the fact that the process is not driven by high absolute hydraulic pressure (like in reverse osmosis) and incorporates larger membrane pores compared to other membrane techniques, the risk of clogging is lowered, which eliminates the need for intensive chemical pretreatment of water before entering the modules [49]. Furthermore, it features a lower physical footprint and can operate at lower hot-feed temperatures than conventional Vacuum Thermal Distillation (VTD).

Despite the extensive interests of scientific community in MD technology and its application in desalination, there are some engineering drawbacks which have hindered its up-scaling process. The main barrier is lack of long-term membrane fabrication and module design that can simultaneously enhance permeation flux and provide low wettability. Another issue in the way of commercializing MD is complexity of energy consumption and economics, considering the fact that operating conditions in the MD process differ considerably from bench-scale to larger-scale due mainly to the significant variation of temperatures through the MD module itself. Other localized challenges include pore wetting, conductive dissipation, permeation rate decay[2] due to temperature polarization[3], long term performance and flux stability.

3.5.5 Comparative analysis

To provide a comprehensive overview of the thermal desalination pathways suitable for low-enthalpy geothermal integration, a qualitative comparative screening between Vacuum Thermal Distillation (VTD) and Vacuum Membrane Distillation (VMD) is established.

The primary thermodynamic divergence between the two technologies lies in their thermal sensitivity and structural configuration. VTD relies on a high-temperature threshold (70-75°C). to feed its single-effect evaporation plates under a deep vacuum shell, resulting in intensive localized geothermal resource exploitation and limited reservoirs availability. Conversely, VMD couples a vacuum-assisted permeate channel with a membrane-controlled vapor transport

[2] Permeation rate decay: the decline in the speed or volume at which the target vapor/fluid passes through the membrane.

[3] Temperature polarization: the formation of a thermal gradient where the temperature of the fluid right at the membrane surface is much lower than the temperature in the main fluid "bulk". It happens because the phase change (e.g., liquid evaporating into vapor) absorbs heat faster than the fluid can replenish it.

mechanism, allowing the system to operate efficiently at lower geofluid temperatures (55-65°C).

From a material perspective, VTD requires high-grade titanium plates to mitigate the severe galvanic corrosion risks triggered by the hyper-saline boiling environment, whereas VMD inherently avoids corrosion mechanisms by using lightweight, modular advanced polymers. However, VMD faces specific challenges regarding membrane pore wetting, temperature polarization, and lower commercial diffusion compared to the mature industrial benchmark represented by VTD.

The key qualitative design parameters are summarized and compared in Table 4.

Table 4: Comparison between different technologies for thermal distillation

Feature	Vacuum Thermal Distillation (VTD)	Vacuum Membrane Distillation (VMD)
Driving force	Vacuum-induced boiling & pressure gradient	Thermal gradient (vapor pressure) assisted by vacuum
Thermal requirement	Higher temperature required (70-75°C)	Flexible low temperature (55-65°C)
Maturity	Industrial benchmark (mature)	Innovative/Emerging
Corrosion risk	Managed via expensive titanium plates	Absent (polymeric membranes and frames)
Footprint	Moderate	Low (highly modular)
Main issues	Vacuum maintenance, scaling, heavy metallic weights	Membrane fouling, pore wetting, low market diffusion

3.6 Geothermal-assisted aquaculture

Aquaculture is one of the most promising sectors for offshore platforms because it is an increasingly important contributor to economic growth and global food supply. While it includes fish, molluscs, and seaweed cultivation, this section focuses primarily on fish production, as it is the most suitable application for geothermal heat integration. However, a brief reminder of seaweed cultivation in offshore context will be presented to have a global view of this sector.

3.6.1 Aquaculture for fish production

Aquaculture is the fastest-growing animal food-producing sector on the planet. While capture fisheries production decreased by 2.6% from 1992 to 2012, aquaculture's contribution to the global supply rose from 15% to 42% [51].

Shifting from nearshore to offshore farms offers significant environmental and operational benefits. At offshore sites, a greater water exchange makes it easy to remove farm waste and offers better salinity stability. Furthermore, larger and deeper cages that are located further offshore would provide a safer environment for some European species, such as seabass and seabream [51].Offshore fish farms have the potential to develop and increase organic production.

Despite the benefits, there are environmental concerns regarding moving fish farms offshore such as nutrient and chemical pollution, habitat damage, disease introduction, and the interbreeding of wild stock with escapees from farms. The productivity of a farm depends on location choice, and so spatial planning is required to ensure that farms have no impact on their surrounding ecosystems and to ensure the sustainable growth of offshore aquaculture. In addition, offshore farms can be exposed to wild predators such as otters, sea lions, seals and birds. Lastly, there are higher costs for farm operations with offshore aquaculture [51] and the requirement to use large and complex fish pens in order to withstand the exposed – more challenging environment.

In recent years, many offshore fish pen designs have been proposed, and some have been built and deployed. They range from structurally advanced versions to submerged structures, and

some have even integrated offshore fish pens with offshore renewable energy production devices [52]. However, a consensus has not been reached as to which of these new offshore design concepts will become globally accepted and give confidence in sustainable and profitable offshore fish farming to the aquaculture operators [52].

3.6.2 The role of geothermal energy and fish biology

The integration of geothermal energy in aquaculture has grown over the last 25 years in similar sectors like greenhouses, agro-industrial processes, and fish farming [53]. Temperature is a critical factor as it directly affects fish metabolic processes such as circulation, food intake, digestion, growth and bio-energetical re-acclimation [54]. For the most common Mediterranean species (sea bass and gilthead sea bream), the optimal range is approximately 18-26°C [55]. In comparison, salmon prefers 16–18°C [54]. Geothermal heat allows these optimal conditions to be maintained year-round, significantly accelerating growth cycles.

Successful production depends on maintaining specific farming conditions. The stocking density should not exceed 13-15 kg/m^3 for sea bass and gilthead sea bream in the seawater phase to minimize injury and stress [55]. In the context of water quality, dissolved oxygen levels and current velocities (which affect swimming patterns and schooling) must be strictly controlled [54]. Maintaining high dissolved oxygen (DO) levels is critical, especially when geothermal heat is used to increase water temperature (as oxygen solubility decreases with temperature). The best approach is to use an oxygenation system that generates microbubbles for highly efficient oxygen dissolution (e.g. SOLVOX Oxystream [56]). However, it’s necessary to provide oxygen to the platform. The final phase of the aquaculture is related to harvesting. To ensure welfare and quality, electrical stunning is recommended for Mediterranean species, followed by transfer into ice slurry [55].

A comprehensive offshore aquaculture model must also consider the early life stages of the fish. While the grow-out phase occurs in large seawater cages, the initial stages (hatchery and nursery) traditionally require freshwater. On a repurposed platform, this could be achieved by utilizing the permeate produced by the Reverse Osmosis (RO) or thermal desalination units. These early stages can be hosted in specialized indoor tanks on the platform's deck, where geothermal heat ensures the precise thermoregulation required for fry development. This "on-

board lifecycle" minimizes the logistical risks associated with transporting juvenile fish from the mainland.

3.6.3 Infrastructure, logistics and the Italian context

An offshore fish farm is a complex system comprising steel structures, mooring systems, automatic feeding barges, and monitoring units (video/audio) [54]. Modern closed-system plastic tanks are increasingly used to prevent waste and feed residues from polluting the seabed [57]. A well-engineered chamber and pumping system allows the fish to swim in the current, and the amount of food can be optimized. Additionally, pipelines are needed for water treatment and food transport [57]. Concerning aquaculture, after selecting the most promising species for the area, it is necessary to identify the kind of cages and their mutual position, the feeding system, the maintenance requirements and the general management [58].

To optimize logistics and mitigate environmental issues at coastal landing sites (such as odors and waste accumulation), primary processing (gutting and cleaning) can be performed directly on the platform. This can have a double benefit, because both waste valorisation and logistic improvement are present. Indeed, if fish viscera and processing scraps are not discarded, they can be treated via anaerobic digestion or used to produce high-value fish oils and fertilizers. Moreover, cleaning the fish on board reduces the weight of the transported product leading to lower fuel consumption for transport vessels.

The following basic requirements should be taken into account when installing and operating a Sea Bass fish farm [59]:

- In order to secure a good waste dilution to the fish stock, the water depth at the site should ideally be around 30 m or deeper, in presence of a significant water current. The minimum required depth by the Italian legislation is 20 m.

- Individual cages must be as far as possible from the nearest cages, to allow good circulation of clean water between and within cages.

- Sedimentary bottoms are preferred, due to the reduced impact on benthic biocenosis[4] and to the greater ease of mooring installation and tensioning.

The Italian scenario

Italian aquaculture is grown as a very diversified activity thanks to the high environmental diversification that characterize the territory. The national market is interested mainly at the sea bass, gilt-head bream and eels production [60].

In the rather warm Mediterranean Sea, fish farming is the most promising offshore activity from an economic point of view, due to the use of mature and reliable technologies and to the mild water temperature. However, the shift of fish-farming from near-shore to offshore may cause a relevant social opposition due to the many operating traditional factories.

In the specific case of the “Amelia B" platform, offshore aquaculture has been already successfully tested in the area through mussel collection on platform legs, involving local fishermen [58].

3.6.4 Environmental impact and mitigation

Effluents from fish farms contain undigested feed, metabolic excretions, faeces (solid organic waste), and dissolved organic and inorganic nutrients composed largely of carbon, nitrogen, and phosphorus. If the flow of these compounds released into the environment exceeds the natural assimilation capacity of a body of water, ecological changes can occur in both the water column and the sediment, causing, as a consequence, phenomena of eutrophication, reduction of dissolved oxygen, increased turbidity, and alterations to microbenthic communities in the sediment [60].

The extent of the ecological impact depends primarily on the physical and oceanographic conditions of the site, seawater temperature, and dissolved oxygen concentrations, but also on the size of the facilities, the biomass being farmed, and the management practices used. In the case of marine cage facilities, a simple study of the site's hydrodynamic characteristics can

[4] Benthic biocenosis: it refers to a specific, naturally occurring community of living organisms (plants, animals, and microorganisms) that inhabit the seafloor or the bottom sediments of a body of water (the benthic zone).

provide important information. To allow the widest distribution of organic effluent on the sediment, it is advisable to choose areas with high current velocities or with a distance between the bottom of the cage and the seabed greater than twice the height of the cage itself [60]. In these cases, the impact of organic matter on the sediment and macrobenthic communities is limited to a localized area of 30-50 meters around the cages and is unlikely to cause significant changes on a larger scale.

3.6.5 Seawood cultivation

Seaweed farming is an emerging sector, often integrated into the "Multi-Use" framework alongside offshore wind farms (e.g. North Sea Farm #1) [61]. Although large-scale offshore seaweed farming currently faces high CAPEX and technical challenges due to rougher seas, it offers a sustainable source for proteins, fertilizers, and biostimulants [62]. Integrating seaweed near fish cages (Integrated Multi-Trophic Aquaculture) could further improve circularity by absorbing excess nutrients from fish waste.

3.7 Repurposing for artificial reefs

Differently from the other proposed scenarios, repurposing as artificial reef doesn't exploit geothermal resources. While this pathway doesn't generate direct economic revenues from energy or products, it avoids the high costs of total platform removal and prevents the destruction of the established ecosystem beneath the structure. This scenario is particularly suitable for "minor" platforms with limited deck surface (mono and bi tubular structures) that cannot host complex industrial equipment.

The submerged steel lattice structures, known as "jackets", provide a hard substrate that attracts large numbers of invertebrates. In turn, these creatures attract various fish species, creating a self-sustaining ecosystem. Studies indicate that these steel structures, once colonized, can maintain their structural integrity against corrosion for several centuries [63].

3.7.1 Different modes of artificial reef creation

Artificial reef can be created through three general methods [64]:

1. Tow-and-place: it involves severing the structure from the sea floor either using explosives or mechanical cutting techniques and then towing it to the selected reef for deployment.

2. Topple-in-place (Toppling): it involves detaching the structure from the seabed and then toppling it onto its side.

3. Partial removal (Topping): generally, it does not use explosives. The top portion of the structure is severed at a permitted navigational depth, typically around 26 m deep, and placed on the sea floor next to the base of the remaining structure.

In all three configurations, the deck is always removed and brought to dry land to be dismantled or recycled. Figure 23 provides a visual representation of these configurations.

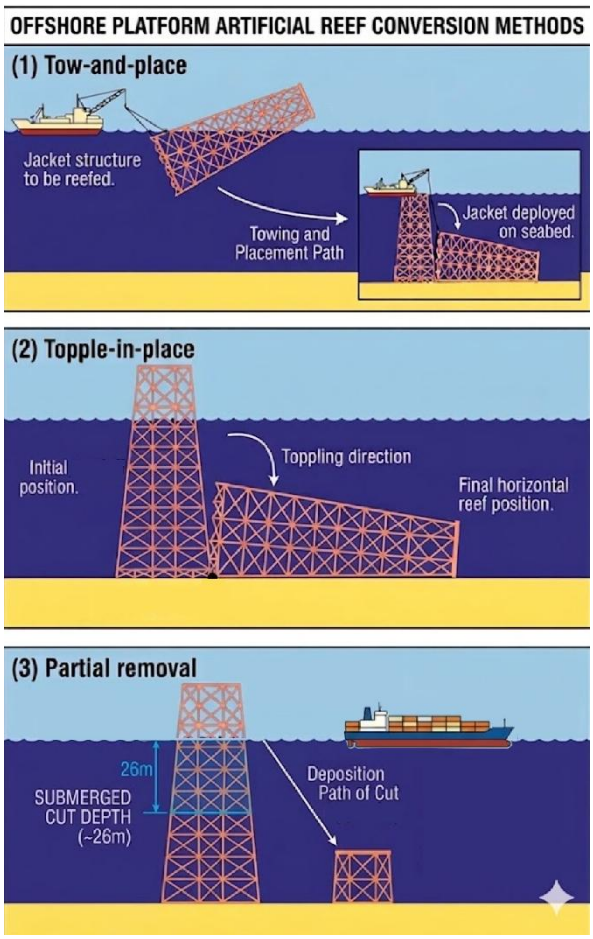


Figure 23: Offshore platform artificial reef conversion methods [64], AI generated image

It is important to underline that not all platforms are suitable for reefing: there're engineering and environmental standards for converting a platform to a permanent artificial reef. Platform size, complexity, structural integrity and location are key considerations in evaluating its reefing potential. Complex, stable, durable and clean platforms (free from hazardous materials) are generally the best candidates for reefing [64].

3.7.2 The Gulf of Mexico and California cases

Since the 1980s, over 600 structures in the Gulf of Mexico have been successfully converted into artificial reefs [64]. These platforms have seen a significant increase in fish numbers, becoming popular fishing and diving sites. In contrast, in California, fishing is prohibited in most areas surrounding the production platforms: it is therefore not unreasonable to believe that for decades they have served as protected marine reserves, benefiting especially the most exploited species [63].

3.7.3 The Italian example: the Paguro wreck

The Paguro wreck originated from a jack-up platform that sank in 1965, supplemented since 1990 by other decommissioned structures relocated to the site. Today, it is a recognized hotspot of biodiversity and, since 2019, has been protected as a Special Area of Conservation (SAC). Currently, recreational scuba diving is the only commercial activity allowed in the area. The wreck and the decommissioned structures act as an artificial reef, supporting a complex trophic net and diverse fauna. The holistic approach applied to the Paguro study case empowers its attitudes to scientific research, promotes local tourism and encourages its conservation by also engaging the larger public of non-scuba divers. The Paguro experience serves as a foundational model for reusing Oil & Gas assets to enhance marine ecosystems and foster the Blue Economy through new sustainable business opportunities [63].

Since the Italian seabed is generally shallow the Partial Removal configuration could be problematic due to insufficient bathymetry for navigation safety. Among the proposed methods, the Tow-and-place configuration appears most useful for the Italian context especially if several small platforms are grouped to create a "super-reef", similar to what was partially achieved with the Paguro site.

3.8 Multi-Use Platforms Approach

A Multi-Use Platform (MUP) can be defined as a marine area that combines different activities such as aquaculture, tourism, transportation, energy production and oil and gas operations. These activities can be completely integrated into a single shared structure or simply co-located with the same marine space. Integrating different functions allows for significant benefits such as lowering installation and maintenance costs, increasing resource utilization and reducing the environmental impact [51].

3.8.1 Potential offshore energy resources

To achieve a true multi-use approach, it is necessary to integrate energy production on the platform. Some studies have proposed the combining of marine energies as a better alternative instead of using a single source of energy. Proposed methods include [51]:

- Wind, wave, and tidal energy converters.
- Floating solar farms.
- Ocean thermal energy converter (OTEC).
- Marine biomass energy.

Regarding marine biomass, algae can produce various biofuels including biodiesel, bioethanol, biogas and bio-jet fuels. Although these are still not economically feasible due to the high costs of the operation, cultivation, processing, and separation of biofuels, integrating algae farms into offshore MUPs could improve the technology's efficiency and make it available on a commercial scale.

In practice, several barriers are hampering the implementation of MUPs, ranging from regulatory, financing, liability and insurance issues to environmental concerns, stakeholder perceptions and lack of appropriate skills. Currently, there are very few examples of multi-purpose installations, typically in connection with offshore wind farms [59].

When converting a platform into a MUP, especially in the context of the Adriatic Sea, certain challenges must be considered [59]:

- Lower energy density: the area is characterized by the lower marine energy potentials compared to other parts of the Mediterranean; therefore, a single purpose installation for energy conversion is unlikely to be economically feasible.

- Spatial conflicts: the presence of well-developed infrastructure including harbours, commercial and touristic maritime routes, suggests possibles potential conflict of use.

3.8.2 Mineral extraction from brine

In geothermal energy production, hot mineral-rich brine is pumped from deep underground formations to the surface. In addition to its use in energy production, this brine offers the potential to extract valuable coproduct minerals such as lithium (in Europe and United States), silica (in New Zealand), helium (in China), as well as zinc, manganese and other critical raw materials [53]. This extraction process adds another layer of circularity to the MUP approach, turning a byproduct into a strategic resource.

There's also another mineral-rich brine that can be used. It's the one that comes outside the desalination process. This could be a strong advantage because using the same machinery it's possible to extract more minerals starting from different inputs.

3.8.3 Example of MUP starting from the proposed scenario

A good example of MUP in this context is based on the use of geothermal heat extracted from the depleted reservoir, this thermal energy is used for the desalination process and the freshwater produced is used for fish farm. Moreover, the harvesting process produces waste that can be further used to produce biofuels. This proposed scenario further underlines the circularity of the MUP approach.

3.9 Summary of pre-feasibility scenarios for platform repurposing

Scenario	Chemical & Thermal parameters			SEC	Operational needs			Environmental & Safety		Resource & Technology	
	Chemical reaction/Process	T (°C)	p (bar)	Heat/ Energy	Substances	Area	Structural Aspects	Criticalities	Circularity	Geothermal exploitation	Maturity*
Biologic methanation	$CO_2 + 4H_2 \rightarrow CH_4 + 2H_2O$	25-65	1-10	Thermal - 100% geo-thermal + Electric	CO_2, H_2, nutrients, freshwater	Medium	Moderate weight, gas tanks required	Bacterial sensi-tivity to changes in T and pH, CO_2 and H_2 management	High (CO_2 valorisation, closed carbon loop if renewable H_2)	High	Medium
LOHC Hydrogenation (DBT)	$C_{21}H_{20} + 9H_2 \rightarrow C_{21}H_{38}$	150-200	10-50	Electric + high-T thermal (geother-mal preheat + auxiliary boiler)	Catalysts (Pt/Al), DBT, H_2	Medium	Pressure reactors, heat exchangers, auxiliary boiler	High exothermicity of the reaction	Medium (reusable carrier but degradation losses and catalyst impacts)	Low-medium (preheat)	Medium
NH_3 production	$N_2 + 3H_2 \rightarrow 2NH_3$	250-400	100-200	Electric + high-T thermal (geother-mal preheat + auxiliary boiler)	Catalysts, air (N_2), H_2	High	Pressure reactors, heat exchangers, auxiliary boiler	High toxicity of NH_3, high p and T (explosion/ corrosion risk)	Low-Medium (depends on N_2 source and H_2 origins)	Low (pre-heat)	High
Reverse osmosis	Filtration (mechanical) DF: pressure gradient	20-40	50-70	Electric mainly + geothermal heat only to preheat feed water	Sea water, filters, additives	Medium	Pre-treatment unit, vibration management, high pressure pumps, fresh-water storage tanks	Brine disposal, high noise, high power demand, sensitive mem-brane (fouling), concentrate-brine disposal	Medium	Low (not tempera-ture-driven, only indirect via electricity)	Standard technology
Vacuum thermal distillation	Evaporation/Condensation DF: pressure gradient	60-90	0.15	Thermal - 100% geo-thermal + Electric	Seawater, antiscalants	High (big heat exchangers)	High weight due to water tank	Scaling in heat exchangers,	Medium	High	Standard technology

								concentrate-brine disposal			
Membrane distillation	Evaporation/Condensation DF: thermal gradient	55-85	0.3	Thermal - 100% geo-thermal + Electric	Seawater, antiscalants	Small	Compact modules (skid)	Pore-wetting, concentrate-brine disposal	Medium	High (70-80°C)	Emerging / Pilot scale
Thermally assisted fish farming	Fish growth & metabolic acceleration (Biological)	20-30	Ambient	Thermal - 100% geo-thermal + Electric (pumps, feeding)	Oxygen, feed, fingerlings	High (the area around the platform is occupied by cages, this may restrict vessel circulation)	Large tanks, high weight load	Oxygen depletion, waste management, species escape, spread of diseases, logistics	High (nutrient recycling)	High (direct use)	High for cages, Medium for offshore thermal integration
Artificial reef	Habitat restoration	Ambient	Hydrostatic	None (passive habitat)	None (recycled steel)	None (passive habitat)	Submerged jacket structures	Potential invasive species	100%	Absent	Very high

DF: Driving Force
SEC: Specific Energy Consumption

* Maturity level is evaluated based on onshore applications, as the proposed processes were selected for their ability to exploit waste heat rather than their current offshore presence (excluding reverse osmosis, thermally assisted fish farming and artificial reef scenarios). Regarding hydrogen-based technologies, their implementation is significantly limited by the logistic challenges of offshore production and transport. Consequently, numerical data are often scarce and primarily based on pre-feasibility studies rather than established industrial operations.

Since the focus of this project is geothermal exploitation, it's reasonable to underline a common criticality for all the scenarios that use the geothermal reservoir. The main criticality is the chemical corrosion of caused by underground brines that can contain H_2S or CO_2. This requires the use of special steels (inox or duplex) or expensive corrosion inhibitors (this topic was addressed in Section 2.3.2).

4 Thermodynamic performance and energy assessment of reconversion scenarios

In the previous chapter, several technologies were investigated from a qualitative perspective, focusing on their fundamental working principles, state-of-the-art developments, and main operational criticalities within an offshore context. The next step consists in translating these qualitative insights into engineering data**.** The purpose of this chapter is to execute a rigorous quantitative comparative analysis of the proposed configurations. Specifically, the assessment focuses on their mass balances, electrical and thermal requirements, and localized geothermal exploitation potential, alongside the definition of a preliminary plant layout for each technology. To ensure a coherent and thermodynamically sound comparison between highly heterogeneous processes, a standardized set of invariant project boundaries and baseline constraints has been established and will be presented in the following section. The quantitative engineering outputs obtained in this section will serve as the raw, objective inputs for Chapter 5, where the core challenge shifts from simple sizing to the formulation of a structured decision-making methodology to mathematically select the best overall reconversion pathway.

4.1 Definition of the project framework and constraints

The overall conceptual boundary conditions and core infrastructure of the integrated platform are schematically mapped in Figure 24. This structural block diagram identifies the primary subsystems and logistics analysed across the decommissioning and reconversion projects. For each distinct technology detailed in the subsequent sections, specific operating parameters, including localized stream temperatures, pressures, and mass flow rates, will be uniquely defined and quantified.

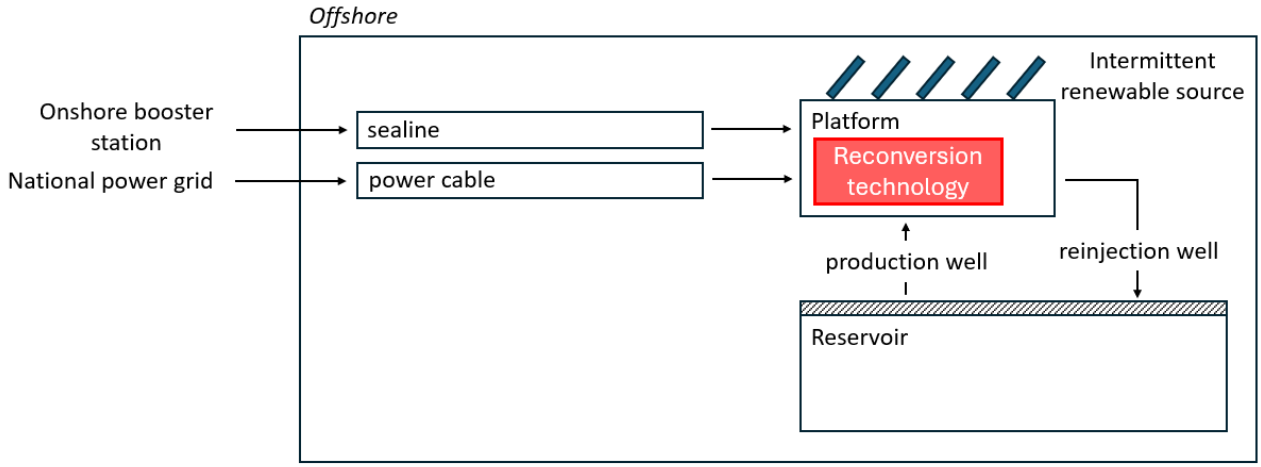


Figure 24: Overall block diagram of the platform plant configuration

While offshore assets are conventionally linked to the mainland power grid via subsea high-voltage cables to ensure a stable electrical supply, this study evaluates two distinct operational power regimes to reflect different future energy transition strategies. On one hand, a continuous mainland grid supply configuration is considered, operating under stable steady-state conditions with minimal system shutdowns. On the other hand, a prospective decentralized off-grid scenario is modelled, where the reconverted platform is powered entirely by localized, weather-dependent marine renewable sources (such as offshore wind or solar arrays). The inherent volatility of these intermittent sources forces the integrated facilities to undergo frequent operational transients and shutdowns. To rigorously address these dynamic conditions, both operational cases – frequent intermittent supply versus continuous supply – are formally defined and quantified in Section 4.2.5.

Regarding the geothermal resource configuration, the fluid is characterized by a baseline temperature of 75°C within the deep reservoir. To account for wellbore heat dissipation during the fluid ascent along a nominal 2 km well string, a conservative thermal loss of 10°C was implemented, resulting in an available brine temperature of 65°C at the platform deck utilities.
A preliminary screening of the Italian offshore asset indicates that only 7 existing infrastructures (excluding light monotubular structures) are connected to reservoirs exhibiting a temperature strictly above 75°C. However, this geofluid constraint presents significant margins for optimization; by minimizing wellbore thermal losses through advanced insulation and

by extending the feasibility boundary to include reservoirs with an initial water temperature above 70°C, the total pool of candidate platforms expands significantly to 17 structures.

To evaluate the engineering feasibility of platform repurposing, the quantitative analysis investigates seven technological pathways grouped into two macro-categories based on their thermodynamic coupling with the geothermal resource:

- **Synthesis of chemical energy carriers (Biological methanation, LOHC Hydrogenation, and Ammonia production):** these processes occur within dedicated reactors driven by catalytic or biological pathways. While these synthesis reactions are strongly exothermic under steady-state continuous operation, they require a thermal power input during the transient start-up phase to lift the structural reactor mass and the chemical reactants to their specific activation temperatures. This start-up thermal duty represents a singular localized energy investment, as the system becomes thermally self-sustaining or net-heat-exporting during steady-state operations.

- **Marine based and desalination pathways:** applications that absorb low-enthalpy geothermal heat on a continuous baseload operation. This category includes three desalination configurations for freshwater production (Reverse Osmosis, Vacuum Thermal Distillation, Membrane Distillation) driven by hydraulic or phase-change forces, alongside thermally assisted fish farming, where continuous geothermal heat maintains optimal metabolic water temperatures for biomass growth.

4.2 Energy and mass balances for chemical synthesis scenarios

To establish a baseline for the chemical synthesis configurations, the mass and molar flow rates of the primary chemical reactants were systematically determined. A major operational constraint concerns the logistics of hydrogen (H_2) supply. To minimize space requirements, equipment weight, and parasitic electrical consumption on the offshore platform, H_2 compression is assumed to be performed entirely at the onshore booster station prior to injection into

the subsea pipeline (*sealine*). Consequently, the H_2 temperature remains constant at approximately 15°C, matching the steady temperature of the seabed, while its delivery pressure is dynamically adjusted onshore to satisfy the specific structural and operating requirements of each offshore reactor network.

To ensure a consistent, rigorous, and scalable thermodynamic comparison across highly diverse chemical pathways, a baseline hydrogen mass flow rate of **9.09 kg/h (4.54 kmol/h)** is established as the invariant constraint for all the subsequent synthesis scenarios investigated in this study.

Hydrogen supply strategy

Regarding feedstock sourcing, previous offshore hydrogen production studies indicated that a 1000 m^2 photovoltaic (PV) array can yield approximately 3500 kgH_2/year under Mediterranean conditions. However, the available weather deck surface of a typical platform in Adriatic Sea (GREEN1) is constrained to 440 m^2, restricting the local green hydrogen production rate to roughly 1700 kg/year (equivalent to a continuous rate of approximately 0.2 kg/h, assuming 7960 h/year of operation).

This localized production rate is insufficient to meet the baseline chemical demand of 9.1 kg/h established in this study. To overcome this spatial limitation, a co-feeding configuration – combining local PV-driven electrolysis (0.2 kg/h) with stored hydrogen extracted from the geological reservoir (8.9 kg/h) – represents a promising prospective development for the model. However, to maintain a conservative operational baseline for the current study, a full shore-based supply delivered via the subsea pipeline is selected as the primary investigated option.

4.2.1 Thermodynamic and technical feasibility of Biological Methanation

To verify the thermodynamic and technical feasibility of the proposed Trickle Bed Reactor (TBR) configuration, a preliminary mass and energy balance was performed. While biological methanation processes are generally characterized by operational ranges in literature, the design values for the current system were simplified by adopting the average thermodynamic parameters, resulting in a fixed reactor temperature of 55°C and an operating pressure of 10 bar.

The baseline reference flow rate of captured CO_2 is derived from the storage basic design analysed by F. Pertuso "*Conversion of an Oil & Gas platform and the associated depleted reservoir into a carbon dioxide storage plant. Basic design.*" [65], which establishes a continuous daily injection of 1.43 tons/day (59.6 kg/h). To ensure an operational buffer and absorb process fluctuations, a steady-state design flow rate of 50.0 kg/h (1.14 kmol/h) was selected for the reactor feed, requiring a stoichiometric hydrogen input of 9.09 kg/h (4.54 kmol/h). The theoretical biomethane (CH_4) production is 18.2 kg/h.

A critical engineering challenge emerges from the physical supply conditions and the extreme pressure drops associated with CO_2. The CO_2 is back-produced from the depleted reservoir as a supercritical fluid at a pressure range of 79-145 bar [65], while the H_2 is imported via sealine at approximately 15°C (seabed temperature) and 20 bar. Since both feeds are available at pressures well above the reactor operating pressure (10 bar), the parasitic electrical consumption for gas compression is completely eliminated. The only auxiliary electrical load is the liquid recirculation pump which circulates the water solution containing nutrients within the trickle bed. Assuming a design volumetric flow rate of 1.5 m^3/h and the pump head of 6 m, the recirculation loop requires a negligible power input of approximately 0.04 kW_{el}.

Regarding the thermal balance, the geothermal energy required during the transient **start-up phase** must account for the sensible heat of both the liquid bulk and the gaseous feeds. Assuming a reactor volume of 2 m^3, heating the initial water volume over a 24-hour cycle requires approximately 4 kW_{th}. Additionally, before entering the TBR, the high-pressure CO_2 must undergo a depressurization step down to 10 bar. Due to the Joule-Thomson effect, this isenthalpic expansion causes the gas temperature to drop significantly to approximately $-25°C$. For preliminary feasibility purposes, hydrogen is assumed to be delivered to the offshore platform at conditions compatible with reactor injection pressure. Therefore, no dedicated expansion or compression stage for H_2 was considered in the present analysis. Preheating the gaseous reactants from their inlet conditions up to the thermophilic reaction temperature (55°C) requires an additional net thermal lift of 2.7 kW_{th}, resulting in a total start-up thermal duty of 6.6 kW_{th}.

Conversely, during the continuous **steady-state operational phase**, the biological Sabatier reaction is strongly exothermic, releasing 165 kJ of thermal energy per mole of reacted CO_2. At

the design flow rate, this synthesis generates a continuous thermal power output of 52.1 kW_{th}. Consequently, the thermal management strategy undergoes a strategic reversal: the external jacket shifts from a heating utility to a heat-recovery application. The exothermic heat is continuously recovered by an auxiliary cooling loop (e.g., leveraging the raw seawater feed that could be used for the desalination unit), thereby stabilizing the biological culture at 55-60°C and preventing thermal runaway.

Finally, to assess the impact of this transient thermal demand on the geothermal asset, the required geothermal brine volumetric flow rate was calculated. Assuming an inlet temperature of 65°C at the platform deck and a 5°C temperature drop across the reactor's jacket, the maximum start-up thermal load of 6.6 kW_{th} requires a brine flow rate of just 1.13 m^3/h. This low flow requirement confirms that the thermal baseline of the methanation unit is fully sustainable for a 2 m^3 reactor, leaving the possibility to use multiple modular reactors to better exploit the potential of the reservoir.

To provide a clear and intuitive visualization of the proposed plant layout, a simplified process flow diagram is illustrated in Figure 25. This schematic framework is intended to map the overall system configuration, highlights the primary mass streams, and explicitly tracks the operational temperatures and pressures across each stage.

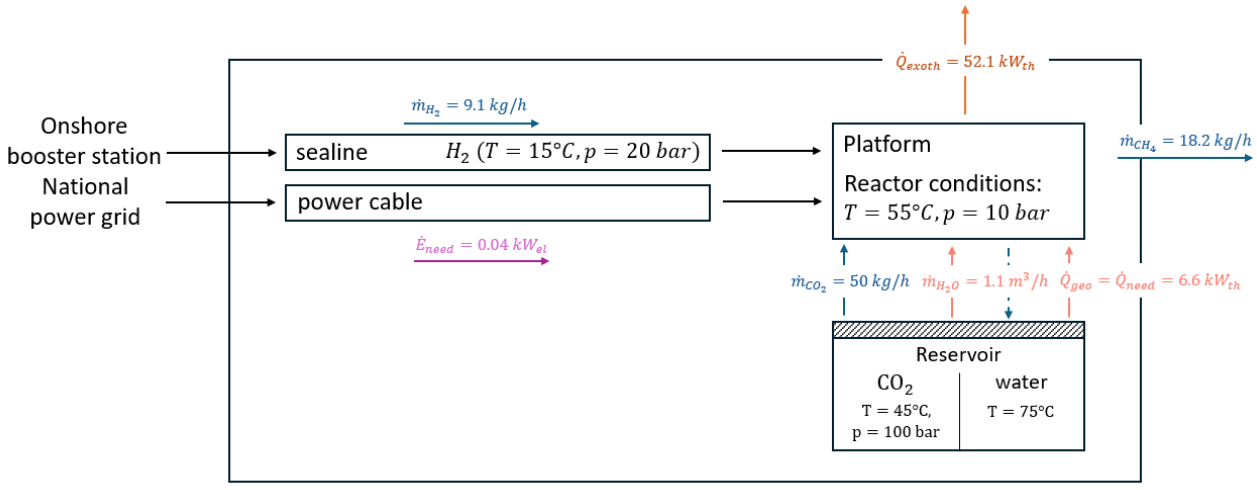


Figure 25: Simplified process flow diagram of the biological methanation scenario

The results of this screening analysis are summarized in Table 5:

Table 5: Quantitative summary of the mass, thermal, and electrical results for the biologic methanation system

Parameter	Value	Unit	Note / Source
CO_2 input design flow rate	50.0	kg/h	Derived from basic design
H_2 required flow rate	9.1	kg/h	Stoichiometric ratio (4:1 molar)
CH_4 theoretical production	18.2	kg/h	Biomethane synthesis output
CO_2 storage pressure range	79-145	bar	Subsurface reservoir conditions
Reactor operating pressure	10	bar	Biological thermophilic standard
CO_2 post-expansion temperature	-25	°C	Calculated via isenthalpic Joule-Thomson flash
Total start-up thermal duty	6.6	kW_{th}	Covered by Geothermal Fluid
Geothermal fluid mass flow rate	0.3	kg/s	Mass flow rate necessary to satisfy the geothermal start-up thermal duty
Geothermal coverage share	100	%	Given by the ratio between the heat given by the geothermal source and the total heat required
Steady-state exothermic heat	52.1	kW_{th}	Released by reaction (to be removed)
Gas compression electrical power	—	kW_{el}	H_2 is supplied via sealine directly at reactor operating pressure. The high-pressure CO_2 is depressurized from the reservoir, eliminating any requirement for auxiliary gas compression power

Parameter	Value	Unit	Note / Source
Recirculation pump electrical power	0.04	kW_{el}	Calculated for liquid recycling (H = 6 m, Q = 1.5 m^3/h)

4.2.2 Thermodynamic and technical feasibility of LOHC hydrogenation

To evaluate the thermodynamic and technical viability of the Liquid Organic Hydrogen Carrier (LOHC) system, a preliminary mass and energy balance was performed, using the same baseline hydrogen flow rate 9.09 kg/h (4.55 kmol/h) to maintain cross-technology consistency. Based on stoichiometric calculations for the hydrogenation of dibenzyltoluene (DBT), the required inlet flow rate of the lean oil ($C_{21}H_{20}$) is 138 kg/h yielding a rich LOHC product flow rate ($C_{21}H_{38}$) of 147 kg/h at the reactor outlet.

The thermal balance of the process is highly dependent on the operational phase. During the **start-up phase**, thermal energy must be supplied to overcome system inertia and heat the reactants from an ambient temperature of 15°C up to the catalytic reaction temperature of 170°C. Preheating the continuous feeding streams across this $\Delta T = 155\ K$ gradient requires a thermal power of 18.1 kW_{th}. Additionally, to account for the substantial thermal inertia required to heat the mass of the reactor shell and to compensate for localized thermal dissipation (radiation losses) during this initial heating phase, a precautionary oversizing factor of 30% is applied to the calculated fluid preheating duty. Consequently, the total cumulative start-up thermal duty required from the external heating utility is established at 23.5 kW_{th}.

Conversely, during the **steady-state operational phase**, the catalytic hydrogenation is strongly exothermic, releasing 65.4 kJ of energy per mole of consumed H_2. At the design capacity, this chemical pathway generates a continuous thermal power output of 82.7 kW_{th}.

From an electrical consumption perspective, the system layout benefits from strategic upstream optimization. The H_2 feed is assumed to reach the platform directly at the required operating pressure (30 bar). By adjusting the thermodynamic properties onshore, the need for heavy compression infrastructure offshore is eliminated, mitigating space and operational

constraints. Furthermore, since the organic carrier remains in a single liquid phase and undergoes a single-pass conversion, no gas-liquid recycling loops are necessary, reducing the fluid recirculation electrical consumption to zero.

To provide a clear and intuitive visualization of the proposed plant layout, a simplified process flow diagram is illustrated in Figure 26. This schematic framework is intended to map the overall system configuration, highlights the primary mass streams, and explicitly tracks the operational temperatures and pressures across each stage.

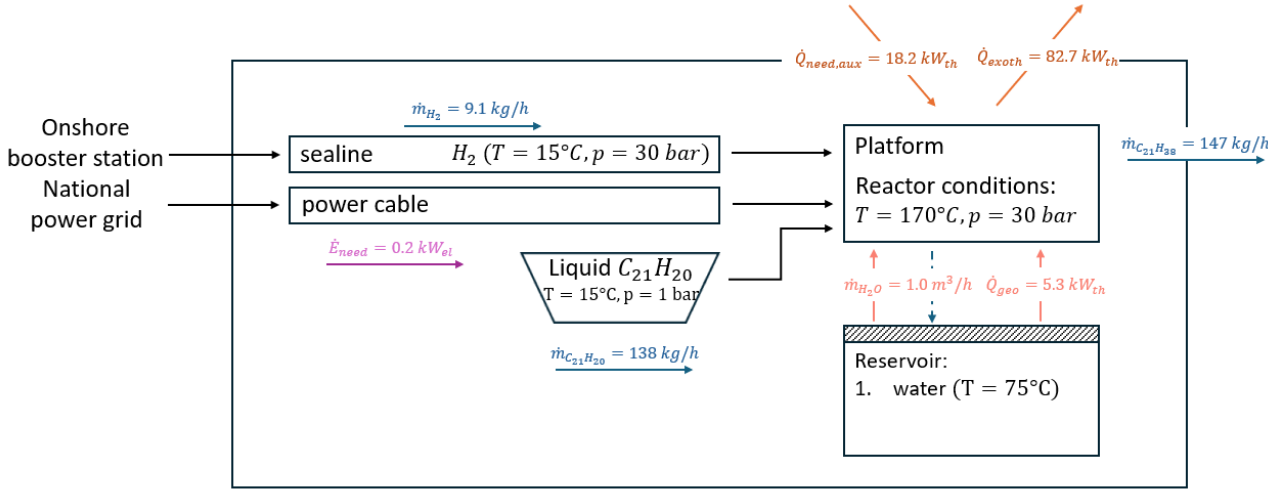


Figure 26: LOHC hydrogenation simplified process flow diagram

To maximize efficiency, the low-enthalpy geothermal source (70°C) is integrated to supply the initial share of the preheating load. The geothermal fluid can safely heat the cold reactants up to an intermediate temperature of approximately 60°C, while the remaining high-temperature thermal lift up to 170°C is supplied by an auxiliary thermal oil loop. Therefore, the total continuous thermal power required $\dot{Q}_{tot}$ can be decomposed into two distinct contributions:

$$\dot{Q}_{tot} = \dot{Q}_{geo} + \dot{Q}_{aux}$$

Where:

- $\dot{Q}_{geo}$ is the thermal power provided by the geothermal brine for the initial preheating stage;
- $\dot{Q}_{aux}$ is the thermal power required to reach the operating temperature.

The effective coverage share of the geothermal source (η_{geo}) within the LOHC architecture is evaluated as the ratio between the geothermally supplied heat and the total thermal demand:

$$\eta_{geo} = \frac{\dot{Q}_{geo}}{\dot{Q}_{tot}}$$

Finally, to satisfy the required $\dot{Q}_{geo}$ baseline, the necessary mass flow rate of the geothermal brine ($\dot{m}_{geo}$) extracted from the well is quantified through the standard energy balance:

$$\dot{m}_{geo} = \frac{\dot{Q}_{geo}}{c_{p,w} \cdot \Delta T_{geo}}$$

Where $c_{p,w}$ is the specific heat capacity of the brine (3.9 kJ/kgK [71]) and ΔT_{geo} is the controlled temperature drop across the preheating heat exchanger (assumed equal to 5°C). All the resulting mass, thermal, and electrical metrics for this LOHC configuration are summarized in Table 6.

Table 6: Quantitative summary of the mass, thermal, and electrical results for the LOHC (DBT) hydrogenation system

Parameter	Value	Unit	Note / Source
H_2 required flow rate	9.1	kg/h	Derived from biologic methanation case study
$C_{21}H_{20}$ input design flow rate	138.0	kg/h	Stoichiometric ratio
$C_{21}H_{38}$ theoretical production	147.0	kg/h	Charged DBT synthesis output
Reactor operating pressure	30	bar	Typical values are between 10-50 bar
Reactor operating temperature	170	°C	Typical values are between 150-200°C
Total start-up thermal duty	23.5	kW_{th}	Covered by geothermal fluid and auxiliary system
Geothermal start-up thermal duty	5.3	kW_{th}	Heat provided by the geothermal fluid to preheat the reagents and the oil from 15°C to 60°C

Parameter	Value	Unit	Note / Source
Geothermal fluid mass flow rate	0.3	kg/s	Mass flow rate necessary to satisfy the geothermal start-up thermal duty
Geothermal coverage share	22.3	%	Given by the ratio between the heat given by the geothermal source and the total heat required
Steady-state exothermic heat	82.7	kW_{th}	Released by reaction (to be removed)
Compression electrical power	0.17	kW_{el}	Power required to compress liquid DBT from 1 to 30 bar. H_2 reaches the reactor at the required operating pressure
Recirculation pump electrical power	—	kW_{el}	The chemical reaction occurs in a single liquid phase with high single-pass conversion

4.2.3 Thermodynamic and technical feasibility of Ammonia production

To evaluate the thermodynamic and technical viability of the offshore ammonia synthesis, a preliminary mass and energy balance was performed using the same baseline hydrogen input 9.09 kg/h (4.55 kmol/h) to maintain cross-technology consistency. Based on the stoichiometry of the Haber-Bosch reaction, the process requires a continuous nitrogen feed of 42.6 kg/h (1.52 kmol/h), yielding a theoretical anhydrous ammonia production of 51.5 kg/h (3.03 kmol/h).

Unlike the previous scenarios, this architecture requires the installation of an offshore Pressure Swing Adsorption (PSA) unit to extract nitrogen directly from the atmospheric air on the platform. Because the Haber-Bosch catalytic conversion must operate at an elevated pressure

of 150 bar, a massive pressure increase from atmospheric conditions is required. To avoid unacceptable discharge temperatures that would compromise gas density and equipment integrity, a multi-stage gas compression train with intercooling phases is mandatory.

To provide a clear and intuitive visualization of the proposed plant layout, a simplified process flow diagram is illustrated in Figure 27. This schematic framework is intended to map the overall system configuration, highlights the primary mass streams, and explicitly tracks the operational temperatures and pressures across each stage.

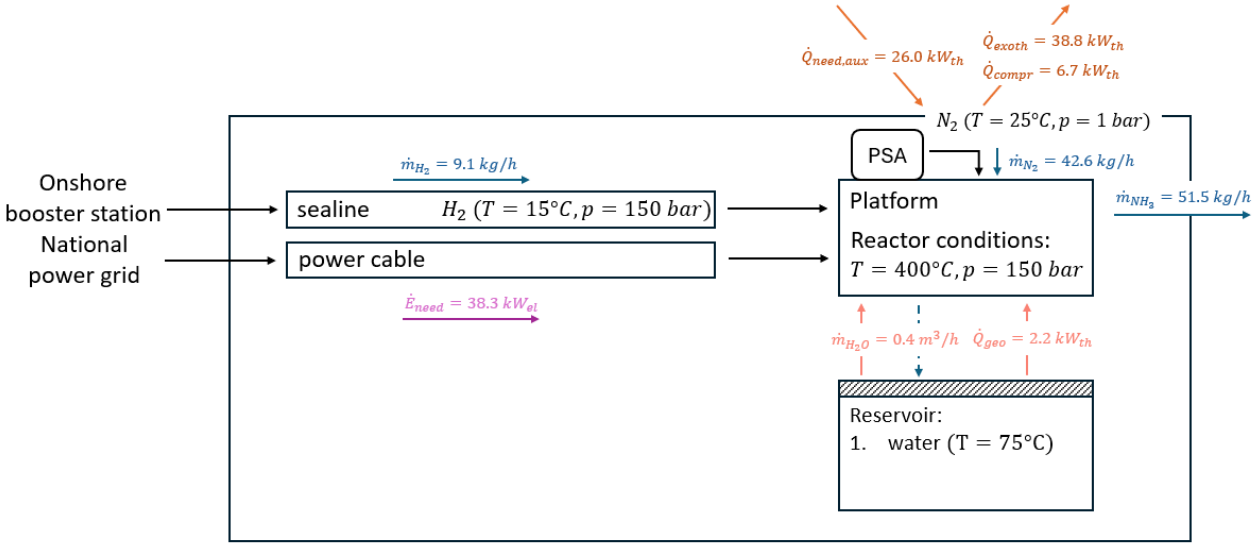


Figure 27: NH_3 production simplified process flow diagram

The compression train for the nitrogen stream was modelled by doing the following assumptions:

- An optimized 4-stage configuration.
- An equal pressure ratio per stage $\left(\beta = \frac{p_{out}}{p_{in}} = 3.5\right)$.
- An intercooling target where the gas is cooled back to 40°C (313.15 K) after each stage (except for the first stage, which draws air at an ambient temperature of 25°C (298.15 K)).

Under these boundary conditions, the ideal isentropic power (P_{isent}) required for each stage is calculated as follows:

$$P_{isent} = \dot{n} \cdot \frac{k}{k-1} \cdot R \cdot T_{in} \cdot \left[(\beta)^{\frac{k-1}{k}} - 1\right]$$

To accurately account for mechanical friction, fluid-dynamic losses, and electrical inefficiencies, the actual electrical power demand (P_{el}) for the multi-stage system is defined by separating the isentropic efficiency (η_{isent}) and the motor electrical efficiency (η_{el}):

$$P_{el} = \frac{P_{isent}}{\eta_{isent} \cdot \eta_{el}}$$

Applying the first law of thermodynamics to each intercooling phase, the thermal power that must be rejected to the sea cooling loop ($\dot{Q}_{intercooling}$) to return the nitrogen to its setpoint temperature is expressed as:

$$\dot{Q}_{intercooling} = \dot{m}_{N_2} \cdot c_{p,N_2} \cdot (T_{out} - T_{in})$$

Where $T_{out} = T_{in} \cdot \beta^{\frac{k-1}{k}}$.

Based on these thermodynamic steps, the outlet temperatures (T_{out}) and thermal cooling duties ($\dot{Q}$) for each compression stage were quantified and are structured as follows:

Table 7: Outlet temperatures and thermal cooling duties for each compression stage

Stage	$p_{in}(bar)$	$p_{out}(bar)$	$T_{in}(K)$	$T_{out}(K)$	$\dot{Q}\ (kW_{th})$
1	1	3.5	298.15	426.5	1.6
2	3.5	12.2	318.15	455.1	1.7
3	12.2	42.9	318.15	455.1	1.7
4	42.9	150	318.15	455.1	1.7

Cumulatively, the total thermal heat that must be continuously removed during the nitrogen compression phase is established at 6.7 kW_{th}.

The overall energy balance is highly constrained by the specific operational phases. During the **start-up phase**, external heat must be supplied to overcome the massive thermal inertia of the thick, high-pressure reactor shell and to pre-heat the gaseous reactants from ambient conditions up to the required catalytic activation threshold of 400°C. This initial preheating stage dictates a thermal load of 18.8 kW_{th} strictly dedicated to the gas streams. To structurally account for the significant metal-mass heat capacity of the high-pressure reactor shell and the

associated heat losses during transient warm-up, a conservative, precautionary oversizing factor of 50% is added to the fluid energy requirement. Consequently, the total cumulative thermal duty during the start-up phase is established at a peak value of 28.2 kW_{th}.

Because the low-enthalpy geothermal source available from the platform wells only reaches 65°C, it cannot fully sustain this high-temperature demand. Therefore, the geothermal brine is strategically exploited to perform an initial pre-heating lift of the cold gases up to 60°C, while the remaining high-temperature thermal gap up to 400°C is supplied by electrical resistance heaters. The geothermal start-up thermal duty is 2.2 kW_{th}.

Conversely, once **steady-state** operational conditions are achieved, the Haber-Bosch synthesis becomes strongly exothermic, releasing 46 kJ of energy per mole of synthesized ammonia. At the design mass flow rate, this reaction generates a continuous net thermal power output of 38.8 kW_{th}. Due to the thermodynamic equilibrium limitations of the Haber-Bosch pathway, the single-pass conversion efficiency is restricted to approximately 15% [66]. Consequently, the remaining 85% of unreacted gases must be recycled back to the reactor inlet. This requires a continuous gas-loop recirculation compressor working against a localized loop pressure drop of 4 bar, introducing an auxiliary electrical load of 2.2 kW_{el}, which runs in parallel to the main gas compression trains.

All the final mass, thermal, and electrical parameters resulting from this integrated ammonia synthesis assessment are cross-compared and summarized in Table 8.

Table 8: Quantitative summary of the mass, thermal, and electrical results for the ammonia synthesis using Haber Bosch process

Parameter	Value	Unit	Note / Source
H_2 required flow rate	9.1	kg/h	Derived from biologic methanation case study
N_2 input design flow rate	42.6	kg/h	Stoichiometric ratio
NH_3 theoretical production	51.5	kg/h	Ammonia synthesis output by using Haber Bosch process
Reactor operating pressure	150	bar	Typical values are between 100-200 bar

Parameter	Value	Unit	Note / Source
Reactor operating temperature	400	°C	Typical values are between 250-400°C
Total start-up thermal duty	28.2	kW_{th}	Covered by geothermal fluid and auxiliary system
Geothermal start-up thermal duty	2.2	kW_{th}	Heat provided by the geothermal fluid to preheat the reagents and the oil from 15°C to 60°C
Geothermal fluid mass flow rate	0.11	kg/s	Mass flow rate necessary to satisfy the geothermal start-up thermal duty
Geothermal coverage share	7.5	%	Given by the ratio between the heat given by the geothermal source and the total heat required
Steady-state exothermic heat	38.8	kW_{th}	Released by reaction (to be removed)
Electrical consumption for onboard N_2 production	20.5	kW_{el}	Power required for N_2 production using a PSA unit with a specific consumption of 0.6 kW/Nm^3 [67]
Compression electrical power	15.6	kW_{el}	Power required to compress N_2 from 1 to 150 bar. H_2 reaches the reactor at the required operating pressure
Heat to be removed during N_2 compression phase	6.7	kW_{th}	Heat to be removed during the multi-stage compression phase from 1 to 150 bar

Parameter	Value	Unit	Note / Source
Recirculation compressor electrical power	2.2	kW_{el}	Power required to restore initial pressure after pressure losses that occur in the reactor

4.2.4 Final thermodynamic comparison between different exothermic reactions

A comprehensive thermodynamic and technical comparison can be established by evaluating the mass and energy balances of the selected technologies. To ensure engineering coherence and a rigorous baseline for the comparative framework, the analysis is anchored to a constant mass flow rate of hydrogen (9.09 kg/h) as the primary reference input. Since all three chemical pathways rely on hydrogen as a fundamental reactant, maintaining this fixed boundary condition enables a direct, transparent evaluation of how each process scales in terms of utility requirements, thermal outputs, and parasitic electrical loads. The definitive cross-technology parameters resulting from these calculations are structured and summarized in Table 9.

Table 9: Thermodynamic and electrical utility requirements for the analysed Power-to-X technologies (referenced to a baseline H_2 flow rate of 9.09 kg/h)

Process	Biologic methanation	LOHC (DBT)	Ammonia (H-B)
Mass flow rate of the product (kg/h)	18.2	147	51.5
Total start-up thermal duty (kW_{th})	6.6	23.5	28.2
Steady-state exothermic heat (kW_{th})	52.1	82.7	38.8
Pump/Compression electrical power (kW_{el})	—	0.17	15.6
Recirculation pump/ compressor electrical power (kW_{el})	0.04	—	2.2
Geothermal power (kW_{th})	6.6	5.3	2.2
Geothermal fluid mass flow rate (kg/s)	0.32	0.27	0.11
Geothermal coverage share (%)	100	22.3	7.5

Regarding thermal management, while the biologic methanation operates at a low temperature (55°C), allowing the geothermal source to fully cover its modest start-up load ($\eta_{geo} = 100\%$), the high-temperature processes suffer from severe thermodynamic limitations. The LOHC and ammonia configurations require activation thresholds of 170°C and 400°C, respectively. Consequently, the 75°C geothermal brine can only perform a preliminary sensible heat lift of the cold reactants up to 60°C. This restricts the geothermal coverage share to 22.3% for the LOHC network and a low 7.5% for the Haber-Bosch loop, leaving the remaining high-temperature duty to be covered by auxiliary electrical heaters. However, during steady-state operations, all three systems switch to net-exothermic regimes, generating significant waste heat (ranging from 38.8 kW_{th} to 82.7 kW_{th}) that represents a strategic asset for internal platform recovery or integration with the thermal desalination units.

From an electrical utility perspective, the primary parasitic loads shift dramatically depending on the physical phase of the reactants. The biological methanation represents the less intensive configuration due to the low-pressure baseline and the expansion of the storage CO_2. In contrast, the ammonia loop demands a significant compression power (15.6 kW_{el}) to elevate the nitrogen stream up to 150 bar, coupled with a steady 2.2 kW_{el} penalty dedicated to the high-volume gas recirculation fan required to overcome the 15% single-pass equilibrium limit. On the other hand, the LOHC pathway completely bypasses the gas-loop recycling constraints since it operates in a single liquid phase, demanding a negligible power input solely for the high-pressure liquid DBT feeding pump.

In conclusion, while biological methanation emerges as the most self-sustaining and geothermally-compatible option for small-scale offshore deployment, the LOHC and ammonia frameworks provide higher product energy densities at the expense of an increased reliance on the platform's electrical grid for gas compression and high-temperature thermal upgrading.

4.2.5 Energy analysis and operating scenarios

To dynamically account for system interruptions, the evaluation was shifted from power requirements to annual energy balances. While power ratings provide an instantaneous thermodynamic snapshot of the system, they neglect the factor of time-dependent operational constraints. Depending on the infrastructure configuration, offshore facilities may either face

severe supply intermittency or benefit from a stable connection to the mainland grid. Therefore, annual thermal and electrical energy consumption profiles offer a more comprehensive metric for technology comparison.

The annual energy demands were computed by multiplying the previously defined steady-state power requirements by the net operating hours of the plant. To assess the impact of different supply conditions, two operational case studies were defined:

- **Case 1: Frequent interruptions** (inconstant supply): this scenario assumes 200 operational interruptions per year (approximately one event every two days). Each event lasts 4 hours in total, split into 2 hours of complete shutdown and 2 hours of transient plant start-up, resulting in 7960 hours of steady-state production per year.

  This configuration models a prospective scenario where the synthesis plant experiences periodic operational halts due to power grid instability, severe renewable electricity supply fluctuations, or localized system trips. Even with a continuous hydrogen feed, the unavailability of electrical power forces the plant to undergo frequent operational transients, standby modes, and cyclical restarts. Given its high relevance for future fully-renewable off-grid systems, **Case 1 is established as the Base Case** for the multi-criteria adaptability analysis in Chapter 6.

- **Case 2: Rare interruptions** (continuous mainland supply): this scenario assumes only 2 interruptions per year (e.g., for scheduled maintenance), each lasting 4 hours (2 hours of shutdown and 2 hours of start-up), leading to 8752 hours of steady-state production per year.

The alternating nature of these operational phases (transient start-up versus steady-state exothermic reaction) is conceptually illustrated in Figure 28.

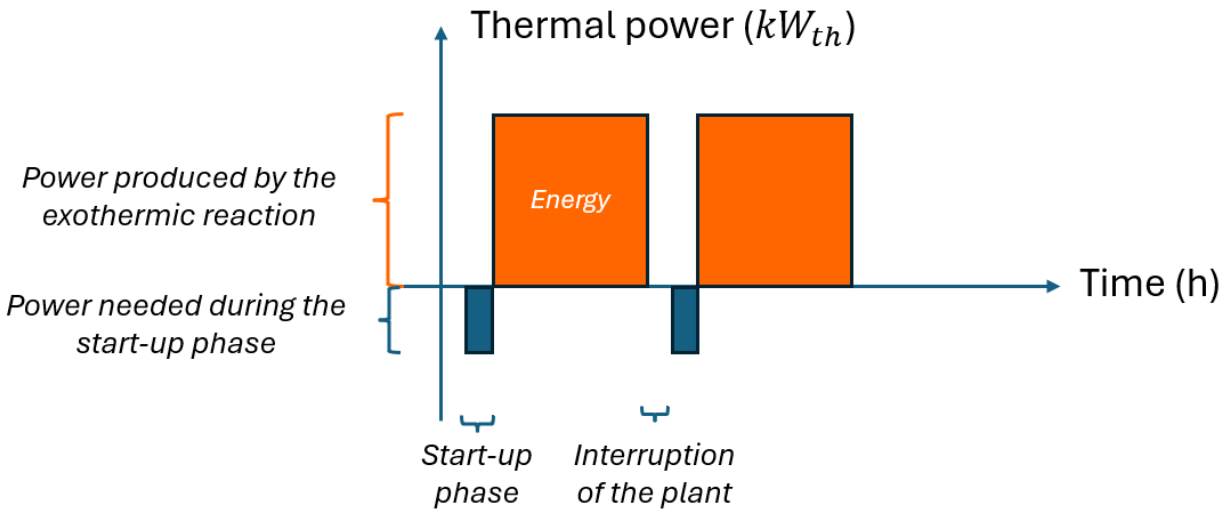


Figure 28: Representation of the two main operational phases of the plant

Moreover, another factor is introduced to evaluate the exploitation of the geothermal source over the operating schedule of the plant. The Exploitation Factor is defined as the ratio between the annual geothermal energy effectively consumed and the maximum theoretical energy that the reservoir could deliver if it operated continuously at peak capacity throughout the entire year (8760 hours):

$$Exploitation\ Factor\ (\%) = \frac{E_{geo,annual}}{P_{geo,max} \cdot 8760\ h} \cdot 100$$

In the previous paragraphs, a different metric involving the geothermal source was introduced: the Geothermal Coverage Share. The main difference between them is associated with their physical context. The Geothermal Coverage Share compares instantaneous thermal powers (kW) to underline the thermal compatibility of each technology with the specific temperature constraints of the reservoir. On the other hand, the Exploitation Factor is a ratio between annual energies (MWh) and accounts for the effective working time of the geothermal source. Consequently, this factor is identical for all three technologies, as it depends exclusively on the total annual duration of the start-up phases.

The operational times for both cases are summarized in Table 10:

Table 10: Operational times of Case 1 and Case 2

Scenario	Case 1: Frequent interruptions	Case 2: Rare interruptions	Comment
Stationary phase duration (h/year)	7960	8752	$h_{year} - N_{avv} \cdot \Delta t_{inter}$
Start-up duration (transient phase) (h/year) *	400	4	$N_{avv} \cdot t_{start-up}$
Yearly pump/ compressor working time (h/year)	8360	8756	$h_{year} - N_{avv} \cdot t_{inter}$

**Note: it is assumed that the geothermal source is exploited exclusively during the 2-hour start-up phase to provide the required transient thermal duty. During the shutdown period, all primary plant operations are halted; consequently, the geofluid extraction pumps are turned off, reducing geothermal energy consumption to zero.*

Table 11 summarizes the total annual mass production yields along with the integrated electrical and thermal energy flows computed for the three chemical pathways. These numerical results quantify the baseline requirements and the heat generated over the year for both operational scenarios. A detailed graphical comparison of these energy profiles, together with a critical discussion on the actual exploitation and strategic role of the geothermal source, is provided in the following section.

Table 11: Integrated annual mass and energy balances for biological methanation, LOHC hydrogenation, and ammonia synthesis under Case 1 (intermittent supply) and Case 2 (continuous supply) operating conditions.

Process	Biologic methanation		LOHC (DBT)		Ammonia (H-B)	
Scenario	**Case 1**	**Case 2**	**Case 1**	**Case 2**	**Case 1**	**Case 2**
Mass flow rate of the product $(ton/year)$	144.9	159.3	1170.1	1286.5	409.9	450.7
Annual start-up thermal energy $(MWh/year)$	2.6	0.03	9.4	0.09	11.5	0.12
Annual steady-state exothermic heat $(MWh/year)$	414.7	456.0	658.3	723.8	308.8	339.6
Electrical energy $(MWh/year)$	0.33	0.35	1.4	1.5	148.8	155.9

Process	Biologic methanation		LOHC (DBT)		Ammonia (H-B)	
Scenario	**Case 1**	**Case 2**	**Case 1**	**Case 2**	**Case 1**	**Case 2**
Geothermal energy $(MWh/year)$	2.6	0.03	2.1	0.02	0.9	0.009
Exploitation factor of the geothermal source (%)	4.6	0.046	4.6	0.046	4.6	0.046

4.2.6 Exploitation and strategic role of the geothermal source

This section evaluates the strategic role of the geothermal resource within the three chemical synthesis pathways. The analysis uses a dual-scale approach: a steady-state assessment of nominal power capacities and a time-integrated evaluation of annual energy balances.

Figure 29 shows the nominal thermal power balances for biological methanation, LOHC hydrogenation, and ammonia synthesis. A clear thermodynamic trend emerges: once the activation temperature is reached, all three reactions are strongly exothermic. They generate a significant surplus of thermal power compared to the initial heating requirements.

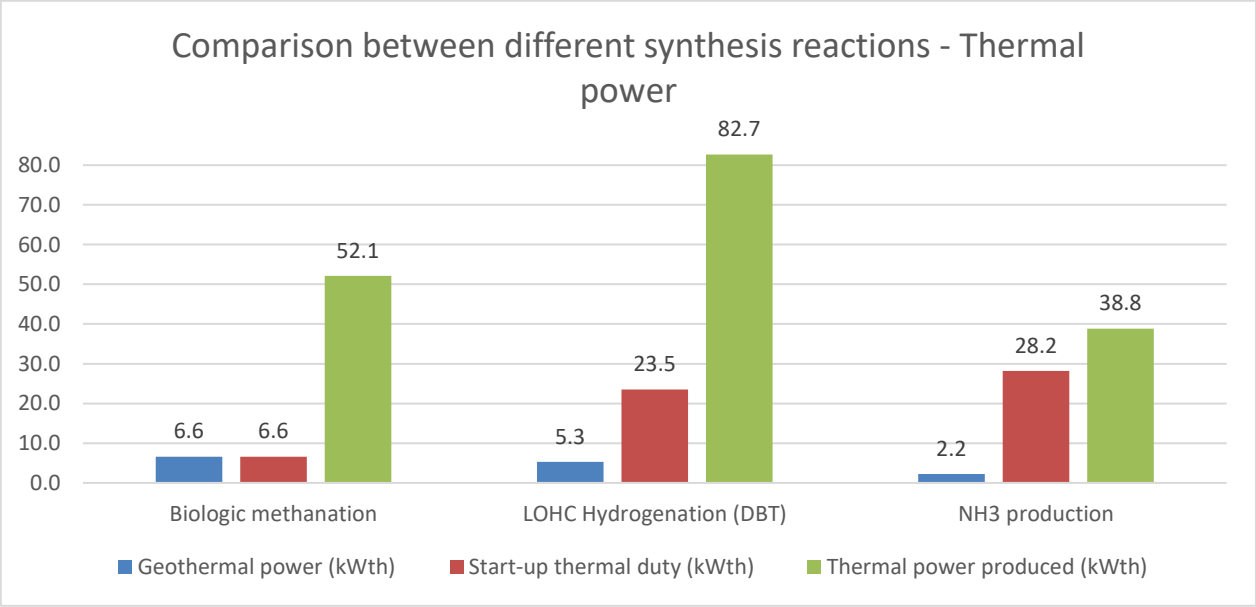


Figure 29: Comparison of nominal thermal power capacities (heating demand vs. exothermic heat production) for the three synthesis pathways under steady-state conditions

Consequently, under steady-state continuous operations, these processes are entirely self-sustaining from a thermal standpoint. The external low-enthalpy geothermal geofluid loop is

strictly utilized as a transient utility during the initial start-up phase to overcome the system's massive thermal inertia and trigger the catalytic mechanism. Once the chemical loop is activated, the geothermal supply is completely bypassed, and the system switches to a cooling configuration to safely reject or re-route the high-temperature reaction heat surplus.

However, a power-based analysis does not account for the operational time. Therefore, annual energy balances are required to evaluate the long-term impact of the two operating cases (intermittent versus continuous supply).

Figure 30 reports the annual thermal energy produced by the exothermic reactions in both Case 1 (intermittent supply) and Case 2 (continuous supply). Despite the significant difference in total operating hours between the two scenarios (respectively 7960 h and 8752 h) the annual energy outputs are remarkably similar.

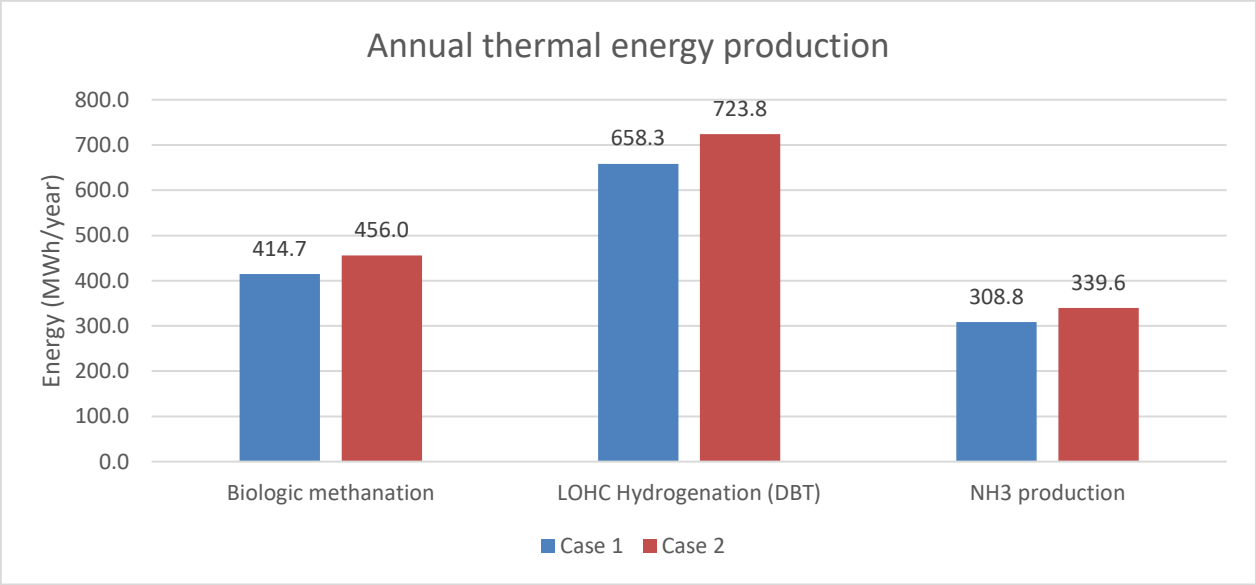


Figure 30: Total annual thermal energy produced by the exothermic reactions – comparison between Case 1 (intermittent supply) and Case 2 (continuous supply)

Regarding the thermal energy required for the start-up phase, Figure 31 shows the results exclusively for Case 1. In Case 2, the system experiences only 2 interruptions per year, making the total start-up energy consumption negligible across all scenarios (< 0.15 MWh/year).

Comparing Figure 30 and Figure 31 reveals an enormous gap between the energy produced and the energy consumed during start-up, differing by two orders of magnitude. Furthermore, the low geothermal exploitation factor (4.57% for Case 1 and 0.05% for Case 2) confirms that the

geothermal source plays a minor role in the overall annual energy balance of these synthesis processes.

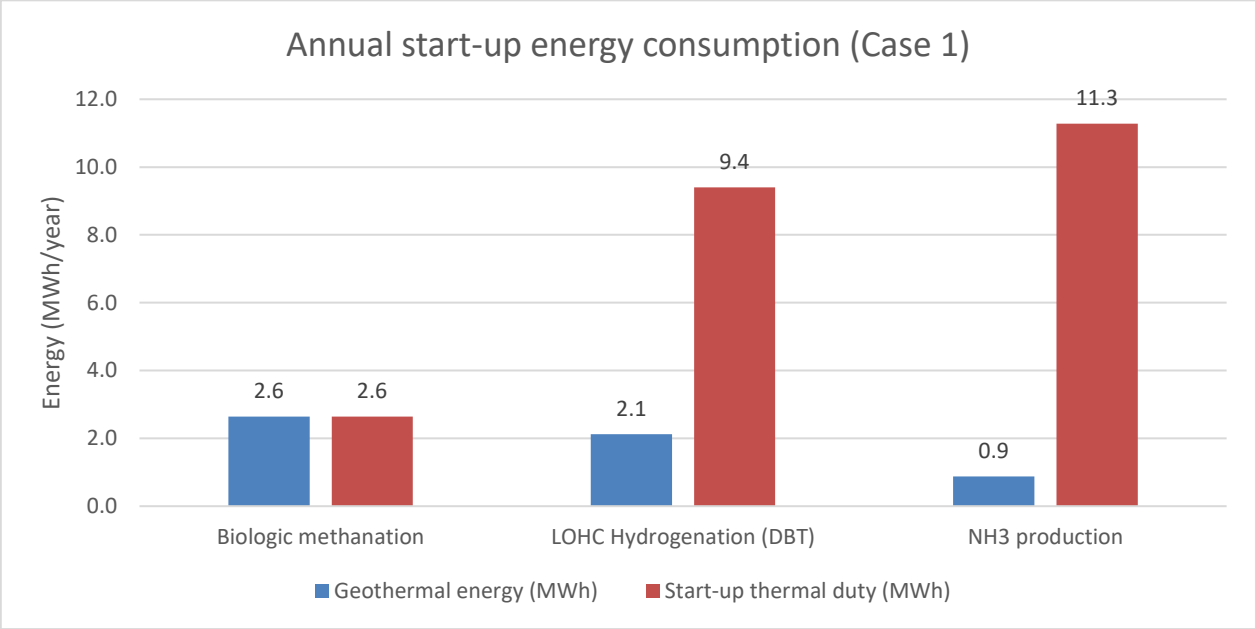


Figure 31: Annual thermal energy required for transient start-up phases across the three chemical technologies under Case 1 operating conditions

4.3 Energy and mass balances for seawater-based pathways

To establish the design basis for the freshwater production subsystem, the baseline volumetric and mass flow rates were derived from the offshore platform community requirements analysed by A. Aliberti "*Conversion of a decommissioning Oil & Gas platform for the installation of a photovoltaic plant to feed a desalination unit. Preliminary design.*" [68]. Assuming a total workforce of 50 operators distributed across the cluster of platforms surrounding the main hub, and a standard per-capita daily freshwater requirement of 150 l/day, the net required permeate volume is established at 7500 l/day (7.5 m^3/day).

A major thermodynamic and operational departure from the reference study [68] concerns the plant capacity factor. While the previous literature assumed a partialized operation of only 8.5 hours/day due to the daytime physical constraints of an offshore photovoltaic array, the current framework leverages a continuous electrical and geothermal energy availability. Operating uninterruptedly 24 hours a day, 7 days a week, the required hourly permeate flow

rate is drastically smoothed down to a steady-state design capacity of **310.0 kg/h (0.31 m³/h)**. To ensure a rigorous, standardized, and unbiased thermodynamic comparison between diverse water-separation mechanism frameworks, this fixed permeate production capacity (310.0 kg/h) is enforced as the invariant constraint for all three investigated desalination architectures.

4.3.1 Thermodynamic and technical feasibility of Reverse Osmosis

To evaluate the operational integration of the freshwater production subsystem, a comprehensive mass, thermal, and electrical assessment was performed for the Reverse Osmosis (RO) architecture. Assuming a commercial baseline recovery ratio (Y) of 0.25 for the selected Lenntech LennRO SW 500 module [69], the required continuous seawater feed flow rate ($\dot{m}_{feed}$) is established at 1240.0 kg/h (0.344 kg/s).

While Reverse Osmosis is conventionally treated as a purely electrical, pressure-driven separation process, this architecture introduces an innovative hybrid electro-thermal integration by exploiting the low-enthalpy geothermal source. The technical feasibility of the system is constrained by a manufacturer-specified maximum inlet temperature threshold of 30°C to preserve membrane polymer integrity and prevent premature flux compaction. Consequently, the geothermal brine (75°C) is strategically routed to an upstream titanium plate heat exchanger to upgrade the raw seawater from its ambient unheated state ($T_{sw,amb} = 20°C$) to the maximum optimized setpoint of 30°C ($T_{feed,opt}$). The thermal power required from the geothermal well ($\dot{Q}_{RO,th}$) to sustain this $\Delta T = 10\ K$ continuous sensible preheating lift is quantified through the thermal balance:

$$\dot{Q}_{RO,th} = \dot{m}_{feed} \cdot c_{p,sw} \cdot (T_{feed,opt} - T_{sw,amb})$$

Where $c_{p,sw}$ is the specific heat capacity of seawater (approximately 3.985 J/(kg K)).

This thermal lift induces a favourable reduction in fluid viscosity, which directly depresses the feed osmotic pressure. Consequently, the required high-pressure pumping energy drops from the 60.73 bar demanded under unheated conditions (20°C) down to 52.06 bar at 30°C [70]. This thermodynamic optimization yields a reduction in the Specific Energy Consumption (SEC) from 4.88 kWh/m³ to 4.18 kWh/m³ (standard baseline at 25°C is 4.5 kWh/m³), corresponding to a net parasitic electrical power saving on the high-pressure pump network of $0.22\ kW_{el}$ (14.3%).

Starting from the geothermal power required it's possible to calculate the geothermal fluid mass rate:

$$\dot{m}_{geo} = \frac{\dot{Q}_{VTD,th}}{c_{p,brine} \cdot (T_{geo,in} - T_{geo,out})}$$

Where $c_{p,brine}$ is the specific heat capacity of the geothermal brine (3.9 kJ/(kgK) [71]), and by estimating a $\Delta T = 30°C$ ($T_{geo,in} = 65°C$ and $T_{geo,out} = 35°C$). The result is 0.12 kg/s (approximately 0.43 m^3/h).

The quantitative mass, thermal, and electrical metrics comparing the cold baseline and geothermally-preheated operations are summarized in Table 12.

Table 12: Quantitative mass, thermal, and electrical metrics for the Reverse Osmosis (RO) desalination system under cold and geothermally-preheated operation

Operational configuration	Seawater feed (kg/h)	Freshwater permeate (kg/h)	Operating pressure (bar)	Specific energy consumption (kWh/m^3)	Net electrical power (kW_{el})	Geothermal duty (kW_{th})
Standard Baseline (20°C)	1240.0	310.0	60.73	4.88	1.51	—
Geothermal Optimized (30°C)	1240.0	310.0	52.06	4.18	1.30	13.7

4.3.2 Thermodynamics and technical feasibility of Vacuum Thermal Distillation

To evaluate the operational integration of the freshwater production subsystem, a comprehensive mass, thermal, and electrical assessment was performed for the Vacuum Thermal Distillation (VTD) architecture. Based on the daily permeate target of 7.5 m^3/day and the operational ranges identified in literature (Figure 18), the Alfa Laval Aqua Blue E1-Ctype C80 module was selected. Since proprietary commercial datasheets do not explicitly report the system recovery ratio (Y) for varying seawater feed qualities, a baseline design value of 0.25 was implemented, resulting in a continuous raw seawater feed flow rate of 1240.0 kg/h (0.344 kg/s).

A distinct operational constraint of the VTD module is that the heating medium water must enter the evaporator heat exchanger at a temperature between 70°C and 75°C [47]. Consequently, not all the identified offshore geothermal reservoirs are directly suitable for this

technology. This represents a significant thermodynamic difference from the Reverse Osmosis (RO) configuration, where the feed input is strictly constrained to a lower temperature range (20-30°C). Although it would be technically feasible to integrate an exothermic chemical synthesis reaction upstream of the VTD unit to lift the feed water temperature, such an approach would deviate from the primary objective of this research, which remains the direct exploitation of the low-enthalpy geothermal resource.

Since vacuum thermal distillation relies strictly on a liquid-to-vapor phase transition, it is necessary to supply the specific latent heat of vaporization (ΔH_{evap}) to break the intermolecular hydrogen bonds of the liquid phase. The continuous thermal power requirement ($\dot{Q}_{VTD,th}$) is governed by the following energy balance:

$$\dot{Q}_{VTD,th} = \dot{m}_{perm} \cdot \Delta H_{evap}$$

Within the Aqua Blue E1-Ctype C80 configuration, the internal shell operates under vacuum conditions at approximately 0.15 bar [47], which depresses the boiling point of seawater to a vaporization temperature of 54°C. At this thermal state, the associated latent heat of vaporization extracted from the thermodynamic steam tables is $\Delta H_{evap} = 2373.2\ \frac{kJ}{kg}$. The required thermal duty is 204.4 kW_{th} which is significantly higher than the thermal loads quantified in the RO preheating scenarios. This macro-difference stems directly from the underlying physics of the separation mechanisms: VTD demands latent heat for phase change, whereas RO only leverages a minor fraction of sensible heat to modulate fluid viscosity without phase alteration.

Since the geothermal water supplying this thermal duty must remain entirely in the liquid phase to prevent scaling and outgassing within the heat exchangers, the required geofluid mass flow rate ($\dot{m}_{geo}$) is:

$$\dot{m}_{geo} = \frac{\dot{Q}_{VTD,th}}{c_{p,brine} \cdot (T_{geo,in} - T_{geo,out})}$$

Assuming a specific heat capacity ($c_{p,brine}$) of 3.9 kJ/(kg K) for the thermal brine [71], the delivery temperature at the platform deck utilities is modelled through a resource-focused geological constraints framework. Within the reservoir asset, the geofluid is characterized by an initial

temperature of 75°C. Based on a conservative engineering approach, a thermal loss of 5°C is assumed during the fluid ascent from the subsurface reservoir to the platform deck, resulting in an available inlet temperature ($T_{geo,in}$) of 70°C at the desalination utilities.

From a strategic screening perspective, it is worth noting that only 7 existing Mediterranean offshore structures (excluding light monotubular platforms) possess a depleted reservoir with a thermal profile strictly exceeding 75°C.

By implementing an optimized design temperature drop (ΔT) of 15°C across the heat exchanger network – thereby establishing a brine discharge temperature ($T_{geo,out}$) of 55°C – the required continuous geothermal mass flow rate is quantified at 3.5 kg/s (approximately 12.6 m^3/h). This flow rate represents a highly intensive exploitation of the single-well delivery capacity, reflecting the high thermal energy demand (204.4 kW_{th}) characteristic of single-stage thermal evaporation without advanced heat recovery.

Beyond the dominant thermal power footprint, auxiliary electrical power is required to drive the raw seawater feed pump, the distillate extraction pump, and the liquid-ring vacuum pump necessary to maintain the internal sub-atmospheric conditions. Because these parasitic electrical loads are heavily dependent on localized site conditions and are not tabulated as standalone figures in the commercial module datasheets, a Specific Energy Consumption (SEC) benchmark for industrial single-effect vacuum distillers was estimated at 4 kWh/m^3. The net parasitic electrical power ($P_{VTD,el}$) is calculated as the product of the volumetric permeate flow rate ($\dot{V}_{perm}$) and the SEC:

$$P_{VTD,el} = \dot{V}_{perm} \cdot SEC = 1.2\ kW_{el}$$

4.3.3 Thermodynamics and technical feasibility of Membrane Distillation

As introduced in the qualitative state-of-the-art review (Paragraph 483.5), a major barrier to the commercializing of Membrane Distillation (MD) is the intrinsic complexity of its energy consumption profile and economic scalability. Operating conditions and performance indices differ considerably from bench-scale prototypes to industrial-scale configurations, primarily due to significant temperature polarization and localized thermal gradients across the MD module itself. A review of experimental literature indicates that while several MD pilot systems

have been constructed and analysed [72], they generally operate at very low permeate capacities (<60 l/h), where thermal insulation losses and small-scale pump inefficiencies distort the energetic benchmarks.

For instance, the study by Ong et al. [72] evaluating a compact unit at a permeate flow rate of 125 l/h reports a Specific Thermal Energy Consumption (STEC) of 128.1 kWh_{th}/m^3 but an extremely penalizing Specific Electrical Energy Consumption (SEEC) of 70.2 kWh_{el}/m^3. Although the authors demonstrate that under specific optimized operating variables – a high hot-water inlet temperature ($T_{hot,in} = 75°C$), a low cold-water inlet temperature ($T_{cold,in} = 20°C$), and a minimized feed salinity – the electrical parasitisation can theoretically be compressed down to 4.5 kWh_{el}/m^3, these values still reflect non-upscaled laboratory boundary conditions.

Considering the continuous freshwater capacity constraints established for the current platform layout (310 kg/h), such laboratory-scale modules are physically undersized due to their highly restrictive active membrane surface area. Therefore, for the purpose of this industrial upscaling framework, a commercial modular system based on the Memsys MDS 500 platform was evaluated. The manufacturer technical datasheet [73] for the MDS 500 strictly reports the baseline boundary constraints, specifying a minimum hot-loop heating power and a cold-loop cooling power of 50 kW each. However, explicit fixed values for the net specific thermal and electrical consumption are omitted by suppliers, as these operational metrics are strongly coupled with localized raw feed salinity, fouling factors, and dynamic temperature driving forces.

Consequently, to model a realistic commercial offshore deployment, consolidated industrial benchmarks for multi-stage Vacuum Membrane Distillation (VMD) configurations were adopted. Specifically, a standardized Specific Thermal Energy Consumption (STEC) of 200 kWh_{th}/m^3 and an optimized auxiliary Specific Energy Consumption (SEC) of 1.5 kWh_{el}/m^3 were selected, reflecting the performance of commercial multi-stage modules equipped with integrated internal vacuum recovery lines. Leveraging these industrial targets, the continuous net energy duties for the MD block are quantified as:

$$\dot{Q}_{MD,th} = \dot{V}_{perm} \cdot STEC = 62.0\ kW_{th}$$

$$P_{MD,el} = \dot{V}_{perm} \cdot SEC = 0.47\ kW_{el}$$

Starting from the primary thermal energy consumption metrics, the required continuous geothermal mass flow rates ($\dot{m}_{geo}$) can be calculated through the following thermal balance:

$$\dot{m}_{geo} = \frac{\dot{Q}_{MD,th}}{c_{p,brine} \cdot (T_{geo,in} - T_{geo,out})}$$

To ensure a rigorous and standardized comparison under identical asset boundary conditions, the geothermal resource variables are kept consistent with the framework detailed for the VTD configuration (Paragraph 4.3.2). Therefore, assuming the same wellbore thermal loss profile, the geofluid delivery temperature ($T_{geo,in}$) at the deck utilities is established at 70°C (originating from a 75°C deep reservoir constraint, which limits the immediate application to 7 specific Mediterranean candidate structures).

By implementing the same optimized design temperature drop (ΔT) of 15°C across the multi-effect heat exchange channels ($T_{geo,out} = 55°C$), the required continuous geothermal mass flow rate for the MD unit is quantified at 1.06 kg/s (approximately 3.8 m^3/h).

It is important to emphasize a key thermodynamic divergence arising from this comparative analysis. Although both desalination technologies are evaluated at the same inlet temperature (70°C) to reflect identical platform resource constraints, the MD architecture exhibits a significantly higher operational resilience. While the single-effect VTD configuration operates near its structural evaporation limit under deep vacuum conditions, the VMD process could theoretically tolerate a degradation of the geothermal source down to 55-60°C.

4.3.4 Final thermodynamic comparison between different desalination systems

To determine the most suitable configuration for offshore platform integration, a comprehensive thermodynamic screening was executed by comparing the simulated performance metrics of Geothermal-Optimized Reverse Osmosis (RO), Vacuum Thermal Distillation (VTD), and Membrane Distillation (MD). To guarantee an unbiased analysis, the net freshwater production was strictly held constant at the invariant constraint of 310 kg/h for all three architectures. The quantitative results are summarized in Table 13.

The comparative analysis highlights a stark engineering trade-off between electrical parasitisation and geothermal heat utilization:

- **Reverse Osmosis (RO):** represents the most efficient configuration from a purely thermal standpoint, demanding the lowest geothermal duty since the geofluid is exclusively parasitised for a 10°C raw seawater sensible preheating lift. However, it features the highest operational pressure (52.1 bar) and a high Specific Energy Consumption (4.2 kWh/m^3), leading to a substantial net electrical load of 1.30 kW_{el} concentrated on the high-pressure pumping network.
- **Vacuum Thermal Distillation (VTD):** completely eliminates the high-pressure hydraulic requirements, thereby compressing the net electrical power down to 1.20 kW_{el}. Nevertheless, due to its single-effect vaporization mechanism that operates under deep vacuum (0.15 bar), it generates a massive and localized thermal footprint, requiring a geothermal duty of 204.4 kW_{th}. This intensive demand risks over-exploiting the single-well capacity of the platform asset.
- **Membrane Distillation (MD):** emerges as the most balanced and optimized solution within the integrated offshore framework. By leveraging an internal multi-effect latent heat recovery configuration, the MD block reduces the external geothermal duty to 62.0 kW_{th} (achieving a 70% thermal saving compared to VTD). Simultaneously, by avoiding both high hydraulic pressures and deep vacuum restrictions, it achieves the absolute lowest Specific Energy Consumption (1.5 kWh/m^3) and a minimal parasitic electrical load of just 0.50 kW_{el}.

Table 13: Thermodynamic and electrical utility requirements for the analysed desalination technologies (referenced to a baseline permeate production flow rate of 310 kg/h)

Process	Geothermal optimized RO (30°C)	Vacuum thermal distillation	Membrane distillation
Seawater feed (kg/h)	1240.0	1240.0	1240.0
Freshwater permeate (kg/h)	310.0	310.0	310.0
Operating pressure (bar)	52.06	0.15	0.30
Specific energy consumption (kWh/m^3)	4.2	4	1.5
Net electrical power (kW_{el})	1.3	1.2	0.5
Geothermal duty (kW_{th})	13.7	204.4	62.0
Geothermal fluid mass flow rate (kg/s)	0.1	3.5	1.1

4.3.5 Energy analysis for desalination systems

To maintain methodological consistency across the platform, the annual energy consumption of the desalination units was evaluated under the same two operational scenarios (**Case 1** and **Case 2**) defined in Section 4.2.5. While the nominal power requirements presented in Section 4.3.4 provide an instantaneous thermodynamic snapshot of the separation processes, the time-integrated annual energy balances account for the operational constraints imposed by network intermittency and maintenance down-times. Unlike the exothermic chemical synthesis loops, which act as net heat producers after activation, the desalination technologies are purely endothermic utilities that continuously rely on external energy inputs throughout their entire operating window.

Table 14 summarizes the integrated annual mass production yields alongside the total electrical and thermal energy requirements for the three analysed desalination systems.

Table 14: Integrated annual mass and energy balances for geothermal optimized Reverse Osmosis, Vacuum Thermal Distillation, and membrane distillation under Case 1 (intermittent supply) and Case 2 (continuous supply) operating conditions

Process	Geothermal optimized RO (30°C)		Vacuum thermal distillation		Membrane distillation	
Scenario	**Case 1**	**Case 2**	**Case 1**	**Case 2**	**Case 1**	**Case 2**
Seawater feed $(ton/year)$	10366	10857	10366	10857	10366	10857
Freshwater permeate $(ton/year)$	2592	2714	2592	2714	2592	2714
Electrical energy $(MWh/year)$	10.9	11.4	10.0	10.5	4.2	4.4
Geothermal energy $(MWh/year)$	114.5	120.0	1708.8	1789.7	518.3	542.9
Geothermal fluid mass flow rate $(ton/year)$	3702	3877	105035	110010	31902	33413
Exploitation factor of the geothermal source (%)	95.4	99.9	95.4	99.9	95.4	99.9

Figure 32 illustrates the annual thermal energy directly extracted from the low-enthalpy geothermal source for both Case 1 (intermittent supply) and Case 2 (continuous supply).

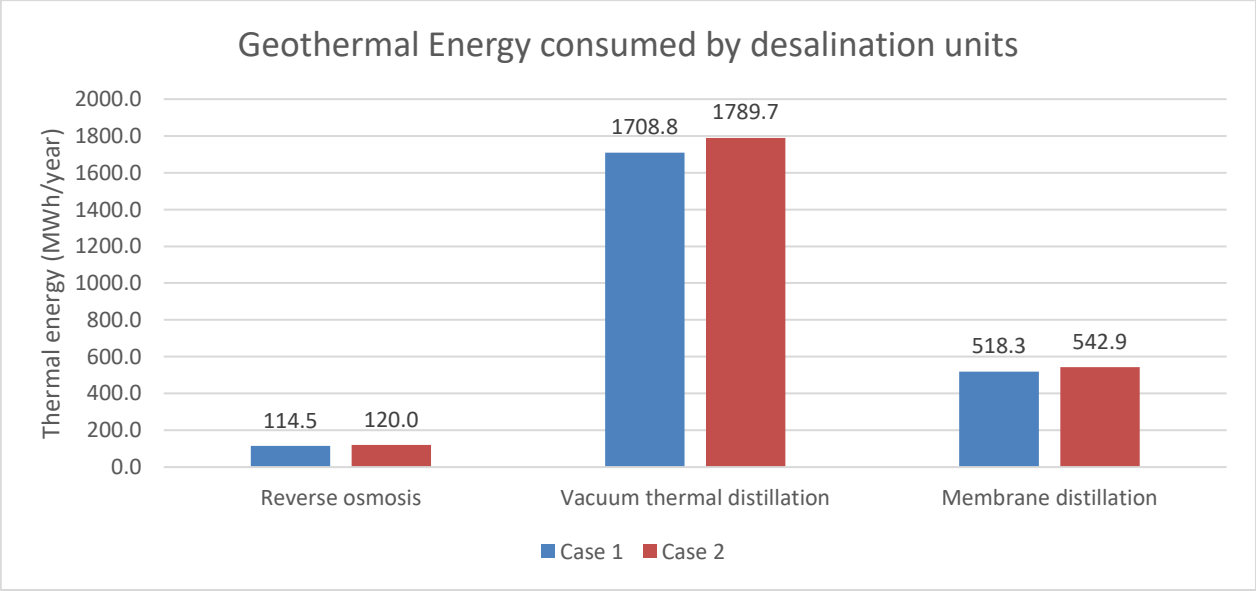


Figure 32: Total annual thermal energy required by the desalinations units: comparison between Case 1 (intermittent supply) and Case 2 (continuous supply)

Vacuum Thermal Distillation (VTD) exhibits the highest thermal energy demand by a significant margin, requiring 1708.8 MWh/year in Case 1 and rising to 1789.7 MWh/year under continuous

operation (Case 2). This massive consumption is directly linked to its high nominal thermal duty (204.4 kW_{th}), necessary to generate the temperature gradient required for seawater evaporation under vacuum. Membrane Distillation (MD) displays a similar, though more moderate, thermal profile, with an annual consumption ranging from 518.3 MWh/year (Case 1) to 542.9 MWh/year (Case 2), reflecting its lower nominal thermal power rating (62.0 kW_{th}). In stark contrast, the Geothermal Optimized Reverse Osmosis (RO) system exhibits a minimal thermal footprint (114.5 MWh/year to 120.0 MWh/year). This is because RO is inherently an electrically-driven process (4.2 kWh/m^3), where the geothermal geofluid is exclusively utilized as a minor utility for the mild preheating of the seawater feed to 30°C to enhance membrane permeability.

A crucial finding of this analysis is reflected in the geothermal exploitation factor, which reaches **95.4%** in Case 1 and **99.9%** in Case 2 across all three configurations. This behaviour represents a complete reversal compared to the trend observed for the chemical synthesis pathways. Because desalination units continuously consume thermal energy to sustain their separation gradients, the geothermal resource is never bypassed during steady-state production. The resource is effectively exploited during all operational hours (both steady-state and start-up transients), and power extraction is interrupted only during complete platform shutdowns. These exceptionally high exploitation factors mathematically demonstrate that coupling a low-enthalpy geothermal geofluid with offshore desalination represents a highly efficient and strategic integration for continuous freshwater production, fully maximizing the potential of the local resource.

4.3.6 Energy analysis for thermally assisted fish farming

Based on a study [58] in the North Adriatic Sea, seabass was selected for fish farming in this region. It is also assumed that the basic module of the fish farm consists of 10 cages with a diameter of 30 m, arranged in 2 columns and 5 rows. Considering the space required for the mooring system, the gap between the modules for free navigation by aquaculture service vessels and other maintenance vessels and the space for the feeding platform for each module, the module requires an area of 320 m · 500 m. At these conditions fish farming requires [58]:

- a continuous base load due to controls, monitoring and communication systems, on average equal to 16 kWh/day, independent from the number of cages;

- a variable electrical load for feeding fish equal to 50 kW for 10 cages (working 6-12 hours/day depending on the season);

- an electrical load of 16.67 kW for 10 cages, for freezing, storage at 0–4 °C, a desalination unit and a breathing air compressor for divers.

Based on these operational literature data [58], the daily electrical demand for a standard offshore fish farming module comprising 10 submerged cages was quantified. To establish a consistent baseline for comparison with the other pathways, daily figures were converted into annual energy metrics assuming continuous operation (365 days/year). The detailed breakdown of daily electrical consumption and corresponding operating assumptions is summarized in Table 15.

Table 15: Daily electrical demand breakdown and operational assumptions for a 10-cage thermally assisted fish farming module (adapted from [58])

Consumption category	Electrical consumption (kWh/day)	Operational description & Assumptions
Base load	16	Continuous control, monitoring, and communication systems (independent of cage count)
Variable electrical load	450	Automated feeding system operating for an average of 9 h/day (50 kW rated power)
Electrical load	400	Continuous operation (24 h/day) of fish cold storage/freezing ($0 - 4$°C), localized desalination, and diver breathing air compressors (16.67 kW total load)
Total daily consumption	866	Given by the sum of base load, variable electrical load and electrical load

The overall annual electrical consumption of the fish farm module is approximately 316 MWh/year. To estimate the corresponding thermal energy demand required for water temperature optimization, specific geometric and hydrodynamic assumptions were made, as these parameters were not explicitly reported in the reference literature [58].

- Geometric sizing: the fish farm baseline module consists of 10 cylindrical cages (D = 30 m). Assuming a standard net depth (h) of 10 m, the total water volume enclosed by a single cage (V_{single}) and by the entire 10-cage system (V_{tot}) is quantified as:

$$V_{single} = \pi \cdot \left(\frac{D}{2}\right)^2 \cdot h = 7068.6\ m^3$$

$$V_{tot} = 10 \cdot V_{single} = 70\,686\ m^3$$

- Hydrodynamic water exchange rate: because flexible offshore net cages allow continuous water exchange with the surrounding marine environment, a conservative residence time (t_{res}) corresponding to 2 complete volumetric water renewals per day ($N_{ex} = 2\ \text{day}^{-1}$) was assumed. The resulting continuous volumetric flow rate ($\dot{V}_{ric}$) is expressed as:

$$\dot{V}_{ric} = \frac{N_{ex} \cdot V_{tot}}{24\ h} = 1.636\ \frac{m^3}{s}$$

Finally, assuming an optimal metabolic water temperature ($T_{opt} = 22°\text{C}$) for European seabass, the continuous thermal power duty ($\dot{Q}_{th}$) and annual thermal energy consumption (E_{th}) required to buffer the seawater temperature are quantified. To adopt a conservative sizing approach, the average annual sea surface temperature was set to $17.1°\text{C}$ based on Northern Adriatic meteorological data[5]. Operating continuously over 8760 hours/year, the continuous thermal power requirement ($\dot{Q}_{th}$) and total annual thermal energy demand (E_{th}) are calculated using seawater density $\left(\rho_{sea} = 1025\,\frac{kg}{m^3}\right)$, seawater specific heat capacity $\left(c_{p,sea} = 3.99\,\frac{kJ}{kg\ K}\right)$, and the target temperature increment ($\Delta T = T_{opt} - T_{sea} = 22°C - 17.1°C = 4.9°C$):

$$\dot{Q}_{th} = \rho_{sea} \cdot \dot{V}_{ric} \cdot c_{p,sea} \cdot \left(T_{opt} - T_{sea}\right) = 32.8\ MW$$

$$E_{th} = \dot{Q}_{th} \cdot 8760\,\frac{h}{year} = 287\,328\ \frac{MW_{th}}{year}$$

The resulting annual electrical and thermal energy demand represents the highest figure among all seven analysed pathways. Rather than indicating an analytical inconsistency, this outcome provides significant engineering insights when contextualized across the comparative framework:

- Strict biological continuity: unlike thermochemical synthesis routes (evaluated between 7960 h/year and 8752 h/year) or desalination plants (8360 h/year to 8756 h/year), living biomass cannot tolerate operational shut-downs or thermal shocks, strictly requiring continuous baseload heating for 8760 h/year.

[5] The average annual sea surface temperature (T_{sea}) is assumed to be $17.1°\text{C}$, corresponding to the historical annual mean recorded for the Northern Adriatic Sea (one of the coldest regions in the Mediterranean basin) [77]. Adopting this baseline temperature throughout the year ensures a conservative approach, allowing for a realistic overestimation of the overall thermal power demand.

- Open boundary conditions and uninsulated fluid volumes: chemical and membrane processes occur within insulated closed vessels. In contrast, fish farming involves continuous, open-boundary volumetric water exchange with the surrounding sea, leading to substantially higher continuous heat duties.
- Disparity in input data maturity and scaling: while the chemical and desalination pathways were modelled directly from fundamental thermodynamic parameters and lab-scale process data, the fish farming scenario relies on empirical operational data from a full-scale offshore aquaculture module [58].

Far from representing a methodology limitation, these quantitative discrepancies highlight the distinct maturity levels and physical constraints of the technologies analysed.

5 Guidelines: definition of the methodology

While the quantitative sizing executed in Chapter 4 provided the mass and energy balances for each individual technology, those raw data alone are insufficient to declare a winning scenario, as they represent conflicting engineering performance. To objectify choice of the best scenario, a Multi-Criteria Decision Analysis (MCDA) based on the Weighted Sum Method (WSM) was applied. This approach allows weighing the importance of several constraints (such as thermal, structural and maturity factors) by analysing them from both a qualitative and quantitative point of view.

This methodology was originally developed by A. Martini in her master's thesis [74]: *Technical-Engineering Methodology for Evaluating the Green Conversion of Offshore Oil and Gas Platforms. Development of the Analysis Process for Defining a Guideline*. In her work, she analysed 66 criteria based on the Basic Design of the 3 reconversions options previously examined in detail by other students.

Since the present research is a prefeasibility study, the level of detail is naturally lower. For this reason, 13 key criteria have been selected with the goal of identifying the most suitable technology. Analysing each scenario in extreme detail at this stage would be impractical. Consequently, the following analysis serves as a Technology Assessment to understand which technology holds the most potential for specific context of the Mediterranean Sea. This operational environment requires a dedicated framework capable of comparing highly heterogeneous deployment outputs – ranging from energy vectors like biomethane, hydrogen carrier, and ammonia, to desalinated water and fish production.

Following the identification of the best option through this screening process, it will be possible to study the most interesting technology for the Mediterranean context in greater depth to verify its technical feasibility. Figure 33 illustrates the synthesis of the working methodology adopted. By establishing this mathematical framework, the thesis moves toward its final challenge: processing the technical criteria to unlock the final adaptability rankings and sensitivity analyses, which will be unveiled and discussed in Chapter 6.

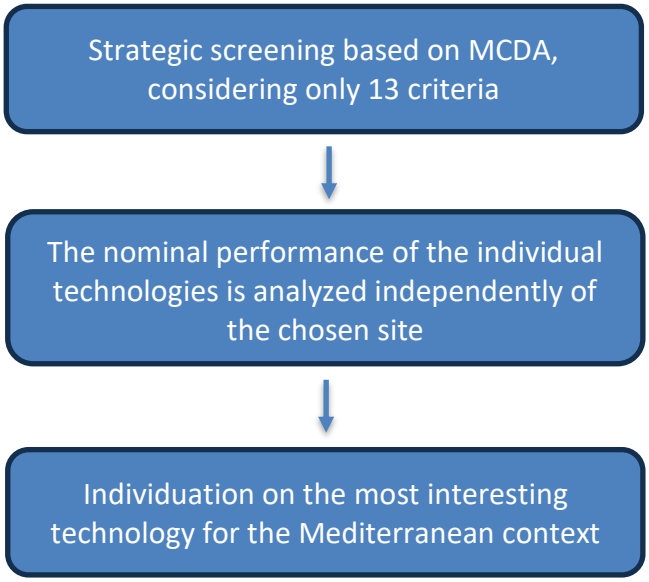


Figure 33: Working methodology for MCDA

5.1 Multi-Criteria Decision Analysis (MCDA)

MCDA provides a systematic and transparent process for decision-making, reducing the risk of bias and ensuring that all relevant factors are considered. By breaking down the decision-making process into clear steps, MCDA ensures that decisions are transparent, auditable and defensible [75].

5.1.1 Advantages and disadvantages of multi-criteria analysis

Working according to this approach has many advantages. They include [75]:

- **Improved clarity:** MCDA helps decision-makers understand the problem structure and the trade-offs between different criteria.
- **Handling uncertainty:** MCDA can incorporate uncertainty and sensitivity analysis to test how changes in criteria weights or alternative scores affect the decision.
- **Enhanced communication:** MCDA provides a common language and framework for stakeholders to discuss and debate the decision.
- **Robust decision-making:** by considering multiple criteria, MCDA reduces the risk of making suboptimal decisions based on a single factor.

However, some drawbacks are also present [75]:

- **Complexity**: especially when dealing with a large volume of criteria and alternatives, MCDA can be time-consuming and complex.
- **High-quality data requirement**: reliable results require robust inputs. This can be problematic if data is incomplete or uncertain.
- **Several types of input data**: they require collaboration from multiple technical fields and stakeholders, which can be impractical.
- **Subjective judgments**: the assignment of weights and the evaluation of alternatives have the potential to introduce unintended bias.

5.2 Weighted Sum Method (WSM)

The Weighted Sum Method (WSM) is selected as the primary mathematical engine for this multi-criteria analysis due to its intrinsic transparency, computational robustness, and widespread validation in engineering decision-making frameworks. Operating under the principle of additive utility, the WSM treats the evaluation as a multi-dimensional matrix, effectively converting disparate qualitative and quantitative technical indicators into a single, dimensionless performance index for each alternative.

To visually conceptualize the structural core of this methodology, the standardized evaluation framework is illustrated in Table 16.

Table 16: Evaluation matrix

	Detail criteria (weight)				
	$C_1\ (w_1)$	$C_2\ (w_2)$	…	$C_m\ (w_m)$	Overall score
Alternatives	PC_{11}	PC_{12}	…	PC_{1m}	$Score_1$
	PC_{21}	PC_{22}	…	PC_{2m}	$Score_2$
	…	…	…	…	…
	PC_{71}	PC_{72}	…	PC_{7m}	$Score_7$

As depicted in the matrix structure, the decision-making domain is organized into three components:

- **Alternatives (rows)**: the horizontal vectors represent the n mutually exclusive decommissioning and repurposing scenarios investigated in this study (where n = 1, 2, ..., 7, spanning from biologic methanation to thermally assisted fish farming). Since the artificial reef option does not represent an active reconversion scenario that directly exploits geothermal resources, it was excluded from the evaluation matrix analysis.
- **Criteria and Weights (columns)**: the vertical axes contain the m specific evaluation criteria (C_m, where m = 1, 2, ..., 13), each coupled with a dedicated weight factor (w_m) that reflects its relative strategic importance within the marine environment.
- **Performance Ratings (PC_{nm})**: each intersecting cell contains a localized performance index (PC_{nm}), which translates the qualitative or quantitative behaviour of alternative *n* under the specific lens of criterion *m*, using the semi-quantitative scaling rules defined in the previous sections.

The governing philosophy of the WSM assumes that all criteria are mutually independent. Under this assumption, the localized performance ratings (PC_{nm}) within the same row are linearly compensated and aggregated. The ultimate goal of the matrix is to compress this multi-variable data array into a standalone Overall Score ($Score_n$) for each scenario, establishing a definitive mathematical hierarchy for platform conversion. The formal mathematical formulation using normalized scaling limits, and the localized weight distribution applied to these macro-categories are detailed thoroughly in Section 5.3.5.

5.3 Guideline analysis procedure

In Italy, the regulatory framework is updated according to the provisions of the Ministerial Decree of 15 February 2019 [76] where Article 5 assigns the Ministry of Environment and Energy Security (MASE) the task of evaluating decommissioned mining platforms for potential reuse. This legislation is essential to justify the development of these guidelines, since it establishes the effective legal possibility of platforms reconversion and reuse for purposes other than hydrocarbon extraction.

To identify the adaptability level of each scenario, environmental, technical, structural, and Green Deal policy aspects are simultaneously considered. The methodology development process is divided into five phases:

1. **Definition of criteria**: selection of relevant parameters for the offshore geothermal context.
2. **Definition of the importance of each criterion**: identification of the characteristics that act as binding thresholds for the implementation of a conversion option.
3. **Assignment of an index to each criterion**: definition of indices to evaluate if the required features are present and valorised on the studied platform.
4. **Assignment of a weight to each criterion**: for not binding criteria, a scale of importance was defined which is different for every reconversion option.
5. **Score evaluations**: calculation of the final score and relative adaptability percentage**.**

5.3.1 Definition of criteria

To evaluate if a platform can be adapted to a specific reconversion option it's necessary to evaluate some key factors that influence its feasibility. They have been divided into four macro-categories:

1. **Technical & Energy**: this category evaluates energy performance of the system and its technological maturity. It includes thermodynamic efficiency in the exploit of low enthalpy fluids (geothermal synergy), the Technology Readiness Level (TRL) for offshore applications and the operation complexity keeping also into account maintenance requirements.
2. **Structural**: it analyses physical constraints imposed by the existing platform. It focuses on the impact of the weight of new modules on the deck (topside load), on the spatial footprint of installations and on dynamic effects such as vibrations and noise that could influence structural fatigue.
3. **Logistics & Infrastructure**: it evaluates industrial feasibility of production phase. It includes reuse potential of well and existing pipelines, storage requirements for energetic vectors (such as CH_4, LOHC and NH_3) and the efficiency of transporting products to the mainland.

4. **Economics & Environment**: it examinates holistic sustainability[6] of the project. It includes both financial feasibility (CAPEX and OPEX) and market value of the products, both ecologic impact with a particular focus on the valorisation of waste fluxes (circular economy) and on the mitigation of environmental risks.

5.3.2 Definition of the importance of each criterion

Once the criteria are defined, it is fundamental to identify those that present binding characteristics for the implementation of a specific conversion option. Consequently, the methodology distinguishes between binding and not-binding criteria.

Binding criteria are those that, if not met, prevent the implementation of a conversion option on a specific platform. Conversely, non-binding criteria, although they may be more or less important, do not prevent the implementation of a given project. An example of binding criteria for all the scenario proposed is the presence of a reservoir. It's important to emphasize that if a criterion deemed binding is not met, the platform's adaptability percentage for a given option is automatically reset to zero, excluding that solution from the conversion analysis. To provide a clear screening framework, the specific binding criteria established for this methodology are summarized in Table 17.

Table 17: Binding criteria

Detail criterion	Macro category	Binding
Presence of reservoirs	Environmental compatibility	All the scenarios
Geofluid temperature > 60°C	Environmental compatibility	All the scenarios
Efficiency of the reservoir >30%	Environmental compatibility	Biological methanation
Presence of cluster	Technologies and design	MUP, desalination units
Enough "free" space around the platform	Technologies and design	Aquaculture, LOHC, NH_3

It is worth noting that the temperature threshold set for the geofluid (> 60°C) serves as a generalized minimum constraint for the overall screening framework. In practice, the strict thermal requirement depends heavily on the specific technology under consideration: options such as

[6] Holistic Sustainability is an integrated approach that balances environmental, social, and economic needs for long-term well-being [78][78].

reverse osmosis or thermally assisted fish farming can operate effectively at lower temperature thresholds, whereas thermochemical synthesis pathways demand higher thermal levels. In a site-specific engineering design, the **characteristics of the site** (reservoir enthalpy and platform infrastructure) dictate which technologies are viable. However, for the purpose of this pre-feasibility study, a baseline platform meeting all the generalized binding criteria is assumed. This site-independent approach enables a comprehensive and standardized comparative analysis, facilitating the identification of the most suitable reconversion solutions for the Mediterranean context.

5.3.3 Attribution of an index to each criterion

Since the definition of criteria identifies the specific characteristics relevant to the conversion solutions, it is essential to determine whether these characteristics are present in the platform–reservoir system. This assessment is structured by assigning descriptive indices to the criteria.

Initially, a scale of 5 indicators was tested to have a wider evaluation range. However, during the preliminary study, this approach proved to be less precise and more prone to subjectivity; when it was difficult to establish a definitive index for a specific scenario, the index 3 (positioned perfectly in the middle) was often selected by default.

To guarantee total objectivity and eliminate arbitrary bias during the evaluation stage, a semi-quantitative scoring framework was developed. Each of the thirteen selected criteria is evaluated using an integer index scale ranging from 1 to 4, where 1 signifies a "Critical" operational bottleneck and 4 represents an "Optimal" engineering or strategic match. The specific boundary conditions, physical thresholds, and technological constraints that govern the assignment of each index are detailed in Table 18. This descriptive matrix serves as the standard reference guideline for mapping the qualitative features of the technologies investigated into definitive numerical values.

Table 18: Multi-criteria evaluation matrix and boundary conditions for index assignment

	ID	Criterion	1: Critical (Low)	2: Limited (Medium-Low)	3: Valid (Medium-High)	4: Optimal (High)
Technical & Energy	C1	**Geothermal Synergies***	Process requires T > 150°C; no thermal match with the fluid.	Requirements (90-150°C) exceed reservoir T; high auxiliary heating needed.	Good match (60-80°C); fluid provides most of the required heat.	Perfect thermodynamic match (< 60°C); process driven entirely by reservoir heat.
	C2	**Technology Readiness**	Concept stage or lab tests only (TRL 1-3).	Prototypes tested onshore or in controlled environments (TRL 4-5).	Technology demonstrated in relevant marine environments (TRL 6-7).	Proven technology with successful offshore track record (TRL 8-9).
	C3	**System Complexity**	High number of moving parts; custom-made components; high maintenance.	Significant complexity; requires frequent specialized technical focus.	Moderate complexity; based on standard industrial equipment.	Simple, modular, or passive design; low maintenance requirements.
Structural	C4	**Topside Load Impact**	Massive weight (>50 t); requires primary structural reinforcements.	Significant weight; requires deck local strengthening.	Manageable weight; fits within existing design margins of the platform.	Minimal impact; lightweight modules or subsea integration.
	C5	**Spatial Footprint**	Requires multiple decks or major structural extensions.	Large footprint; requires relocation of existing equipment.	Standard footprint; fits easily into available deck spaces.	Very compact; can be installed in "dead" or unused spaces.
	C6	**Vibration & Noise**	Heavy machinery causing potential structural fatigue/vibration.	Noticeable vibration levels; requires advanced damping systems.	Low vibration levels; standard industrial insulation is sufficient.	No moving parts or vibration-isolated; negligible impact.
Logistics & Infra-	C7	**Infrastructure Reuse**	No reuse possible; requires new wells and sealines.	Limited reuse; requires major cleaning or partial replacement of lines.	Good reuse; most existing wells and subsea lines are compatible.	Full utilization of existing wells, sealines, and on-board facilities.
	C8	**Product Transport**	Complex logistics (e.g. cryogenic); requires new specialized vessels.	Requires significant upgrades to existing transport/pipeline systems.	Compatible with standard utility vessels or slightly modified pipelines.	Seamless integration with existing gas/liquid transport networks.

	ID	Criterion	1: Critical (Low)	2: Limited (Medium-Low)	3: Valid (Medium-High)	4: Optimal (High)
	C9	**Storage Needs**	Requires massive, pressurized, or cryogenic storage tanks.	Moderate storage needs; requires dedicated space and safety systems.	Limited storage; standard atmospheric tanks are sufficient.	No on-board storage needed; continuous export to shore.
Economics & Environment	C10	**Circular Economy**	Linear process; high waste production; no resource recovery.	Low recovery of heat or minerals; limited environmental synergy.	Significant valorisation of waste streams (heat, water, or brine).	High circularity; integrates multiple value chains (e.g. heat + minerals).
	C11	**CAPEX & OPEX**	Prohibitive investment and high annual maintenance/energy costs.	High costs; long payback period (>15 years) expected.	Competitive costs; standard ROI for energy conversion projects.	Low investment and operational costs due to high automation/simplicity.
	C12	**Environmen-tal Risk**	High risk of toxic leaks or brine discharge with ecological impact.	Managed risks; requires continuous chemical monitoring/treatment.	Low impact; follows standard offshore environmental protocols.	Eco-friendly/Zero-discharge; enhances local marine biodiversity.
	C13	**Market Value**	Volatile market or low-demand product; low profit margins.	Stable but niche market; moderate economic attractiveness.	Strong market demand; reliable revenue stream for the asset owner.	High-value commodity (energy vector, premium food) with high demand.

*Note *: It should be noted that the 'Geothermal Synergy' criterion evaluates qualitative thermodynamic suitability (temperature levels) and power self-sufficiency during the critical system activation phase. The actual annual energy exchange, however, is captured and discussed separately in the dynamic energy balance analysis.*

5.3.4 Assigning weight to each criterion

To determine the relative importance of each macro-category, the *Revised Simos method* was employed. This decision-making tool allows for an objective ranking of criteria based on the specific requirements of offshore repurposing. In this study, the categories were ranked according to their impact on the immediate feasibility and safety of the conversion project.

Specifically, the ranking was defined as follows:

- **Technical & Energy** was identified as the highest priority, as geothermal exploitation is the primary driver for the technology selection.
- **Structural** aspects were ranked second, as they determine the capacity of aged structures to support new equipment loads.
- **Economics & Environment** and **Logistics & Infrastructure** were assumed to have equal weight, representing the necessary but secondary pillars of the project.

To emphasize the strategic importance of geothermal synergy, a blank card was inserted between the "Structural" and "Technical & Energy" categories. By setting a ratio $z = 1.75$ between the highest and lowest ranked criteria, the method produced the following normalized weights (W_K):

Table 19: Weight assigned to each macro-category

Macro-category	Weight (W_K)
Technical & Energy	0.35
Structural	0.25
Logistics & Infrastructure	0.20
Economics & Environment	0.20

Regarding the internal criteria ($w_{J,K}$), it was assumed that all sub-criteria within the same macro-category carry equal weight, ensuring a balanced contribution of each specific parameter to the final score.

5.3.5 Allocation of weights and indices

The weights of the criteria were determined using the Simos Method to reflect the decision-maker's priorities, while the final ranking of the technologies was calculated through the Weighted Sum Method (WSM). Once all the preliminary steps have been completed, using the

weighted sum method, the result for each conversion option can be obtained by the following formula:

$$Score_i = \sum_K W_K \cdot \sum_J PC_{J,K} \cdot w_{J,K}$$

Where:

- $Score_i$: is the level of adaptability of the platform considered with respect to the i-th conversion option.
- W_K: weight assigned to the K-th macro-category via the Revised Simos Method.
- $PC_{J,K}$: score (from 1 to 4) assigned to the J-th criterion belonging to the K-th macro-category.
- $w_{J,K}$: weight assigned to the J-th criterion belonging to the K-th macro-category.

To obtain the percentage of adaptability of a specific option compared to the ideal, the following normalization formula is used:

$$Adaptability_i(\%) = \frac{Score_i}{Score_{max}} \cdot 100$$

Where:

- $Score_i$ = adaptability level of the platform for the *i-th* option.
- $Score_{max}$= the maximum theoretical score achievable if a technology obtained a vote of 4 across all 13 criteria (equal to 4.0).

This parameter allows us to understand how closely each technology adapts to the ideal optimum defined by the technical, structural, logistical, and environmental criteria.

5.3.6 Elaboration of the results

Once the scores and internal weights are assigned to each specific criterion, the data are aggregated to obtain the partial performance of each scenario across the four macro-categories. The resulting score matrix is presented in Table 20.

Table 20: Results obtained from the evaluation matrix

Scenario	Technical & Energy	Structural	Logistics & Infrastructure	Economics & Environment
Biologic methanation	2.7	3.7	3.3	3.3
LOHC Hydrogenation (DBT)	2.3	3.0	3.0	3.0
NH_3 production	1.7	1.7	2.0	2.5
Reverse osmosis	2.7	3.0	3.7	3.3
Vacuum thermal distillation	3.7	3.3	3.7	3.0
Membrane distillation	2.7	4.0	3.7	3.0
Thermally assisted fish farming	3.3	2.7	2.7	3.3

As shown in the matrix, the intermediate values highlight significant differences in the behaviour of the analysed alternatives:

- **Technical & Energy**: desalination and aquaculture achieve the highest partial scores due to high TRL level and system simplicity, whereas *Ammonia production* is limited to lower score (1.7) due to its complex operational start-up requirements.
- **Structural**: *Membrane distillation* shows an optimal structural behaviour (4.0), reflecting its lightweight footprint and low impact on the deck load capacity of aged offshore platforms. Conversely, *Ammonia production* is heavily penalized (1.7) by the weight and space constraints of its process modules.
- **Logistics & Infrastructure**: freshwater production methods (*Reverse osmosis*, *Vacuum thermal distillation*, and *Membrane distillation*) lead this category with a uniform score (3.7), providing a strong adaptability to existing offshore pipeline networks and no specific constraints in transporting the final product.
- **Economics & Environment:** the partial scores show a more balanced distribution, with *Biological methanation*, *Reverse osmosis*, and *Thermally assisted fish farming* leading

the category (3.3) due to their favourable trade-off between economic feasibility and environmental sustainability.

These intermediate macro-category scores serve as the direct mathematical inputs for the calculation of the adaptability percentage. The final results will be computed and analysed in the following Chapter.

6 Elaboration of the final results

This chapter represents the culmination of the engineering challenge addressed throughout this research. After mapping the qualitative features of the conversion technologies in Chapter 3, sizing their energy and mass balances in Chapter 4, and establishing a rigorous mathematical framework in Chapter 5, the model is finally executed to process the data and unveil the adaptability rankings.

The Multi-Criteria Decision Analysis (MCDA) is initially executed under the **Base Case (Case 1)** conditions. As described in Section 4.2.5, this scenario evaluates the technologies under a decentralized offshore layout characterized by 200 annual interruptions, simulating the typical supply volatility of marine renewable energy.

The objective of this section is not only to present the optimal technological solutions for the offshore asset but also to stress-test their stability. First, the Base Case results are unveiled to define the baseline technological hierarchy under standard project assumptions. Subsequently, the challenge shifts toward verifying the robustness of these findings through two distinct sensitivity analyses: the *Equal Weights Scenario*, and the *Continuous Shore Supply Scenario*, which investigates how changes in mainland logistics impact the platform's performance.

6.1 Base Case results

From the graph in Figure 34, it is possible to notice that the best reconversion options are associated with freshwater production technologies, such as Vacuum Thermal Distillation and Membrane Distillation. This outcome is strictly governed by two engineering factors: a minimal structural weight footprint on the platform deck, which ensures long-term structural integrity, and an optimal thermal match with the low enthalpy geofluid.

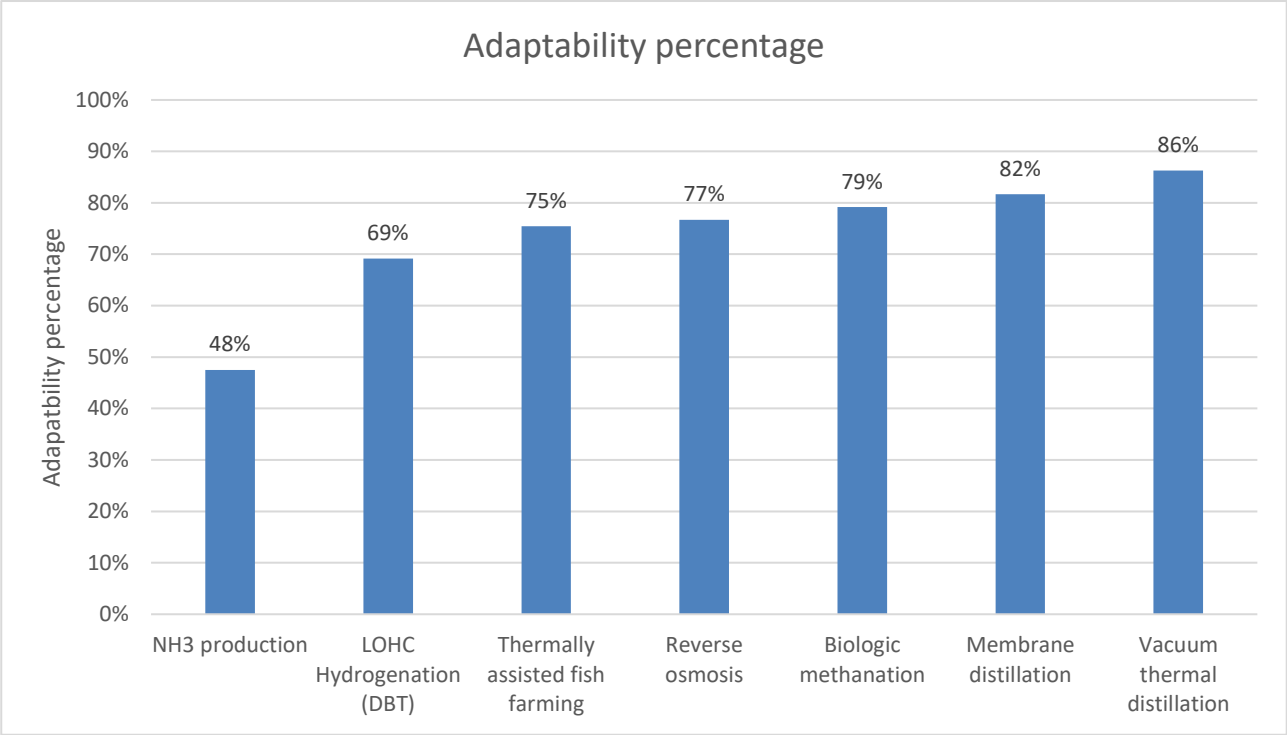


Figure 34: Adaptability percentage of different scenarios

On the other hand, chemical synthesis reactions (Ammonia production and LOHC Hydrogenation) are heavily penalized within this decision framework.

However, despite this optimization attempt and the high market value of the strategic products obtained, these options are still constrained by heavy, complex, and capital-intensive equipment requirements. Furthermore, it must be emphasized that the baseline scoring for geothermal synergy strictly evaluates the qualitative thermodynamic compatibility and power sufficiency during the activation phase, deliberately setting aside the long-term operational time factor at this stage. Under this specific lens, only biological methanation achieves a highly favourable adaptability score (79%), directly reflecting its optimal thermal match with the 75°C reservoir during start-up. In contrast, LOHC hydrogenation (69%) and particularly ammonia production (48%) are constrained by their higher temperature and pressure demands.

Moreover, because these core chemical reactions are highly exothermic once initiated, the geothermal source remains strictly confined to a brief transient utility. The massive annual underutilization of the well capacity is therefore not captured in this static baseline matrix; instead, this temporal dimension and its penalizing effects are systematically addressed in the subsequent sensitivity analysis (*Continuous Shore Supply Scenario*) where the transition to continuous operation shifts the evaluation to a time-integrated perspective.

6.2 Sensitivity analysis: Equal Weights Scenario

To rigorously validate the mathematical stability of the developed Multi-Criteria Decision Analysis (MCDA) model, a sensitivity analysis was performed by testing different weighting scenarios. Specifically, the baseline engineering-weighted configuration was compared against an 'Equal Weights' scenario, where all thirteen criteria were assigned an identical mathematical importance (Figure 35).

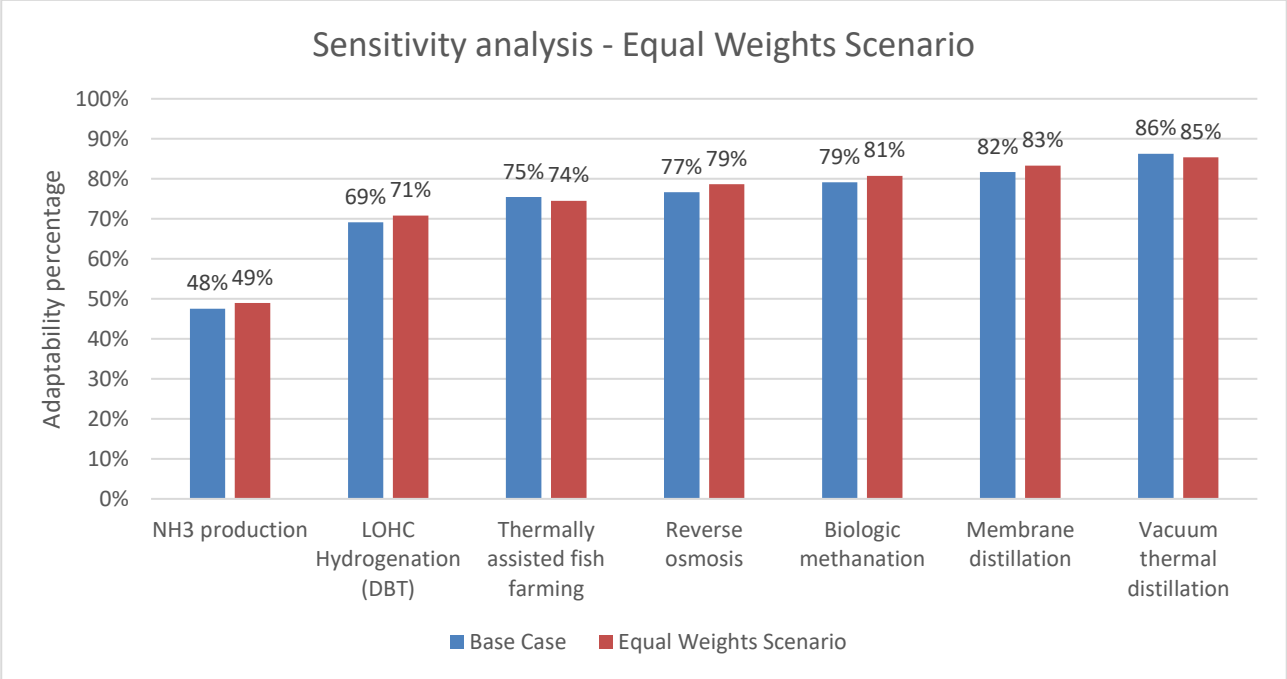


Figure 35: Sensitivity analysis – Comparison between Simos Weights and Equal Weights Scenario

The quantitative outputs, summarized in the final analysis, reveal an outstanding convergence between the two allocation methods. For instance, Vacuum Thermal Distillation consistently emerges as the absolute optimal reconversion strategy for water production, yielding a score of 86% (Base Case) and 85% (Equal Weights Scenario). Concurrently, Ammonia production systematically remains the least favourable option due to its severe intrinsic limitations in terms of structural footprint and system complexity.

This lack of significant divergence between the two scenarios does not imply a lack of sensitivity in the criteria, but rather mathematically proves the structural robustness of the evaluation matrix. It demonstrates that the technological hierarchy is fundamentally governed by the objective physical constraints of the offshore asset and the intrinsic thermodynamic merits of the

processes, rather than being artificially biased by the designer's subjective weighting choices. Therefore, the decision-making framework can be considered highly reliable and independent of external prioritization shifts.

6.3 Sensitivity analysis: Intermittent vs Continuous Supply

The Base Case scenario was initially built upon an intermittent operational framework (modelling Case 1 conditions), characterizing a decentralized offshore environment powered by fluctuating marine renewable sources. In this configuration, exothermic chemical synthesis routes require geothermal power exclusively during brief transient start-up phases to overcome initial thermal inertia. Since these chemical processes are exothermic and self-sustaining once operational, the high frequency of plant activations and shutdowns artificially overestimates their synergy with a continuous geothermal source.

To introduce a time-integrated perspective, a sensitivity run – the Continuous Supply Scenario (modelling Case 2 conditions) – was performed. In this scenario, the geothermal synergy index for all three chemical pathways was adjusted to its minimum rating of 1. This adjustment reflects the physical reality that under a continuous mainland grid supply, annual start-up events become negligible (<0.15 MWh/year), leaving the geothermal well capacity almost entirely underutilized by chemical loops over the 8760 hours.

The visual comparison between the Base Case and the Continuous Supply scenario is illustrated in Figure 36. As depicted, this operational variation induces a sharp divergence between the two macro-categories of technologies analysed (chemical synthesis pathways vs. seawater-based pathways, which encompass desalination units and thermally-assisted fish farming), driven by their opposite patterns of geothermal resource consumption:

- **Chemical synthesis pathways**: because these processes rely on the geothermal source only as a transient start-up utility, the transition to a continuous supply layout drastically reduces their long-term integration with the reservoir. Consequently, their overall adaptability scores experience a visible decline: Biologic methanation drops from 79% to 70%, LOHC Hydrogenation decreases from 69% to 66%. Conversely, Ammonia production remains constant at 48%, as its required reaction temperatures

(~400°C) far exceed the low-enthalpy reservoir potential, resulting in a minimal geothermal contribution in both operational regimes.

- **Seawater-based technologies (desalination and fish farming):**
    - **Desalination units**: freshwater production systems are endothermic technologies structurally designed to continuously absorb the low enthalpy geofluid as a primary operational input. Eliminating intermittent supply disruptions allows these units to operate at maximum baseload capacity without transient performance penalties or thermal degradation. As a result, the continuous supply regime further consolidates their technological dominance, shifting their adaptability scores upward: Vacuum thermal distillation increases from 86% to 89%, Membrane distillation rises from 82% to 85%, and Reverse osmosis improves from 77% to 80%.

    - **Thermally assisted fish farming:** this biological application shows an increase in adaptability score, moving from 75% in Case 1 to 85% in Case 2. Because fish farming involves living biomass highly sensitive to thermal shocks, an intermittent supply framework (Case 1) severely penalizes the facility by requiring extensive on-board backup equipment – such as auxiliary thermal storage, emergency electrical systems, and redundant heaters – to ensure biomass survival. The transition to a reliable, continuous grid supply (Case 2) eliminates the need for bulky and costly backup systems, simplifying the topside layout, lowering CAPEX/OPEX, and allowing the facility to exploit its continuous low-temperature baseload heating at maximum efficiency.

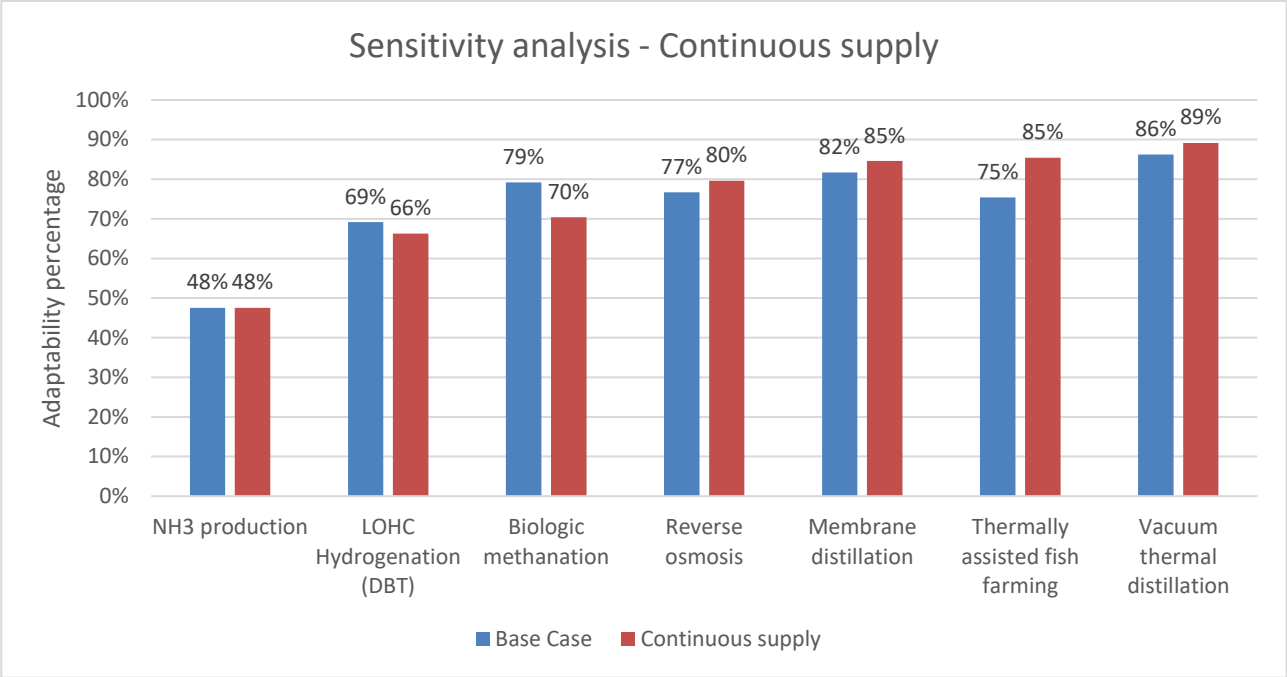


Figure 36: Sensitivity analysis – Comparison between intermittent and continuous supply

This comparison successfully quantifies a fundamental trade-off for the offshore platform design: while an intermittent renewable supply profile favours the justification of a geothermal loop for chemical start-ups, a continuous supply configuration represents the absolute optimal environment for maximizing the true energetic potential of the local low-enthalpy resource through seawater-based applications, specifically water desalination and thermally-assisted fish farming.

7 Conclusion

The repurposing of decommissioned offshore oil and gas platforms can provide an opportunity to extend the value of existing marine infrastructure while supporting the energy transition and reducing the need for complete asset removal. Within this context, this thesis investigated the potential exploitation of low-enthalpy geothermal resources associated with depleted offshore hydrocarbon reservoirs in the Mediterranean Sea, with the aim of identifying suitable reconversion pathways.

The thermal assessment showed that the identified geothermal resource, characterized by relatively low reservoir temperatures, is not suitable for conventional electricity generation under the conditions considered. The analysis therefore focused on direct thermal applications and evaluated seven reconversion scenarios through a multi-criteria decision-making framework.

Overall, the results suggest that low-enthalpy geothermal resources are particularly promising for offshore reconversion when they can be directly coupled with continuous low-temperature thermal demand, while Power-to-X pathways may retain strategic value for their energy-carrier production and potential integration with subsurface storage.

7.1 Critical engineering assessment

The results highlight several key engineering considerations for the repurposing of offshore platforms:

- **Compatibility between geothermal supply and thermal demand**: low-enthalpy geothermal energy is most effectively exploited when the thermal demand is continuous and located directly on or close to the platform. This limits heat losses and avoids the need for extensive thermal transport infrastructure.
- **Different roles of the two technology families**:
    - Seawater-based technologies showed the highest compatibility with the available geothermal resource, as their operating conditions allow a more continuous

exploitation of low-temperature heat. Their technological maturity and comparatively lower process complexity also favour their potential integration into offshore environments.

  - Power-to-X technologies, conversely, showed a lower degree of geothermal utilization because the exothermic synthesis reactions can largely sustain their thermal requirements once operating conditions are reached. Nevertheless, these pathways may become particularly attractive when the depleted reservoir can also be exploited as a site for hydrogen and/or CO_2 storage, enabling the integration of geothermal heat exploitation, energy-carrier production and geological storage within the same offshore asset.

- **Importance of asset-specific constraints**: the feasibility of platform repurposing cannot be assessed from the energy resource alone. Structural integrity, available deck space, equipment weight, marine environmental conditions, safety requirements and the residual lifetime of the asset are critical parameters that must be evaluated on a platform-by-platform basis.

- **Role and limitations of the decision-making framework**: the developed MCDA framework provides a structured approach for comparing heterogeneous reconversion options under multiple technical, structural, logistical, environmental and socio-economic criteria. Its modular structure also allows additional technologies to be incorporated as new data and reconversion concepts become available. However, the results remain dependent on the quality of the available data and on the attribution of the index to each criterion, which introduces an inherent element of subjectivity into the assessment.

- **Model assumptions and energy requirements**: the energy demand associated with seawater intake pumping was not included in the present assessment. This assumption may affect the overall energy balance and should therefore be considered in future, more detailed assessments.

7.2 Future developments

The limitations of the present model, discussed in Section 7.1, also highlight the main areas for further investigation. Several aspects should be further developed to progress from the preliminary assessment presented in this thesis towards a more detailed engineering evaluation:

- **Reduction of resource uncertainty**: future studies should incorporate more detailed well-level and reservoir data, including flow potential, pressure history, casing and cement conditions, and residual well and platform lifetime. However, the availability of such data is often limited by commercial confidentiality and proprietary constraints. Collaboration between Oil & Gas companies and research institutions is therefore essential to enable access to more detailed and reliable information. Moreover, the most suitable reconversion pathway is inherently site-dependent and should therefore be assessed on a case-by-case basis, considering the specific characteristics and constraints of each asset.
- **Thermo-fluid dynamic modelling**: detailed modelling of downhole and riser temperature and pressure losses to quantify the thermal power available at the wellhead under variable flow regimes.
- **Structural and layout assessment**: future work should evaluate the structural capacity and available deck space of representative platforms, considering equipment weight, load distribution, marine environmental loads, safety clearances and the integration of new process units.
- **Economic assessment**: a more comprehensive techno-economic analysis should compare retrofit CAPEX and OPEX with decommissioning costs, potential cost savings from infrastructure reuse and the expected revenues over the extended operational lifetime of the platform.
- **Extension of the technology portfolio**: the MCDA framework could be expanded to include additional emerging reconversion technologies, allowing the methodology to evolve together with the development of offshore energy and marine applications.
- **Integration with geological CO_2 storage**: future work could investigate the feasibility of coupling geothermal heat exploitation with CO_2 storage in depleted offshore reservoirs. This would require assessing reservoir pressure management, injectivity, well

integrity and monitoring requirements, while evaluating whether the combined use of the subsurface resource could provide additional technical or economic benefits.

Bibliography

[1] "Conversione di Piattaforme Off Shore per usi multipli eco-sostenibili (PLACE) — Ingegneria Civile, Chimica, Ambientale e dei Materiali – DICAM," Accessed: May 18, 2026. [Online]. Available: https://dicam.unibo.it/it/ricerca/progetti-di-ricerca/place

[2] SEASTAR, "CONSEGNA I Progetti Basic per la riconversione della piattaforma GREEN1," 2023.

[3] L. Santos, A. Dahi Taleghani, and D. Elsworth, "Repurposing abandoned wells for geothermal energy: Current status and future prospects," Renew. Energy, vol. 194, pp. 1288–1302, Jul. 2022. Available: https://doi.org/10.1016/j.renene.2022.05.138.

[4] M. Leporini, B. Marchetti, F. Corvaro, and F. Polonara, "Reconversion of offshore oil and gas platforms into renewable energy sites production: Assessment of different scenarios," Renew. Energy, vol. 135, pp. 1121–1132, May 2019. Available: https://doi.org/10.1016/J.RENENE.2018.12.073.

[5] MASE, "ELENCO DELLE PIATTAFORME MARINE E STRUTTURE ASSIMILABILI," Feb. 2026.

[6] MASE, "Elenco delle piattaforme in dismissione mineraria – Ministero dell'ambiente e della sicurezza energetica," Accessed: Mar. 10, 2026. [Online]. Available: https://unmig.mase.gov.it/dismissione-mineraria-delle-piattaforme-marine/elenco-delle-piattaforme-in-dismissione-mineraria/

[7] Y. Tan et al., "Cost and environmental impact estimation methodology and potential impact factors in offshore oil and gas platform decommissioning: A review," Environ. Impact Assess. Rev., vol. 87, p. 106536, Mar. 2021. Available: https://doi.org/10.1016/j.eiar.2020.106536.

[8] "Produzione nazionale di idrocarburi – Ministero dell'ambiente e della sicurezza energetica," Accessed: May 21, 2026. [Online]. Available: https://unmig.mase.gov.it/ricerca-e-coltivazione-di-idrocarburi/produzione-nazionale-di-idrocarburi/

[9] M. J. Kaiser, "BSEE decommissioning cost estimates in the shallow water US Gulf of Mexico," Ships and Offshore Structures, vol. 18, no. 10, pp. 1482–1496, Oct. 2023. Available: https://doi.org/10.1080/17445302.2022.2126117.

[10] IEA, "Geothermal Annual Report 2024," Jan. 2026.

[11] C. Alimonti, E. Soldo, and D. Scrocca, “Looking forward to a decarbonized era: Geothermal potential assessment for oil & gas fields in Italy,” Geothermics, vol. 93, p. 102070, Jun. 2021. Available: https://doi.org/10.1016/J.GEOTHERMICS.2021.102070.

[12] F. Vagnon, “Geothermal Energy [lecture note],” 2025, Politecnico of Torino.

[13] IEA, “The Future of Geothermal Energy,” Dec. 2024, Accessed: Mar. 10, 2026. [Online]. Available: IEA – International Energy Agency

[14] V. G. Gude, “Geothermal source potential for water desalination – Current status and future perspective,” Renewable and Sustainable Energy Reviews, vol. 57, pp. 1038–1065, May 2016. Available: https://doi.org/10.1016/J.RSER.2015.12.186.

[15] S. K. Chakraborty and M. Mazzanti, “Geothermal energy: A sustainable and cost-effective alternative for clean energy production and climate change mitigation,” Sustainable Futures, vol. 10, p. 101247, Dec. 2025. Available: https://doi.org/10.1016/j.strueco.2021.08.006.

[16] R. C. Selley and S. A. Sonnenberg, “Sedimentary Basins and Petroleum Systems,” Elements of Petroleum Geology, pp. 377–426, 2015. Available: https://doi.org/10.1016/B978-0-12-386031-6.00008-4.

[17] “GEOTHERMAL DATA - International Geothermal Association,” Accessed: May 19, 2026. [Online]. Available: https://worldgeothermal.org/geothermal-data

[18] J. W. Lund and A. N. Toth, “Direct utilization of geothermal energy 2020 worldwide review,” Geothermics, vol. 90, p. 101915, Feb. 2021. Available: https://doi.org/10.1016/J.GEOTHERMICS.2020.101915.

[19] M. Jochmann, O. Vestavik, M. Wangen, and A. Helstrup, “Advanced Closed Loop Geothermal Energy Solution for Longyearbyen Svalbard, Arctic Norway”.

[20] N. A. Cano et al., “Power from Geothermal Resources as a Co-product of the Oil and Gas Industry: A Review,” ACS Omega, vol. 7, no. 45, p. 40603, Nov. 2022. Available: https://doi.org/10.1021/ACSOMEGA.2C04374.

[21] J. Ma, L. Liu, N. Sai, and L. Gao, “Offshore Geothermal Energy and Repurposing of Oil and Gas Platforms for Integrated Offshore Energy Systems: A Review,” Processes 2026, Vol. 14, Page 2146, vol. 14, no. 13, p. 2146, Jul. 2026. Available: https://doi.org/10.3390/PR14132146.

[22] P. Vannoli, G. Martinelli, and G. Valensise, “The Seismotectonic Significance of Geofluids in Italy,” Front. Earth Sci. (Lausanne)., vol. 9, p. 579390, Feb. 2021. Available: https://doi.org/10.3389/FEART.2021.579390/BIBTEX.

[23] B. Della Vedova, S. Bellani, G. Pellis, and P. Squarci, “Deep temperatures and surface heat flow distribution,” Anatomy of an Orogen: the Apennines and Adjacent

Mediterranean Basins, pp. 65–76, 2001. Available: https://doi.org/10.1007/978-94-015-9829-3_7.

[24] MASE, “Zonazione geotermica del territorio italiano – Ministero dell’ambiente e della sicurezza energetica,” Accessed: Mar. 10, 2026. [Online]. Available: https://unmig.mase.gov.it/risorse-geotermiche/zonazione-geotermica-del-territorio-italiano/?utm_source=chatgpt.com

[25] GHFDB, “GHFDB Research Data Portal,” Accessed: Mar. 10, 2026. [Online]. Available: https://portal.heatflow.world/explore/

[26] “The SLB Energy Glossary | Energy Glossary.” Accessed: Apr. 29, 2026. [Online]. Available: https://glossary.slb.com/en/

[27] A. Rajbongshi and S. B. Gogoi, “A review on oilfield produced water and its treatment technologies,” Petroleum Research, vol. 9, no. 4, pp. 640–656, Dec. 2024. Available: https://doi.org/10.1016/J.PTLRS.2024.06.003.

[28] U. Department of Energy Geothermal Technologies Office, “GeoVision: Harnessing the Heat Beneath Our Feet Chapter 2”.

[29] N. Andritsos, J. Karabelas, and P. G. Koutsoukos, “SCALE FORMATION IN GEOTHERMAL PLANTS,” Jan. 2002. Accessed: Apr. 29, 2026. [Online]. Available: https://www.researchgate.net/publication/248390587_SCALE_FORMATION_IN_GEOTHERMAL_PLANTS

[30] J. Havukainen and M. Horttanainen, “BIOLOGICAL BIOMETHANATION: IN-SITU, EX-SITU AND HYBRID METHODS FOR UPGRADING OF BIOGAS OR SYNGAS,” Lappeenranta–Lahti University of Technology LUT, 2023.

[31] H. C. Yörüklü et al., “A comprehensive review on biological methanation processes: from gaseous feedstocks to biomethane,” Energy Convers. Manag., vol. 341, p. 120075, 2025. Available: https://doi.org/10.1016/j.enconman.2025.120075.

[32] M. Sposob, R. Wahid, and K. Fischer, “Ex-situ biological CO2 methanation using trickle bed reactor: review and recent advances,” Reviews in Environmental Science and Bio/Technology 2021 20:4, vol. 20, no. 4, pp. 1087–1102, Aug. 2021. Available: https://doi.org/10.1007/s11157-021-09589-7.

[33] ENI, “Idrogeno, un vettore energetico per un’energia senza emissioni | Eni,” Accessed: Mar. 17, 2026. [Online]. Available: https://www.eni.com/it-IT/azioni/fonti-energetiche/idrogeno.html

[34] K. Al and A. Kantürk Figen, “Dibenzyltoluene-based liquid organic hydrogen carrier systems: Recent advances, challenges and future perspectives Clean Energy Technologies Journal ARTICLE INFO,” Clean Energy Technol J, vol. 3, no. 1, pp. 30–38, 2025. Available: https://doi.org/10.14744/cetj.2025.0003.

[35] J. Ba et al., “Progress in catalysts for hydrogen storage/release in MBT/DBT based LOHCs: a review,” Chemical Communications, vol. 61, no. 48, pp. 8619–8631, Jun. 2025. Available: https://doi.org/10.1039/d5cc01352f.

[36] F. D’Ambra, V. Faucheux, E. Nicolas, T. Cantat, G. Gébel, and P. Hajiyev, “Direct Enthalpy Measurement for Hydrogenation of Liquid Organic Hydrogen Carriers by Differential Scanning Calorimetry under H2 Pressure,” Ind. Eng. Chem. Res., vol. 63, no. 30, pp. 13157–13168, Jul. 2024. Available: https://doi.org/10.1021/acs.iecr.4c01739.

[37] I. Paz-Paredes, F. Jiménez, J. A. D. Muñ Oz, and J. Ancheyta, “Recent Developments in Distributor Trays for Improving Catalyst Utilization in Hydrotreating Units,” Ind. Eng. Chem. Res., vol. 62, pp. 18122–18132, Oct. 2023. Available: https://doi.org/10.1021/acs.iecr.3c02586.

[38] P. Preuster, C. Papp, and P. Wasserscheid, “Liquid Organic Hydrogen Carriers (LOHCs): Toward a Hydrogen-free Hydrogen Economy,” 2016. Available: https://doi.org/10.1021/acs.accounts.6b00474.

[39] V. S. Arutyunov, “Hydrogen Energy: Significance, Sources, Problems, and Prospects (A Review),” Petroleum Chemistry 2022 62:6, vol. 62, no. 6, pp. 583–593, Jun. 2022. Available: https://doi.org/10.1134/S0965544122040065.

[40] S. Karytsas and I. Choropanitis, “Barriers against and actions towards renewable energy technologies diffusion: A Principal Component Analysis for residential ground source heat pump (GSHP) systems,” Renewable and Sustainable Energy Reviews, vol. 78, pp. 252–271, Oct. 2017. Available: https://doi.org/10.1016/j.rser.2017.04.060.

[41] S. Karytsas and I. Choropanitis, “Barriers against and actions towards renewable energy technologies diffusion: A Principal Component Analysis for residential ground source heat pump (GSHP) systems,” Renewable and Sustainable Energy Reviews, 2017.

[42] E. Vieren, K. Couvreur, M. De Paepe, and S. Lecompte, “High-temperature heat pumps in industrial heating networks: A study on energy use, emissions, and economics,” Appl. Therm. Eng., vol. 259, p. 124799, Jan. 2025. Available: https://doi.org/10.1016/j.applthermaleng.2024.124799.

[43] “Air Source Heat Pump vs Gas Boiler. Which is the Better Choice?” Accessed: Mar. 18, 2026. [Online]. Available: https://completesolar.net/insights/air-source-heat-pump-vs-gas-boiler/

[44] E. Spatolisano and L. A. Pellegrini, “Haber-Bosch process intensification: A first step towards small-scale distributed ammonia production,” Chemical Engineering Research and Design, vol. 195, no. 32, pp. 651–661, Jul. 2023. Available: https://doi.org/10.1016/j.cherd.2023.06.031

[45] Q. Muhammad, B. Mohamed, N. A. Darwish, and H. Nidal, “Reverse osmosis desalination: A state-of-the-art review,” Desalination, 2019.

[46] C. P. Koutsou, E. M. Kritikos, A. J. Karabelas, and M. Kostoglou, “Analysis of temperature effects on the specific energy consumption in reverse osmosis desalination processes,” Desalination, vol. 476, p. 114213, Feb. 2020. Available: https://doi.org/10.1016/j.desal.2019.114213.

[47] “Alfa Laval AQUA Blue E1 C-type Single Stage Fresh Water Generator,”. [Online]. Available: AQUA - Single stage freshwater generator | Alfa Laval

[48] W. Jantaporn, A. Ali, and P. Aimar, “Specific energy requirement of direct contact membrane distillation,” Chemical Engineering Research and Design, vol. 128, pp. 15–26, Dec. 2017. Available: https://doi.org/10.1016/j.cherd.2017.09.031.

[49] M. R. Rahimpour, N. M. Kazerooni, and M. Parhoudeh, “Water Treatment by Renewable Energy-Driven Membrane Distillation,” Current Trends and Future Developments on (Bio-) Membranes: Renewable Energy Integrated with Membrane Operations, pp. 179–211, Jan. 2019. Available: https://doi.org/10.1016/B978-0-12-813545-7.00008-8.

[50] V. Okati, A. J. Moghadam, M. Farzaneh-Gord, and M. Moein-Jahromi, “Thermo-economical and environmental analyses of a Direct Contact Membrane Distillation (DCMD) performance,” J. Clean. Prod., vol. 340, p. 130613, Mar. 2022. Available: https://doi.org/ 10.1016/J.JCLEPRO.2022.130613.

[51] W. M. Nassar, O. Anaya-Lara, K. H. Ahmed, D. Campos-Gaona, and M. Elgenedy, “Assessment of Multi-Use Offshore Platforms: Structure Classification and Design Challenges,” Sustainability 2020, Vol. 12, vol. 12, no. 5, pp. 1–23, Mar. 2020. Available: https://doi.org/10.3390/su12051860.

[52] Y. Il Chu et al., “Offshore Fish Farms: A Review of Standards and Guidelines for Design and Analysis,” Journal of Marine Science and Engineering 2023, Vol. 11, no. 4, Mar. 2023. Available: https://doi.org/10.3390/JMSE11040762.

[53] ETIP Geothermal, “Geothermal Horizons - From cities to regions,” 2024. Accessed: Mar. 10, 2026. [Online]. Available: https://www.egec.org/wp-content/uploads/2024/09/ETIP_NewVision_FINAL-new.pdf

[54] Y. Wei et al., “Context analysis of Offshore Fish Farming”. Available: https://doi.org/10.1088/1757-899X/700/1/012065.

[55] Food Business, “Welfare issues in European sea bass and gilthead sea bream”.

[56] Linde, “SOLVOX Oxystream for seawater, brackish water and freshwater,” Accessed: Apr. 09, 2026. [Online]. Available: https://www.linde-gas.com/what-we-offer/equipment/aquaculture/solvox-oxystream

[57] AGRU, “Offshore & Fish farming.” Accessed: Apr. 01, 2026. [Online]. Available: https://www.agru.at/en/markets/emerging-markets/offshore-/-fish-farming

[58] B. Zanuttigh, E. Dallavalle, and F. Zagonari, “A novel framework for sustainable decision-making on reusing Oil & Gas offshore platforms with application to the Adriatic Sea,” Renewable and Sustainable Energy Reviews, vol. 211, p. 115252, Apr. 2025. Available: https://doi.org/10.1016/j.rser.2024.115252.

[59] B. Zanuttigh, G. Palma, G. Brizzi, G. Bellotti, A. Romano, and R. Suffredini, “Design of a multi-use marine area off-shore the Mediterranean Sea,” Ocean Engineering, vol. 221, p. 108515, Feb. 2021. Available: https://doi.org/10.1016/J.OCEANENG.2020.108515.

[60] S. Cautadella and M. Spagnolo, “Lo stato della pesca e dell’acquacoltura nei mari italiani,” 2012. Accessed: Apr. 08, 2026. [Online]. Available: https://www.masaf.gov.it/flex/cm/pages/ServeBLOB.php/L/IT/IDPagina/5164

[61] European SeaWeed Association, “NSF1 - European Seaweed Association,” Accessed: Apr. 01, 2026. [Online]. Available: https://www.northseafarmers.org/projects/nsf1

[62] European SeaWeed Association, “Applications - European Seaweed Association,” Accessed: Apr. 01, 2026. [Online]. Available: https://www.northseafarmers.org/seaweed/applications

[63] RGIA, “La dismissione delle piattaforme offshore in Italia,” Sep. 2019, Accessed: Apr. 09, 2026. [Online]. Available: Pronti alla dismissione delle piattaforme italiane?

[64] BSEE, “Rigs-to-Reefs | Bureau of Safety and Environmental Enforcement,” Accessed: Apr. 09, 2026. [Online]. Available: https://www.bsee.gov/what-we-do/environmental-compliance/environmental-programs/rigs-to-reefs

[65] F. Pertuso, “Riconversione di una piattaforma petrolifera in dismissione e del relativo reservoir per l’installazione di un impianto di stoccaggio di anidride carbonica. Progettazione preliminare,” 2022.

[66] G. Song et al., “Techno-economic and life cycle greenhouse gas assessment of green ammonia produced by low-pressure Haber-Bosch process,” Energy Nexus, vol. 17, p. 100379, Mar. 2025. Available: https://doi.org/10.1016/J.NEXUS.2025.100379.

[67] “Understanding Nitrogen Purity in PSA Nitrogen Generators.” Accessed: May 27, 2026. [Online]. Available: https://absstem.com/understanding-nitrogen-purity-in-psa-nitrogen-generators/

[68] A. Aliberti, “Riconversione di una piattaforma petrolifera in dismissione per l’installazione di un impianto di dissalazione alimentato da energia fotovoltaica. Progettazione preliminare,” Politecnico di Torino, 2021.

[69] “LennRO 500 L/h Small sea water desalination plant (LennRO SW-S 500).” Accessed: Jun. 13, 2026. [Online]. Available: https://www.lenntech.it/prodotti/LennRO/LennRO-SW-S-500/500-L/h-Small-sea-water-desalination-plant/index.html

[70] “Temperature Correction.” Accessed: Jun. 13, 2026. [Online]. Available: https://www.watertreatmentguide.com/temperature_correction.htm

[71] C. Bosia *et al.*, “Evolution of Brine Geochemical Composition during Operation of EGS Geothermal Plants (Alsace, France)” *Proc. West. Mark. Ed. Assoc. Conf.*, vol. 46.

[72] A. Najib, J. Orfi, H. Alansary, and E. Ali, “Assessing the Impact of Operating Conditions on the Energy and Exergy Efficiency for Multi-Effect Vacuum Membrane Distillation Systems,” *Water 2021, Vol. 13, Page 1500*, vol. 13, no. 11, p. 1500, May 2021. Available: https://doi.org/10.3390/W13111500.

[73] “Datasheet MDS 500.” Accessed: Jun. 17, 2026. [Online]. Available: https://www.memsys.eu/files/memsys-product-MDS-500.pdf

[74] A. Martini, “Metodologia tecnico-ingegneristica per la valutazione della riconversione green di piattaforme oil & gas offshore. Sviluppo del processo di analisi per la definizione di una linea guida,” Politecnico di Torino, 2024.

[75] “Multi-Criteria Decision Analysis (MCDA).” Accessed: Jun. 20, 2026. [Online]. Available: https://risktec.tuv.com/knowledge-bank/multi-criteria-decision-analysis/

[76] “Gazzetta Ufficiale.” Accessed: Jun. 20, 2026. [Online]. Available: https://www.gazzettaufficiale.it/eli/id/2019/03/08/19A01522/sg.

[77] A. Marcucci, F. Ciciulla, and V. Rosati, “7 6 Rivista di Meteorologia Aeronautica Rivista di Meteorologia Aeronautica LA TEMPERATURA SUPERFICIALE DEL MAR MEDITERRANEO PARTE I Analisi e possibili effetti sullo sviluppo delle celle temporalesche”.

[78] “Term Holistic Sustainability.” Accessed: Apr. 30, 2026. [Online]. Available: https://esg.sustainability-directory.com/term/holistic-sustainability/

Acknowledgments

I would like to express my sincere gratitude to Prof. Andrea Carpignano for the trust he placed in me and for giving me the opportunity to develop this thesis, guiding me with care and support throughout its different stages.

I would also like to sincerely thank Prof. Raffaella Gerboni and Emanuela Bruno for their support, attention, and continuous exchange throughout this work. In addition to contributing to my academic growth, their guidance helped me develop greater independence, curiosity, and awareness in approaching research.

Anna Giuliano